"PNEUMATIC CONVEYING OF SOLIDS"

In a 1", horizontal pipeline with continuous recycling.

A Thesis submitted for the degree of Doctor of Philosophy,
in the Faculty of Science, of the University of London

by

M.McLEMAN, B.Sc. (Aberdeen), D. Chem. Eng. (U.C.L.)

Department of Chemical Engineering,
Imperial College of Science and Technology,
Prince Consort Road,
London, S.W.7.

January, 1960.

Summary

A plant has been constructed for the pneumatic conveying of solids through a horizontal, brass pipeline, 1" internal diameter and 100 ft. long. The solids are continuously recycled and, therefore, it has been possible to reach steady conditions of conveying and to obtain measurements over a prolonged period of continuous conveying. The flow patterns have been observed in a transport test section and pressure gradients have been determined by measuring the difference in pressure between a series of manometer points. The velocity of the particles has been determined by a new method in which the flow of solids is momentarily interrupted and the resultant pulse of air is timedbetween two fixed points.

It has been established that the pressure gradient varies in a cyclic manner with distance along that section of the pipeline in which solid acceleration is at a minimum and that, in order to obtain reproduceable values, it is necessary to make pressure drop measurements over a length of at least 40 ft. of the pipeline; furthermore, this section of the pipe should be situated at least 20 to 40 ft. from the feed point, depending on the density and size of the particles, in order to eliminate the effects of particle acceleration.

The solids investigated have been classified according to the way in which the relative velocity between the air and particles varies with flow conditions and for each class the relative velocity has been related to the terminal falling velocity of the particles. The pressure drops obtained during conveying have been correlated in terms of the controlled variables and the terminal falling velocities.

With two solids - sand and manganese dioxide - the pressure drops increased with time of conveying as a result of the build-up of a static electrical charge on a dust layer on the walls of the pipe. With perspex, measurements do not change with time but the relative velocity and the pressure drop are smaller than would be expected; this is considered to be caused by electrostatic charges, but the effect is different from that in the conveying of sand and manganese dioxide.

Acknowledgements

The author wishes to express his deep gratitude to Dr. J.F. Richardson for his unfailing encouragement throughout the course of the work and for his advice on the problems encountered in the construction of the plant and in the correlation and interpretation of experimental results. The author is also greatly indebted to Mr. A.C.V. Sweeting and his workshop staff, whose invaluable assistance enabled the successful construction of the plant and to Mr. L.R. Tylee and his staff who designed and developed the instruments used for measuring the solid velocity.

The author would also like to acknowledge the assistance obtained from Professor D.M. Newitt who provided facilities for the work to be carried out in his department.

The Tyndall Research Award, granted by the Tyndall Mining Bequest Committee of the Royal Society towards the purchase of equipment, and the subsistence scholarships donated by the Worshipful Company of Salters and the Shell Petroleum Company are sincerely appreciated.

Contents

		Page
Title Page.		1
Summary.		2
Acknowledgements.		3
Contents.		4
Introduction.		5
Chapter 1.	Survey and Discussion of the Literature - Experimental.	7
Chapter 2.	The Presentation and Correlation of Results in the Literature.	17
Chapter 3.	Plant Construction.	25
Chapter 4.	Mensuration.	33
Chapter 5.	Experimental Observations.	50
Chapter 6.	Solid Velocities.	59
Chapter 7.	Correlation of Pressure Drops.	67
Chapter 8.	Comparison of Correlation Methods in the Literature.	75
Chapter 9.	The Wall Effect and Frictional Electrification.	83
Chapter 10.	Conclusions.	96
Appendix 1.	Nomenclature.	102
Appendix 2.	Bibliography - Pneumatic Conveying.	104
Appendix 3.	Bibliography - Frictional Electrification.	107
Appendix 4.	Results.	109
Appendix 5.	Drawings and Graphs.	119

Introduction

Pneumatic conveying was first carried out on a large scale at the end of the nineteenth century when it was first introduced for the unloading of grain ships at the wharf-side and later for the transport of grain on farms. The application of the process to agriculture and industry was, at first, very limited, mainly because manual labour was relatively cheap and because no satisfactory methods had been developed for the design of the equipment. Pneumatic conveying is now widely used in the agricultural, chemical and mining industries because it provides a reliable and convenient method for handling granular solids. However, the fundamental principles which govern the process are still not fully understood and a considerable amount of research is still required.

Plants for pneumatic conveying can be operated either at positive pressure or under reduced pressure. A suction plant has the advantage that the inlet section is simple and can be moved readily. However, the available pressure difference is limited and it is not possible to convey materials over long distances. Commercial plants operating under positive pressure will operate at pressures of up to 120" W.G. and the conveying line may be as much as 600 ft. long and 12" in diameter.

Although the equipment and measuring techniques used for vertical and horizontal conveying are essentially similar, the fundamentals of the processes are considerably different. In vertical conveying, the weight of a particle is counter-balanced directly by the vertical drag force arising from the relative motion between the particle and the air, whereas, in horizontal conveying, the drag force acts in a direction at right angles to the weight and the mode of suspension of the particles is more complex.

The early research work in conveying related mainly to the transport of grain. The data obtained by Gasterstadt, Cramp and Priestley, Segler and Wood and Bailey have been found reliable for the design of grain conveyors and are frequently used, even today. Their reliability no doubt arises from the fact that these workers used large scale plants

in their investigations.

After the completion of this work in the 1930's, few papers were published on the general aspects of pneumatic conveying until about ten years ago, since when a considerable number of papers have been published. Much of the recent work has related to specific problems of pneumatic conveying in relation to the handling of materials in fluidised systems but a number of workers have made fundamental studies of pneumatic conveying. Whereas many authors have had considerable success in correlating the results of their own work by means of semi-empirical equations, no general correlation has been obtained. Further, little progress has been made in developing a fundamental theory for the process.

The present work is a continuation of the programme of research on horizontal conveying which has been proceeding in this department for a number of years. It represents an attempt to obtain reliable and reproduceable results which can be used in the formulation of a general theory for conveying in horizontal pipes.

Chapter 1.

Survey and Discussion of the Literature - Experimental

1.1. Introduction

From a survey of the literature on pneumatic conveying it is seen that, although most of the variables in the process have been studied in detail, no satisfactory theory has yet been developed for general design purposes. In general, the results obtained in each investigation related only to the particular plant and experimental conditions employed and a comparison of results is therefore difficult. In most cases, empirical correlations have been suggested but these do not form a sound basis for the development of a theory for the pneumatic conveying process.

In this survey, the various types of plants used and the measuring techniques which have been adopted are critically examined and the experimentally determined pressure gradients are analysed in an attempt to elucidate the factors which have given rise to the apparently inconsistent results of previous workers. This is regarded as an essential preliminary to the present work.

1.2. Plant layout and construction

Although some workers have used plants operating with air at reduced pressures and others with air at positive pressures, the plant layout is basically similar in all cases. The solids are stored in a feed hopper from which they pass through a feeder into the transport pipe and, after being conveyed by the air through the pipeline, they are recovered from a separator from which the air is vented to the atmosphere.

Authors usually stipulate that in order to obtain reliable results, the bore of the pipe must be smooth, uniform and continuous, especially at joints and pressure tappings and, when pipe bends are used, they must be of a sufficiently large radius to minimise

interference with the flow of solids. Provided that these conditions are observed and that acceleration effects after the feed point and pipe bends are accounted for, there is no evidence to indicate that these factors have any critical effect on the results.

Farbar showed that the geometry and the position of the feeder influenced the flow of solids in pipelines of diameters of less than 1" I.D. However, there is no evidence to suggest that this applies to pipes of larger diameters. The design of column feeders and nozzle ejectors is well developed for plants using reduced or low positive pressures. On the other hand, feeders for plants operating at high positive pressures usually are constructed and positioned by trial and error to obtain optimum flow conditions and the exact arrangement may influence the results for pipelines of small diameters. Feeders for such plants mainly consist of simple orifices but worm or screw feed, or fluidised systems are sometimes used when very fine powders are being conveyed.

1.3. The variables and their measurement

The following variables have been measured in the literature:- the length and diameter of the pipe, and the size, shape, density, terminal falling velocity and flow rate of the solids, the temperature and flow rate of the air and the static and differential pressures at selected positions in the pipeline. All these measurements have been made by standardised methods, the inconsistencies between authors being the different definitions of particle size and shape, the length and position of test sections and the measurement of pressure drops by means of differential or static pressure manometers.

Only a few authors have measured the velocities of the particles in the pipe. The methods so far adopted are the photographic method, the use of an isolator and a method employing photoelectric cells. In the photographic method, used by Gasterstadt, Hinkle, Pinkus and Hitchcock and Jones, the particles in a short length of pipe are photographed on a film moving at a known, high speed or are photographed twice on the same plate, the time between the two exposures being known. The distance through which the solids have moved in a given time is then obtained.

The method is applicable only to low concentrations of readily identifiable particles and gives the velocities of individual particles rather than a bulk average. In the isolator method, used by Mehta, Uspenski, Clark, Charles and Mitlin, the particles contained in a measured section of the pipe are isolated by means of two synchronised shutters or two-way cock valves and the material trapped in the pipe is weighed. The method is rather inaccurate as Mehta reported variations of up to 50% and Mitlin obtained variations of up to 100% in successive and identical experiments. Since Mitlin synchronised the shutters very accurately, the variations in measurements indicate an uneven flow of solids in the pipeline (although in Mitlin's experiments variations were partly due to a change in the cross-sectional area of the isolator, referred to later in section 4.4.). Therefore, a bulk average measurement of the solid velocity is more significant than a measurement made at a point in the pipeline.

Segler deflected the solids out of the whole pipeline (110' long) into a collector and simultaneously stopped the flow of solids from the feed hopper. However, his results are somewhat inaccurate because no correction was made for the time during which the solids were being accelerated.

Adam abruptly stopped the flow of solids into the conveying line and, by means of photoelectric cells, measured the time of travel of the end of the stream of solids between two positions in the pipeline. The method measures the bulk average velocity but Adam's results for sands must be considered with caution because of the possibility that they were influenced by electrostatic charges.

1.4. Experimental procedure

The normal experimental procedure followed by authors is to charge the feed hopper with solids and to start first the air flow and then the flow of solids at the required rates. After steady flow conditions have been attained in the pipeline, all the required measurements of air flow, temperature and pressure are made; then, after a measured time interval, the flow of solids is stopped and the conveyed solids are recovered and weighed. This batch procedure limits both the time available for making measurements and the number of measurements which

can be made during a run. This is the reason why the solid velocity has invariably been measured in experiments separate from those above. Hitchcock and Jones and Adam overcame these drawbacks by photographing all the manometer instruments, grouped together, concurrently with their photographic measurements of the solid velocity.

The development of a continuous recycling process, as attempted by Clark and Charles, would provide ample time for a more detailed measurement and study of the pressure gradient in the pipeline. This is desirable in order to check the effect of the duration of conveying on the behaviour of the pressure gradient in the pipeline and to ensure that measurements are made under conditions of steady flow. Many experiments in several investigations have lasted too short a time for steady conditions to be attained and this factor may have contributed to the inconsistency of the results obtained.

1.5. Flow patterns

Several authors, particularly Zenz and Hillyar-Russ, give qualitative descriptions of the flow patterns which they observed during conveying. Similar patterns have been observed in the present work and are referred to in detail in chapter 5. In general, particles are suspended in the air stream at high air velocities and the degree of the dispersion of the particles at a given air velocity is inversely related to the terminal falling velocity. As the air velocity is reduced, the degree of dispersion decreases and particles concentrate more on the bottom of the pipe until eventually some particles settle out of the main stream. This phenomenon is referred to as "saltation" and gives rise to pressure fluctuations throughout the pipeline which increase in magnitude as the velocity is progressively reduced until blockage occurs.

Since authors do not always describe the flow patterns associated with their results, it is possible that many of the discrepancies are associated with differences in flow patterns.

The behaviour of individual particles in a fluid has been studied by a number of authors including Bagnold, Adam, Gasterstadt,

Lapple and Shepherd, Davis, Wagon and Ambrose. Several of these authors have given mathematical interpretations for their observations. However, it is the opinion of several authors that the behaviour of individual particles is quite different from that of concentrated groups of particles as in conveying and the results of Farbar and of Albright and co-workers show a different behaviour for high, and for very low feed rates.

1.6. The suspension of particles

On the basis of experimental evidence a number of mechanisms have been suggested for the suspension of particles in pneumatic conveying. Bouncing is often observed in saltation flow but otherwise only in pipes of large diameters or at very low feed rates in pipes of small diameters. The unsymmetrical shape of particles and / or the existence of a velocity gradient over the pipe's cross-sectional area can give rise to an Aerofoil Effect. Gasterstadt's photographs show that particles can spin at rates of up to 20,000 r.p.m. which can give rise to a considerable amount of lift due to the Magnus Effect. Fluid Turbulence can give rise to secondary turbulent eddies and, as these eddies are estimated in the literature to have velocities of about 15% of the linear fluid velocity, these can give rise to vertical drag forces on the particles.

Little is known as to the relative importance of each of those effects in suspending particles or in contributing to the pressure drop in conveying. However, the effects of fluid turbulence in supporting the particles would be expected to be a maximum at high air velocities and for particles of low falling velocities. Bouncing is probably of greatest significance with large particles.

1.7. The pressure gradient in the pipeline

If the solids are introduced into the conveying line without an initial velocity component in the direction of flow of the airstream, then the pressure gradient decreases with distance downstream of the feed point over the region in which the solids are being accelerated.

It is generally acceptod that the end of this region is reached when the pressure gradient becomes constant and that any further acceleration of the solids, due to air expansion, is negligible. The two regions will be referred to as the Acceleration Region and the Equilibrium Region, respectively. This generalisation is fundamentally important because it implies that reliable measurements should be obtained provided that they are made over a length of pipe, however short, in the equilibrium region. The evidence in the literature on which the generalisation is based, consists of a small number of plots of the total pressure drop, or the static pressure, versus length. However, the variation of the pressure gradient within the equilibrium region has not been studied in detail and there is some evidence that variations do occur in an apparently unsystematic manner.

Such evidence is provided in the earlier work on pneumatic conveying at Imperial College which preceded the present investigation. Hillyar-Russ used a 1" I.D. horizontal pipeline, 16 ft. long, and this pipeline was subsequently extended by Clark and Mitlin to give a total pipe length of over 120 ft. which included two straight runs, 45 ft. long, after pipe bends; in all cases, a batch procedure was employed. Under otherwise identical conditions, Clark obtained a higher pressure gradient at 40 ft. after a bend than did Hillyar-Russ at 16 ft. from the feed point. Again, Mitlin found that the pressure gradient 30 ft. from a bend could be either greater or less than that at 40 ft. by about 10%.

The results of Hitchcock and Jones show that the pressure gradient at 60 ft. from the feed point is usually greater than that at 80 ft. in a 2" I.D. pipe, whilst it is lower at 60 ft. than at 80 ft. in a 3" I.D. pipe.

Gasterstadt showed that the pressure gradient, measured over a 300 ft. long pipeline, varied systematically with changes in flow conditions. However, when the pressure gradients, calculated from his measurements for the section 154 ft. to 165 ft. from the feed point and for the section 84 ft. to 132 ft. after the return bend, are compared, it is found that they vary in a most unsystematic manner, entirely different from that for the whole pipeline; sometimes, the pressure gradient is less than that for air flow alone.

These apparent discrepancies in results may be attributed, in part, to errors in measuring pressures but are sufficiently marked to warrant a thorough investigation of the variations of the pressure gradient in the equilibrium region.

1.8. Analysis of the measured pressure drop

The measured pressure drop, ΔP, is often analysed as the sum of several components as follows:-

$$\Delta P = \Delta p + \Delta p_{acc} + \Delta p_x$$

where Δp and Δp_{acc} are the contributions due to the flow of air and the acceleration of the solids respectively, and Δp_x, which will be called the Excess Pressure Drop, is that due to the presence of the solids.

In table 1.1., which gives the range of variables investigated by the principal authors, it is possible to see which results are influenced by effects due to features of the plant, including feed hoppers, separators and pipe bends and to particle acceleration. In some cases, the test section was so near to the feed point that it is highly probable that the effects of particle acceleration influenced the results. In order to simplify the analysis of the pressure drop, it is important to eliminate as many as possible of the variables which affect the pressure drop. For this reason, it is desirable, in the first place, that measurements should be made in smooth, straight pipes at positions sufficiently remote from the feed point for the effects of particle acceleration to be reduced to a minimum. Unfortunately, it is possible to ascertain that this has been done, only in the work of Segler, Hillyar-Russ, Clark, Charles, Mitlin and Pattantyus and Papai and, therefore, many of the other results are difficult to compare. A further difficulty arises in that many workers measured pressure gradients over pipe sections less than 10 ft. long, some being only 2 ft. long; as there is considerable evidence that conditions are not reproduceable over successive short lengths of pipe, results for such short sections are, therefore, likely to be peculiar to the selected test section.

A study of the acceleration region is preferable only after the mechanisms of conveying in the equilibrium region have been elucidated

PLANT DATA FROM THE LITERATURE. TABLE 1.1.

1. Author.	2. Type	3. Length, Material	4. Test Section	5. Acc. End.	6. D"	7. d"	8. W. lb./cu.ft.	9. F. lb./min.	10. u. ft./sec.	11. Solids Conveyed.
Albright + Co.	Hor.	58' Copper.	0-58'	Acc. End.	.8; .375. .5"	200 Mesh.	87.	.01 + .35	7-32.	Coal dust.
Belden + Kassel.	Vert.	13.5' Steel.	0-13.5'	Acc. E	1.023. .473.	.038" .078"	53.7. 60.9	2 + 17	3-54.	Catalysts.
Charles.	Hor.	100' Brass.	35'-45' from bend.	No.	1"	.104" .075"	70.. 160	0-30	50-90.	Seeds. Sand. Perspex.
Clark	Hor.	100' Brass.	35'-45'.	No.	1"	.04" - .075"	70. 160	0-30	50-90.	Seeds. Perspex.
Cramp + Priestley.	Vert.	30' Steel.	30'	Acc.	2.54"	.15"	74.	-	32-65	Wheat.
Farbar.	Hor. Vert.	7' Pyrex.	3'-5'	Acc.	.67"	.008"- .0016"	61	0 - 8.	50 -150.	Catalysts.
Gasterstadt	Hor.	325' Steel.	0- 325'	Acc. End.	3.5 - 3.75.	.15"	74.	10 - 250.	50 - 90.	Wheat.
Hariu + Molstad.	Vert.	40" Glass.	-	-	.26 .53	30-200 Mesh	61 - 166.	2 + 54	12. 40.	Catalysts. Sand.
Hillyar - Russ.	Hor.	16.5' Brass.	16.5' - 2'.	No?	1"	.04". .07"	70. 74.	0 - 30	50 - 90.	Seeds.
Hinkle.	Hor.	25' Glass.	25.	No?	2" 3"	.014" - .33"	65 - 114.4	4 - 40.	66 -120	Tenite. Catalin. Alundum. Polystyrene.
Hitchcock + Jones.	Hor.	100' Steel.	At 60'. & 80'.	No	1", 2". 3".	.08" - .28"	86. 173.	30. 60.	50. 100	Peas. Pills. Glass spheres
Mitlin.	Hor.	100' Brass.	35'-45'	No	1"	.004" .1"	70 - 700.	0 - 30.	50. 90.	Metals. Seeds. Coal. Sand.
Mehta	Hor. (Vert.)	13. Steel.	9'-12'	Acc?	.5"	.0014" - .0038"	158	6 + 40	10- 90.	Glass spheres.
Pinkus.	Hor.	-	-	No.	1"	.006" - .023".	160	.33 + 1.7.	-	Sand.
Pattantyus + Papai.	Hor. Vert.	60' Steel.	25'-58'		3.9" 4.9" 5.1" 5.9"	.16"	74.	78 - 530.	50 - 100.	Grains.
Segler.	Hor. (Vert.)	110' Steel.	20'-80'	No.	1.8" 4.4" 11.6" 16.5"	.07" - .12"	74.	40 - 340.	40. 100.	Grains.
Uspenski.	Hor.	80' Steel	20'-80'	No.	1.7" 1.24" 1.49".	.005" - .216".	87.	-	-	Coal. Ash.
Vogt + White.	Hor. Vert.	15' Steel	2'- 8'	Acc.	.5	.008" - .158"	77 - 450.	.12 - 10	40. 180.	Sand. Steel. Seeds.
Wood + Bailey.	Hor.	25' Steel.	0-25'	Acc.	2.9.	-	70 - 160	-	? -	Sand. Linseed.
Zenz	Hor. Vert.	6 Lucite.	44"	Acc.	1.75.	.0066 .06"	68. 175.	3 - 30	3 - 60.	Sand, Glass. Salt. Rape.

Column Headings.

2. Horizontal or Vertical Conveying. 3. Total length & material of the pipeline. 4. Position with respect to the feed point = 0. 5. Results contain acceleration and/or other effects. 6.-10. Range of variables investigated. 9. $^{+}$ lb/sec. ft^2.

and requires that particular attention must also be paid to obtaining reproduceable methods of introducing the solids into the pipe. It does, therefore, seem evident that a complete reassessment of the factors influencing pressure drops in conveying must be effected before progress can be made in furthering the understanding of the problem.

1.9. The electrostatic wall effect exhibited by siliceous materials

Charles and Mitlin found that when siliceous materials, such as sand, granite and carborundum, were conveyed, the pressure drop increased with the number of experiments for identical flow rates of air and solids. The excess pressure drop increased by as much as tenfold and became steady after a considerable number of experiments, equivalent to approximately 90 minutes of continuous running. They found no such behaviour when they used metals, vegetable seeds, perspex, glass and polystyrene except that Mitlin observed a similar behaviour, although very much smaller in degree, with cross seed. The effect was attributed to the building-up of an electrostatic charge on the walls of the conveying pipe. Mitlin has suggested that the effect is present, to a degree, in the conveying of all solids. Other workers who conveyed sands did not notice this effect, firstly, because of the slow change in pressure drop with time and, secondly, because they seldom repeated experiments.

A survey of the literature on friction charging indicates that charging can be produced when conveying any solid in any pipeline, irrespective of their electrical properties. Indeed, several workers on pneumatic conveying observed far more intense charging than that reported by Charles and Mitlin. Mehta found it impossible to make accurate measurements when conveying glass spheres in a pyrex pipe because of electrostatic interference with the flow of solids. This phenomenon is studied in the present work and is referred to, in detail, in chapter 9.

1.10. Conclusions

From the preceding survey, it is seen that much of the difficulty in interpreting previous results has arisen from a general lack of understanding of the principal features influencing the pressure

gradient in a conveying line. In particular, measurements have generally been made too close to the feed point so that a large and variable effect due to particle acceleration is included and pressure drops have been measured over such short lengths that the effects of cyclic variations of conditions have exerted considerable influence. Furthermore, the effects of electrostatic charging have obscured the significance of some of the results.

The principal requirement in a plant for measurements on pneumatic conveying is a long, straight pipe, free from obstacles at joints or at pressure points. In order to investigate quantitatively the change in measurements with time over a prolonged period of continuous conveying, a recycling system is essential and this , necessarily, must incorporate a pressure feeder which can return solids from the discharge to the high pressure end of the conveyor. The pressure measuring devices should be arranged at short intervals to enable the pressure gradient to be explored over the whole length of the conveying line. Because the solid velocity is considered by several authors to be important in interpreting pressure drops, a method for its measurement is required which should be capable of giving rapid readings so that frequent measurements can be made concurrently with other measurements and without causing interference with the continuous operation of the plant. Previous work has shown that electrostatic effects may be of paramount importance in the conveying of certain materials and the plant should, therefore, incorporate the abovementioned features so that the behaviour of the system can be examined, as electrostatic charges build up with time. For the purpose of continuity with previous work in this department, it was decided to use a 1" I.D., brass pipeline.

Chapter 2

The Presentation and Correlation of Results in the Literature

2.1. Introduction

The experimental conditions necessary for obtaining reliable and comparable results, as outlined in Chapter 1., are definitely fulfilled in the work of Segler and Pattantyus and Papai only. Despite this, however, the methods used by individual authors in presenting and correlating results are important and are surveyed in this chapter. The results from investigations in which the particles were not fully accelerated cannot be considered to be generally significant because, under these conditions, the combined contribution to the pressure drop of air flow and particle acceleration is overwhelmingly large. Nevertheless, the work of Cramp and Priestley on vertical conveying is worthy of note as an inspiring example of theoretical analysis in addition to its practical value in the design of wheat conveyors.

The various authors correlate the measured pressure drop, ΔP, either as such or in terms of some derived function. Thus some authors use the specific pressure drop, α, defined as the ratio of the measured pressure drop to the pressure drop due to air during conveying. Alternatively, the pressure drop may be considered as being made up of a component contributable to air friction and a second representing the excess pressure drop, Δp_x, caused by the presence of the solids; experimental results are then represented in terms of Δp_x or as a function of $\frac{\Delta p_x}{\Delta p} = (\alpha - 1)$. It has been suggested that the excess pressure drop arises from one or all of the following effects:-

1. Air friction on the particle.
2. Friction between the particles and the pipe wall.
3. Friction between the particles themselves.
4. Energy required to suspend the particles.

Although methods have been suggested for calculating the first two effects, no theoretical interpretation of the last two mechanisms has been developed. It is a general opinion in the literature that friction

between particles is negligible but different opinions are held concerning effect 4. above. Some authors suggest that the energy used to suspend particles would, in the absence of particles, be dissipated as fluid turbulence and is, therefore, negligible, whilst others suggest that it is a major component of the excess pressure drop.

2.2. Calculation of the pressure drop due to air flow

Previous workers appear to have selected arbitrarily the conditions for which to calculate the pressure drop, Δp, for the flow of air itself. Because the presence of the particle affects the total pressure at any point in the system, the pressure drop due to the air can only be calculated from measured values of the pressure distribution in the pipeline. In most cases, however, the pressure drop for air has been taken as that for the air flowing alone in the same pipeline, either at the same velocity, $\Delta p'$, or the same mass rate, Δp^+.

For a given air flow in a positive pressure conveyor, the pressure at any point in the conveying line will become greater as the feed rate of the solids is increased, provided that the discharge pressure is unaltered. Thus, for these conditions, at any feed rate,

$$\Delta p' < \Delta p < \Delta p^+$$

Similarly, for a reduced pressure system,

$$\Delta p' > \Delta p > \Delta p^+$$

As the feed rate and the velocity of the air are increased, the difference between these values of the air pressure drop become progressively more marked. This is an important factor in comparing results in the literature but, for the purpose of clarity in the text, the symbol Δp is used in this chapter, irrespective of the method used by authors for calculating the pressure drop due to air in conveying.

2.3. The drag force of the air on the particles

Because the fluid is normally highly turbulent in conveying, the drag force, $\bar{F}$, on a particle, arising from the relative motion between the air and the particle, is generally assumed to be proportional to the square of the relative velocity. It is, therefore, given by:-

$$\bar{F} = \frac{C\rho(u - s)^2 a}{2} \qquad 2.1$$

Where ρ is the density of the air,

u is the velocity of the air,

s is the velocity of the particle,

a is the cross-sectional area of the particle

and C is the drag coefficient.

Equation 2.1. will apply only when the particle is completely suspended in the air stream. The total drag force on all the particles in a length, L, of the pipeline is then given by the expression,

$$\frac{C\rho (u - s)^2 a F L}{2 \quad s m}$$

where, F, is the feed rate and, m, is the weight of a particle. The excess pressure drop over the length, L, may be assumed to be entirely due to the drag force of the air on the particles. Thus, by a balance of forces, the force exerted by the air, as given by the expression, $\Delta p_x A$, where A is the cross-sectional area of the pipe, is equated to the sum of the drag forces on the particles to give the equation

$$\Delta p_x A = \frac{C\rho (u - s)^2 a F L}{2 \quad s m} \qquad 2.2$$

For spherical and uniform sized particles of diameter, d, and density, w, equation 2.2. can be rewritten as

$$\Delta p_x A = \frac{3 C\rho (u - s)^2 F L}{4 \quad w d s} \qquad 2.3$$

as used by Hinkle, Pinkus and Mehta. When the particles being conveyed are non-spherical and non-uniform in size, an "equivalent diameter" is arbitrarily defined by individual authors and used in equation 2.3. instead of the particle diameter. Segler and Hillyar-Russ derived a slightly different equation by means of an energy balance. They obtained their two energy terms by multiplying the left hand side of equation 2.3. by the air velocity and the right hand side by the relative velocity. Their equation is inconsistent in that, for a unit time interval, the two energy terms refer to different lengths of pipeline.

The drag coefficient, calculated by substituting measured values of the other quantities in equation 2.3., is found to vary with flow conditions. Furthermore, if it can be assumed that the same relationship between the drag force and the relative velocity exists both in conveying and when particles settle in air, then the value of the drag coefficient, C, can be determined experimentally and the excess pressure drop can be calculated from measurements of the solid velocity and vice versa. The

calculated values of the excess pressure drop are then usually up to several times greater than the measured values. However, because of the algebraic form of equation 2.3. and the small numerical values of the relative velocity, values of the solid velocity, calculated from measurements of the excess pressure drop and the drag coefficient, usually agree with measured values to within $\pm$ 10%. A further difficulty in using equation 2.3. arises in the choice of a suitable value of the "equivalent particle diameter" for non-uniform sized and non-spherical particles. In many cases, the equation is not applicable because the particles are not all freely suspended in the fluid stream.

2.4. Friction between the particles and the pipe

The contribution to the measured pressure drop of friction between particles and the wall of the pipe has been considered by several authors. Cramp and Priestley, on vertical conveying, and Hillyar-Russ derived equations using an equivalent coefficient of friction which was assumed to act continuously. Wood and Bailey and Clark used a shear stress term, similar to that in the Fanning equation. Vogt and White and Clark considered the loss of energy in collisions between particles and the pipe wall.

However, it was not possible to assess the significance of these factors except in the work of Cramp and Priestley, who reasoned that the equivalent coefficient of friction was directly proportional to the square of the solid velocity divided by the square root of the feed rate. They determined the constant of proportionality but the accuracy of this particular analysis is obscured by the effects of particle acceleration. This treatment, however, has not been applied to horizontal conveying.

2.5. Analogies to the Fanning Equation

A more successful approach for expressing the pressure drop is the use of equations based on the Fanning equation. The total pressure drop and the excess pressure drop have both been correlated by various authors in terms of a variety of density and velocity terms and corresponding friction factors. Sogler showed graphically how the

friction factor, ft, defined by the equation

$$\Delta P = f_t \frac{\rho u^2}{2} \frac{L}{D} \qquad 2.4$$

depended on the air velocity, the feed rate and the pipe diameter, D. Mehta inserted his experimental results in equation 2.3. and in the equation

$$\Delta p_x = f_d \frac{\bar{w} s^2 L}{2 D} \qquad 2.5$$

where $\bar{w} = \frac{F}{s.l}$, is the disperse density and fd is a friction factor defined by equation 2.5. He found that C from equation 2.3. and fd varied in an erratic manner; his results were best expressed by the equation

$$\Delta P = f_c \left[1 + \left(\frac{\bar{w} s^2}{r^2 u^2} \right)^b \right] \frac{L \rho u^2}{D \ 2} \qquad 2.6$$

where b is an experimental constant for each material and was considered to depend on the type of flow. The friction factor, fc, could not be predicted but it was independent of Re for Re $>$ 20,000 and increased, in a similar way as does the Fanning friction factor, as Re decreased for Re $<$ 20,000; it also depended on the feed rate for his smaller particles.

The friction factor, fd, in equation 2.5. may be expressed in terms of the drag coefficient and the relative velocity by substituting for the excess pressure drop as given by equation 2.5. in equation 2.3. However, this type of relationship has not been found to be of any value for expressing experimental results.

Further references to similar analogies to the Fanning equation are found in the publications of Charles, Korn, Hinkle and Pinkus.

2.6. The specific pressure drop

Gasterstadt and Uspenski expressed their results by the equation

$$\frac{\alpha - 1}{r} = \tan \theta \qquad 2.7$$

where α is the specific pressure drop and r is the specific loading defined as the ratio of the mass flow rate of solids to that of air. Gasterstadt found that, for wheat, tan θ decreased and tended to become constant as the air velocity increased. Uspenski found that, for various sized ashes and coal dust, tan θ was a constant for a particular material. Pattantyus and Papai found that their results for grain, conveyed in pipes of different diameters, gave the following empirical relationships:-

$$\frac{\Delta p_x}{L} = \frac{k F u}{A} \qquad 2.8$$

where k is an experimentally determined constant.

By using the Fanning equation,

$$\Delta p = f \rho u^2 L / 2 D \qquad 2.9$$

where, f, is the Fanning friction factor, equation 2.8. may be re-written as, $\frac{\Delta p_x}{\Delta p L} = \frac{k F u}{A} \cdot \frac{2 D}{f \rho u^2 L}$

therefore, $(\alpha - 1) = \frac{k F}{\rho u A} \cdot \frac{2 D}{f}$

therefore, $\frac{(\alpha - 1)}{r} = \frac{k 2 D}{f} \qquad 2.10$

Thus, the results of Pattantyus and Papai show that the term $\frac{(\alpha - 1)}{r}$ is a function of the Fanning friction factor and increases with the air velocity (or the Reynold's Number). Those of Gasterstadt show that the term decreases and tends to be constant as the air velocity increases. This difference may be due to the fact that the two authors calculate values of the air friction, Δp, in different ways. Nevertheless, Pattantyus and Papai found that the value of $\frac{\alpha - 1}{r}$, for a pipe diameter of 3.94", corresponded with the constant value obtained by Gasterstadt in a pipeline of diameter 3.5" to 3.75" at high air velocities. Calculations using Segler's results show that $\frac{\alpha - 1}{r}$ decreases as the air velocity increases and varies inversely with the pipe diameter for diameters between 4" and 16" but varies only slightly with pipe diameter for diameters between 2" and 4".

Vogt and White made the following assumptions:-

That the ratio of the solid velocity to the air velocity is constant for a given material;

That the drag force on a particle is given by Stoke's Law;

That the particles lose a constant fraction of their kinetic energy in collisions with the pipe wall.

On this basis, they derived the equation

$$\frac{\alpha - 1}{r} = \left(\frac{D}{d}\right)^2 \left(\frac{\rho}{w}\right) \left(\frac{1}{Re}\right) \qquad 2.11$$

They found that their own results, unlike those of Gasterstadt and Segler, did not agree with equation 2.11.

2.7. Solid velocities

Measurements of the solid velocity were made by Segler, Uspenski, Mehta, Charles, Clark and Mitlin, who all used an isolator method. In general, their conclusions indicated that the solids used could be classified according to whether the relative velocity, $(u - s)$, or the velocity ratio, $\frac{s}{u}$, was constant. Because the relative velocity is obtained by the difference between the air and solid velocity and is considerably smaller, numerically, than either, very accurate measurements of the solid velocity must be obtained in order to calculate the relative velocity with sufficient accuracy. None of the measurements referred to above met this requirement.

Although photographic measurements of the solid velocity are accurate, those found in the literature refer to only a small range of flow conditions. Gasterstadt's photographic measurements referred to only one air velocity and three feed rates. Hinkle's values of the relative velocity are so much greater than those of other workers that it seems probable that either particle acceleration was incomplete or electrostatic charges influenced the flow of solids. Pinkus concluded that the velocity ratio was a function of the Reynold's Number. Hitchcock and Jones, on the basis of relatively few experimental results and a dimensional analysis, expressed the solid velocity as a function of the feed rate, the air velocity and the density of the air and of the particles, but the form of their relation does not appear to have any theoretical significance.

2.8. Conclusions

The results of experimental investigations of pressure drop in pneumatic conveying have been most satisfactorily interpreted in terms of the "specific pressure drop". The results of Gasterstadt, Uspenski, Pattantyus and Papai and Segler, when expressed in this way, show a general agreement, although there are differences in points of detail. In each case, long pipelines were used so that the effects of particle acceleration were minimised.

Representation of results in terms of a modified Fanning equation is not satisfactory because the constants are difficult to predict.

The semi-theoretical equations based on force or energy balances fail because sufficiently accurate values of relative velocity are not available and because the idealised conditions of suspension are generally not realised in practice.

Measurements of the solid velocity by the isolator method indicate that either the relative velocity or the velocity ratio of a given material may be constant. The more accurate photographic measurements indicate that the solid velocity of a given material may not always be directly proportional to the air velocity and may depend, to a small degree, on the feed rate. There is no indication of how the solid velocity depends on the properties of the solids.

Chapter 3

Plant Construction

3.1. Purpose of the plant.

The plant was designed to incorporate the following features:-

a) A long, straight & horizontal pipeline with a uniform bore and sufficient pressure tappings for the detailed investigation of the pressure gradient in the pipeline. This fulfills the conditions necessary for investigating horizontal conveying as suggested in section 1.10. (the conclusions from the literature survey.)

b) A clean and steady supply of air, the temperature and flow rate of which can be controlled and measured accurately.

c) A rotary valve which transfers solids from the low air pressure end of the plant to the high air pressure feed section. This enables the solids to be recycled and conveyed continuously without affecting the flow conditions or the accuracy of measurements to any appreciable extent.

d) A solids' feeder and control unit which ensures a free flow of solids into the pipeline and an easy method of controlling the feed rate as and when required. Two units, one incorporating a camera iris and the other a simple slide were designed and used.

e) A solids' sampler valve which enables the solids to be withdrawn easily at any time from the system without affecting flow conditions. Two valves one with a slide and the other with a pivoted deflector plate were designed and used.

f) A method of measuring the bulk solid velocity simultaneously with other measurements.

With these provisions all the important variables can be controlled easily and at will; all measurements can be made simultaneously and unhurriedly under steady flow conditions and the electrostatic wall effect can be investigated.

3.2. Plant layout.

In order to obtain a long straight run, the plant was installed on the roof of the departmental building. Much experimentation and modification to the plant was necessary before it could be operated satisfactorily on a continuous, recycling principle. The final layout of the plant used in the present investigation is shown in figure 3.1, together with pertinent data on specific parts.

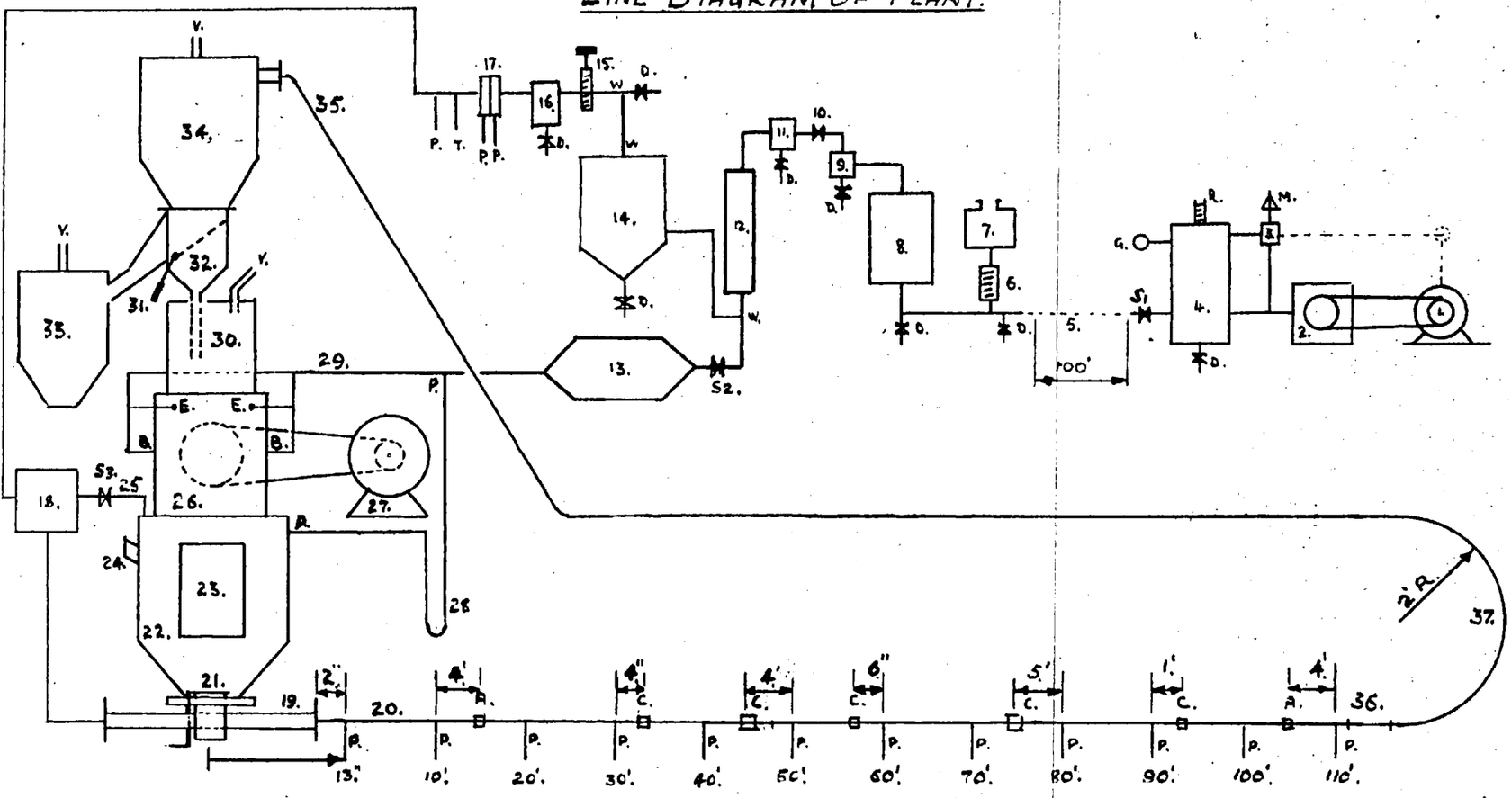
Air from the compressor unit, which is housed at one end of the roof, is led through 100' of 1" I.D. gas piping, exposed to the atmosphere, to a wooden hut, in which most of the equipment is housed, at the other end of the roof. The air is regulated, cooled and cleaned before it reaches the feed inlet where the solids enter the conveying line, through a feed control, from a feed hopper which can be charged with solids through a side inlet. The solids are conveyed by the air through the transport line into a cyclone separator from which they pass into a sampler valve by means of which they can be directed either into a collector or through a pressure relief chamber into a rotary valve. Air from the cyclone separator, from the pressure relief chamber and from the collector is vented to the atmosphere through filter bags. The rotary valve transfers the solids into the feed hopper.

3.3. The pipelines.

The first 114 ft. of the transport line after the feed section is made up of straight lengths of 1.003" I.D brass pipe joined together by brass, "Ermeto" couplings and two alkathene couplings. The brass couplings are a standard size to fit the outside of the pipeline and are sleeved to a 1.003" bore. This pipeline, which is mostly exposed to the atmosphere, is supported at 4 ft. intervals in clamps lined with strips of alkathene to provide electrical

FIGURE 3.1.

LINE DIAGRAM OF PLANT.



ITEM	DESCRIPTION.
1.	15 H.P. 3-PHASE A.C. MOTOR.
2.	2-CYL. AIR COOLED. V-BELT DRIVEN COMPRESSOR 100 CU. FT./MIN. 50 P.S.I.
3.	IGRANIC CONTROL
4.	2·5' DIA. × 6' STEEL CYLINDICAL RESERVOIR.
5.	100' AIR SUPPLY LINE. 1" I.D. GALVANISED STEEL.
6.	BLOW-OFF VALVE. 15-40 P.S.I. ADJUSTABLE.
7.	2' DIA. × 2·5' STEEL CYLINDRICAL SILENCER.
8.	SINGLE FLOW, BRASS, TUBULAR, WATER-COOLER.
9.	WATER SEPARATOR. 4" DIA. × 8" STEEL CYLINDER.
10.	COCK-VALVE.
11.	OIL FILTER, RADIAL FLOW, FELT ON GAUZE
12.	2" DIA. × 3' STEEL CYLINDER PACKED WITH 1/2" COKE.
13.	DAMPING TANK, 2' DIA. × 3' SHEET METAL CYLINDER.
14.	2' DIA. × 3' STEEL CYLINDER, CONICAL END, 2" COKE.
15.	"J & W" 1" DIAPHRAGM REDUCING VALVE 40:0-20 P.S.I.
16.	MIST FILTER, RADIAL FLOW THRO' 10" L. PORCELAIN ANNULUS.
17.	1/2" STAINLESS STEEL ORIFICE PLATE.
18.	2' DIA. × 3' STEEL CYLINDRICAL DAMPING TANK.
19.	TRANSPARENT PERSPEX FEED INLET.
20.	TRANSPORT LINE 1·003" I.D. 1·48" I.D. BRASS.
21.	FEED CONTROL SHUTTER.
22.	FEED HOPPER 1·5' DIA. × 2' STEEL CYL. CONICAL END.
23.	PERSPEX WINDOW.
24.	FILLING PORT.
25.	PRESSURE EQUILIBRIUM LINE.

ITEM	DESCRIPTION.
26.	ROTARY VALVE, CHAIN DRIVEN BRASS ROTOR 10 R.P.M.
27.	1/2 H.P. 3-PHASE A.C. MOTOR GEARED 2000:20 R.P.M.
28.	Hg MANOMETER.
29.	COMPENSATING AIR SUPPLY LINE.
30.	PRESSURE RELIEF CHAMBER.
31.	DEFLECTOR PLATE CONTROL.
32.	SAMPLING VALVE.
33.	SOLIDS COLLECTOR.
34.	CYCLONE SEPARATOR.
35.	RETURN LINE
36.	SIGHT GLASS.
37.	DOWN COMING BEND 2' RAD.
A.	ALKATHENE COUPLINGS.
B.	PORTS TO ROTOR COMPARTMENTS.
C	"ERMETO" BRASS COUPLINGS.
D	DRAIN COCKS
E.	PORTS IN ROTARY VALVE END COVERS.
G.	PRESSURE GAUGE.
M	MAGNEIC RELIEF VALVE
P	PRESSURE TAPPINGS.
R	RELIEF VALVE 40 P.S.I.
S	SCREW-DOWN VALVES.
T	THERMOMETER
V	VENTS TO ATMOSPHERE VIA FILTER BAGS.
W	WIRE GAUZE FILTER PLUGS.

insulation. Each clamp is located in a slot at the end of a $4\frac{1}{2}$' x 2" x $1\frac{1}{2}$" steel "H" channel so that the clamp can be adjusted vertically, by nuts on its screwed stem, and horizontally in the slot at right angles to the axis of the pipeline. By this means the pipeline is set straight and horizontal. Each steel channel is bolted to a 1' square steel plate, cemented to the top of a 4' high, 1' square brick pillar, which is set in a 2' square, 6" high base.

Twelve pressure tappings are brazed in the pipeline at 10' intervals so that they are flush with the inside of the pipe. They are connected by polythene tubing to copper pressure tubing which is led back to differential manometers on a board in the hut. The polythene and alkathene connections insulate the pipeline, to a degree dependent on atmospheric conditions, but it can also be earthed, if required. A sight glass, positioned at the end of the straight length before a 180° bend of 2' radius, enables visual observations to be made of the flow of solids. The return line and the air supply line are made up of lengths of 1" I.D. galvanised gas piping and are supported on steel struts cemented in the base of the brick pillars. The end of the return line rises 10', at an angle of 45°, into the cyclone separator.

3.4. Air supply system

Air regulation

Air is supplied through a reservoir by a twin cylinder, reciprocating compressor which is driven by an electric motor. An "Igranic" control regulates a magnetic valve so that the electric motor is not overloaded when it is started with a high air pressure in the air reservoir. A valve on the air reservoir lifts at 40 p.s.i. and the "Igranic" control stops the motor at a pressure of 41 p.s.i. in order to comply with safety regulations. When small air flow rates are used, the blow-off valve, fig. 3.1, item 6, is adjusted to blow off excess air through a silencer to the atmosphere in order to prevent the air pressure in the reservoir building up sufficiently to cause fluctuations in the air flow or the compressor to be stopped. The adjustable reducing valve, fig. 3.1, item 15, provides a sensitive

control of air flow although it does not maintain a constant downstream air pressure. In order to maintain a free flow of solids, an equilibrium line, fig. 3.1, item 25, is connected from a damping tank, which reduces any pulsations in the air flow caused by the rotary valve, to the top of the feed hopper so as to maintain the pressure above the solids slightly higher than that at the feed point.

Air cooling and cleaning

The air-cooled compressor and the air supply line heat up considerably and a water cooler is used to cool the air to nearly atmospheric temperature. The drop in temperature of the air after the cooler is never more than 2°C., whereas, without cooling, the temperature drop can be up to 15°C., depending on atmospheric conditions. A constant temperature is required in order to permit accurate calculation of the pressure drop due to air flow.

The filters, fig. 3.1. items 9, 11, 12, 14, 16, as well as the drain cocks and wire gauze plugs, are necessary to remove water and oil mist from the air and thus to prevent errors in measurements of air flow and pressure drops due to liquid being deposited on the orifice plate and in pressure tubing.

3.5. The solids' system

Regulation of the flow rate of the solids

The flow of solids was first controlled by means of a suitably modified camera iris, as shown in fig. 3.2., in appendix 5. The iris is screwed to the flange A by the screw N. A spindle T passes through an air-tight gland V in the cylindrical housing C which is attached to the flange A by the screws M. The spindle actuates the bevel gears D which, in turn, open or close the iris W. When the solids are not being conveyed, the shutter B is closed to take the weight of the solids off the iris. The shutter is brazed to the spindle P which passes through a sleeve and air-tight gland S and is pinned to the boss Q by the taper pin R. The control lever F, screwed into the boss Q, controls the shutter. The solids pass through the iris and the bevel gear D and are then guided by the loose fitting conical section E into the perspex section G which is sealed to the glass tube H. This tube is held and sealed, at either end of the inspection box L, by the glands J.

The inspection box has two perspex side windows through which the solids can be viewed as they enter the glass tube H.

The iris operated well although it required to be dismantled occasionally for cleaning purposes. However, a sharp cut-off of the flow of solids, required for the purpose of measuring the solid velocity, could not be obtained due, mainly, to air turbulence between the iris and the glass tube which caused a trickling finish when the flow of solids was stopped by closing the shutter B.

The feed control shown in fig. 3.3., appendix 5., was designed to ensure both a sharp cut-off of the flow of solids and a control of the flow rate. The perspex tube G is cemented in the cylindrical perspex section H and to the square perspex flanges F. The section H is attached to the flange E by the screws R so that the tube G is as close as is practicable to the aperture of the flange E. The hard steel shutter C is operated by the control arm P which is screwed to the boss L to which the shutter spindle M is pinned by the taper pin K.

When granular, non-abrasive solids are used, the stainless steel plate shutter C can be used by itself. When fine non-abrasive powders are used, the shutter is used with the pressure plate B to prevent particles getting between the shutter and the flange E. When abrasive solids are used, the shutter is backed up by the soft rubber pad D and used without the pressure plate B.

The sampling valve

During the early part of the experimental work, the slide valve, shown in fig. 3.4., in appendix 5, was used to withdraw solids from the system during continuous conveying. It consists of a brass block A, which slides in a rectangular brass housing D so that the solids can be directed either into a collector through the tube G or into the pressure relief chamber, through the tube F. The block is operated by the spindle C which passes through the air-tight gland B. After considerable use, the brass panels of the housing, which were soft soldered, became distorted to such an extent that the slide became jammed with dust and could not be used.

The deflector valve, fig. 3.5. in appendix 5, was then used in place of the slide valve and it fulfills the same purpose without any difficulty. The deflector consists of a rectangular rubber sheet E,

sandwiched between two rectangular brass plates C one of which is brazed to the boss H. The boss is attached by three grub screws F, to the spindle G which passes through the glands J and is operated by the lever L. The sides of the brass plate J have $\frac{1}{8}$" clearance from the sides of the housing and the rubber sheet forms a seal with the housing in the two extreme positions of the deflector flap.

3.6. The rotary valve

Fig. 3.6., in appendix 5, shows the major features of the rotary valve originally designed by Clark. This valve gave rise to a large and unsteady air leakage which could not be satisfactorily calculated and which was so large that at high air pressures, solids did not enter the valve from the separator. The air leakage could be reduced by increasing the pressure on the packing and the solids then flowed more readily into the valve but pressure fluctuations in the transport line increased in severity. Before the air leak could be decreased sufficiently, the friction in the gland became so great that the locking mechanisms holding the rotor components together, broke.

Many experiments were carried out in an attempt to obtain operating conditions satisfactory for accurate measurements. Several modifications, shown in figs. 3.6. A.B.C., were made to the casing R and the pressure ring P and a variety of packing material S was used. Although the air leakage could be reduced sufficiently, the packing was always eventually drawn into the rotor and destroyed.

The valve was re-designed, as shown in fig. 3.7. in appendix 5. The casing A is machined flush inside and a steel annular ring B is press fitted into the casing and located by two short $\frac{1}{2}$" steel pipes N screwed through the ports in the casing into the annular ring. A brass rotor M is machined so that the side ends of the vanes are squared off and flush with each other. The rotor is press fitted on and pinned to a hard steel shaft L. A circular brass plate E is brazed on to each end of the rotor and studs H are screwed through this plate into the sides of each vane. The overall width of the rotor and the end plates E is exactly the same as that of the annular ring. Neoprene strips C are bolted to the stepped tips of each vane and pressed into corresponding slots in the end plates E. A circular sheet of Neoprene D is fitted

over each end plate of the rotor. Its diameter is $\frac{1}{4}$" larger than the inner diameter of the annular ring. A brass pressure plate F is fitted over the key K and over each rubber sheet and tightened up evenly, after assembly in the casing, by means of nuts G on the studs H in the vanes. The pressure plate can be spring loaded (J) for use with large, hard particles which may jam in the seal. The rotor is located centrally and laterally by means of thrust ball bearings V in the end covers of the casing, as shown in fig 3.6. (which are larger than those in the original rotary valve).

The rotor sealing arrangement is subjected to little friction. The compartments are large enough to cope with the feed rates used in the investigation with the chain driven rotor turning at 10 r.p.m. The speed of the rotor may be varied by using different sized sprockets. There is a small eccentricity in the rotor which causes a slight air leakage past the lower half of the seal at the non-drive end of the rotor during 180° of each revolution. This gives rise to a small discontinuous air leakage during operation. The origin of this eccentricity was not traced as it was considered unlikely that the rotory valve could be improved upon in view of the many modifications already made.

Before the valve can operate satisfactorily the high pressure air in up-going compartments must not prevent the solids from entering the compartments from the separator: pressure fluctuations, caused by high pressure air entering down-coming compartments from the feed hopper, must be reduced and air leakage must be eliminated or calculated. Many experiments were made to this end and the final arrangement used is shown in figure 3.1. A flow of high pressure air enters the ports B in the casing and the ports E in the end covers of the casing and is adjusted by means of the valve S so that the pressure in the feed hopper is 1 cm. Hg. less than that in the line 29, as measured by the manometer 28. For such conditions the air leakage is almost eliminated and can be calibrated against the air pressure. The damping tanks 13 and 18 satisfactorily reduce pressure pulsations in the orifice meter and the transport line. The pressure relief chamber vents high pressure air from the rotary valve compartments to the atmosphere.

Chapter 4

Mensuration

4.1. Feed rate of the solids

The feed rate is measured by deflecting the solids, by means of a sampling valve, into a collector and weighing the solids collected in a known time, which is normally 60 seconds or longer. When using small quantities of solids in the feed hopper, some of the sampling times must be reduced to as short as 30 seconds. Successive measurements under identical conditions are reproduceable to within $\pm$ 1.5%.

4.2. Pressures and pressure drops

Static pressures and the pressure drop across the orifice plate are measured by means of mercury manometers and other pressure drops by means of water manometers. The manometers can be read to within 0.2 mm. When the rotary valve is in operation with air alone flowing, readings are steady at low flow rates but fluctuations set in at intermediate air flows and increase in magnitude with air flow giving a maximum fluctuation of 2 mm. in each manometer leg. Similar fluctuations occur during conveying but are more severe over the acceleration region. When saltation flow sets in, the fluctuations increase in magnitude and no measurements for saltation flow are presented in which the manometers fluctuated by more than 1 cm. of water in each leg. The pressure drops presented in the text were made over the section 40 ft. to 110 ft. from the feed point and thus errors due to fluctuations in manometers are very small. In general, the error in manometer measurements for the 70 ft. section is less than 1%, although, some measurements for saltation flow have an error of up to 2%. Measurements over 10 ft. sections have larger errors.

4.3. Air flow

The orifice was calibrated against a dry gas meter for low air

flows, a $\frac{3}{8}$" nozzle according to B.S.S. 726 for intermediate air flows and a 1" nozzle according to B.S.S. 1042 for high air flows. These methods give the following equation for the air flow through the orifice

$$Q_o = 0.975 \sqrt{p_o \Delta p_o} \pm 0.1\% \qquad 4.1$$

Where Q_o is in cu.ft./min. at 30" Hg and 60°F.

p_o is the pressure at the orifice in cms.Hg.

and Δp_o is the pressure drop across the orifice in cms.Hg.

The Fanning equation, 2.9. was used to calculate friction factors for each 10 ft. section of the pipeline. At first, several sections gave friction factors up to 5% higher than other sections, but, after sand had been conveyed through the plant for several hours, all the sections, except one, gave friction factors varying from 0 - 2% higher than those given for smooth pipes in fig. 3.3. in "Chemical Engineering" by Coulson and Richardson. However, the section 30 ft. to 40 ft. gave a friction factor which was 5% higher than the others consistently throughout the course of the work. This could not be satisfactorily explained although it was ascertained that it was not attributable to specific pipe couplings, pressure tubing or manometers.

These friction measurements were made first without the rotary valve and then at various intervals of time after the rotary valve had been installed. In the latter case, the air flow was measured by means of a standard nozzle positioned at the discharge end of the pipeline in order to avoid any errors due to air leakage through the rotary valve.

For the section 40 ft. to 110 ft., the measured pressure drop agreed very closely with the value calculated by means of the Fanning equation, 2.9., using the arithmetic mean pressure and friction factors from the above reference. This method was used to calculate the pressure drop due to air flow, Δp, during conveying. The air flow rate, calculated in a similar way using measured values of the pressure drop and the arithmetic mean pressure in the pipe for air flow alone agreed with that indicated by the orifice in experiments with the rotary valve removed (to eliminate errors due to air leakage); furthermore, this calculated flow rate corresponded with that measured by a standard nozzle at the discharge end of the pipeline, with the rotary valve in operation. Thus the air leakage at the rotary valve can be determined by subtracting the actual flow rate through the pipeline, calculated

from pressure measurements over the 40 ft. to 110 ft. section, from that indicated by the orifice. This was done for air flow alone under the conditions outlined in section 3.6. (for reducing the air leakage through the rotary valve and the pulsations in the air flow) and the actual air leakage was calibrated against the pressure in the feed hopper. The air leakage varied between 0 and 4% of the air flowing through the orifice and, using the calibration, the error in air flow measurements is reduced to less than 1%. It was assumed that these conditions of air leakage were simulated during conveying and the above calibration was used to calculate the air leakage during conveying.

The nominal air velocity, in ft./sec., is calculated from the equation

$$u = 0.8025 \frac{Q\,T}{p} \qquad 4.2$$

for the pipeline of diameter 1.003", where Q is the air flow through the pipeline in cu.ft./min. at 60°F and 30"Hg., T is in degrees Kelvin and p is the absolute arithmetic mean pressure (i.e. pressure at 75' for the 40 ft. to 110 ft. section) in cm. Hg. for the 40 ft. to 100 ft. section. The air velocity never varied by more than 2.5 ft./sec. over the 40 ft. to 110 ft. section. The air temperature is always taken into account in calculations of the air velocity and the air friction pressure drop as it varies with atmospheric conditions from 0°C. to 20°C. during the course of the work.

4.4. The solid velocity

When the isolator used by Clark, Charles and Mitlin was assembled in the 1" I.D. pipeline, it had a 3" long section of about 2" diameter at one end. This may explain the fact that the results of Clark and Charles, obtained when the isolator was arranged with this section upstream, were nearly always higher than those with the isolator reversed. Mitlin used the isolator only in the latter position.

A new isolator was made, 13 ft. long, with a uniform bore throughout, using the original shutters. The results with this isolator, however, varied by 50% for identical conditions and they could not be improved upon.

Other methods were, therefore, considered. The solenoid method can only be used for iron particles and may be applied by inserting

single iron particles in the solids being conveyed but it will be satisfactory only if such a particle travels at the same velocity as the others. The photographic method is expensive and has a limited range of application and was not used.

It has been confirmed, in correspondence with the Isotope Division at Harwell, that a radio-active tracer method is possible. For a 1" I.D. pipeline a particle, travelling at 100 ft./sec., and impregnated with a high energy gamma omitter, such as sodium^{24} or cobalt^{60}, to produce 3×10^5 disintegrations per second (8 micro curies), can excite a sodium iodide phosphor scintillation counter, requiring a count of 25 over a distance of 4" (or $\frac{1}{300}$ sec. at 100 ft./sec.) assuming an overall efficiency of 2.5%. Such a labelled particle can be detected 999 times out of 1,000 and the method promises great accuracies for velocities of up to 1,000 ft./sec. However, the cost of photomultipliers and recording apparatus is high, a ready supply of radio-activity is necessary because of the short half-life of the isotopes in question and an air cleansing plant would be required to conform with health regulations. Further, the range of materials which could be suitably treated is quite narrow, although, provided that it travelled at the same speed as the solids being conveyed, a labelled particle of a different material from that being conveyed may be used. For these reasons, it was decided not to pursue the matter further at this stage.

By rapidly closing and opening the feed control shutter, a short break is produced in the flow of the solids. This principle may form the basis of several methods. As the solids generate considerable noise on entering the cyclone, the time taken by the break to traverse the whole pipeline can be measured by stop-watch. Such measurements are reproduceable to within 0.1 second, but acceleration and end effects must be accounted for.

A pressure pulse also accompanies the break in solids' flow and this causes fluctuations in mercury manometers connected to the pipeline. These fluctuations in the mercury columns were used to close electrical circuits which actuated a recording pen on moving paper, but such experiments were not successful, largely because of the inertia of the systems.

Photocells may be used to detect the velocity of the break but it was considered that this method could be used only at large feed rates

(i.e. dense particle concentration) and it was not investigated. Adam, however, has since developed the method successfully.

Preliminary experiments with an oscilloscope and a transducer coupled to the pipeline by a steel point contact, showed that the position of the break could be detected because the sound, generated by the particles colliding with the pipe wall, disappears at the break. After much further experimentation, a sonic method was developed to measure the solid velocity and this is described in detail.

The Sonic Method

Two transducers are coupled to the pipeline by steel point contacts at a known distance apart. The signal (a few m.v. at 10 k.c.) from each transducer is pre-amplified in situ and again amplified in the hut. Each signal is rectified and provides a bias which is just sufficient to hold off a thyratron. When the break in the flow of the solids reaches a transducer, the signal disappears, the bias is reduced and the thyratron becomes conducting. The resultant drop in the anode voltage of the thyratron is used to start or stop a frequency counter which counts microseconds. The disappearance of the signal from the transducer nearer the feed point starts the counter and that from the other transducer stops the counter. Thus, the time taken for the break in the solids' flow to travel a known distance is determined.

The transducers are most sensitive when the steel needles which couple them to the pipe are in a horizontal position and touch the pipe at nearly 90° to the pipe's axis. The behaviour of each signal can be observed on the screen of an oscilloscope. Each transducer, when coupled to the continuous metal pipe, is sensitive to noise over about 6 ft. of pipe and the behaviour of the signal, when a break is made in the solids' flow, is shown in fig. 4.1. When the break passes a transducer the nearly steady voltage between A and B, obtained for a continuous flow of solids, falls off to zero between B and C and then increases again between D and E to its former steady value, after the break has passed the transducer. It is difficult to tune both circuits to ensure that each thyratron fires at the same voltage when the signal is disappearing. To reduce errors due to this, each transducer is coupled to a 2" long pipe section which is connected into the pipeline by rubber pressure tubing so that there is no metallic contact between

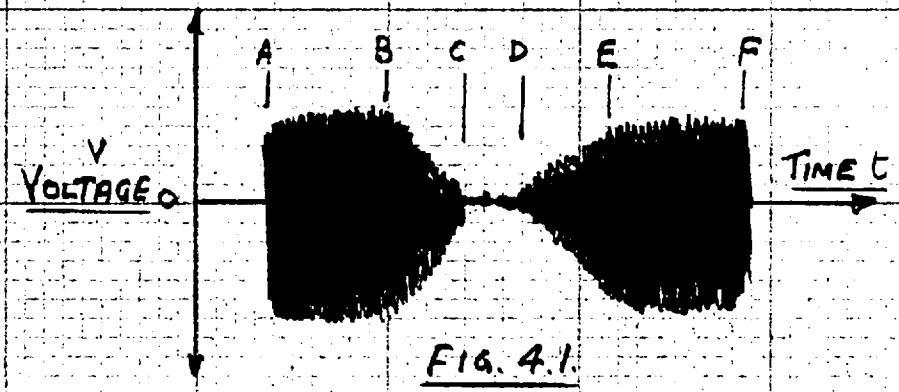


FIG. 4.1.

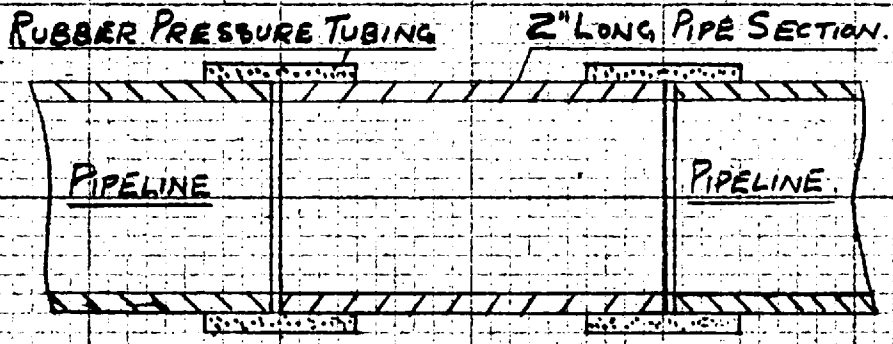


FIG. 4.2. SCALE 1:1.

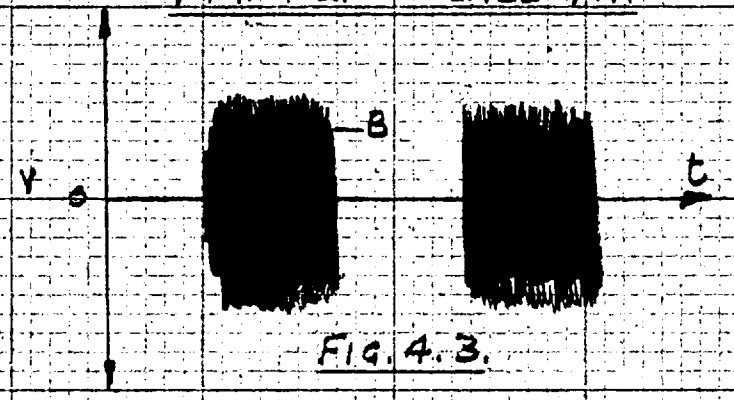


FIG. 4.3.

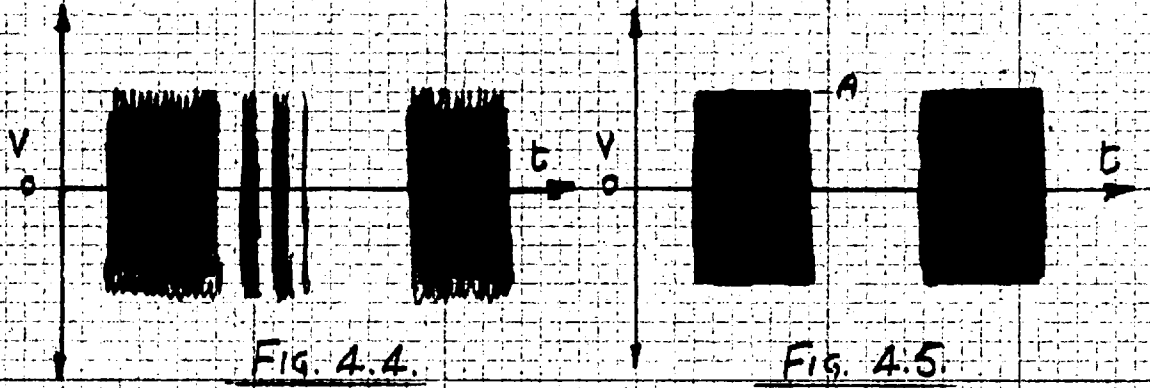


FIG. 4.4.

FIG. 4.5.

the 2" section and the rest of the pipeline, as shown in fig. 4.2. Thus, each transducer is sensitive to sound over only 2" of pipeline as little sound is conducted through the rubber tubing. The behaviour of the signal, in this case, is shown in fig. 4.3 ; it is seen that there is a very sharp drop in voltage. The signal behaves thus only when there is a sharp cut off of the solids' flow. This could not be obtained with the iris feed control because, under those conditions, the solids continued to trickle into the pipe and the result is seen in fig. 4.4. which shows a trickling effect. For this reason, the iris control was replaced by the shutter control. A similar trickling effect arises when the 2" sections referred to above are badly out of line, because they then impede the flow of solids. However, provided these 2" sections are well lined up, as judged by eye, they have no effect either on the flow of solids or on the pressure distribution in the pipeline.

It is seen from fig. 4.3. that the voltage of the signal continuously varies to a small degree. This causes difficulty in tuning both circuits so that the correct bias voltage is applied to each thyratron; as a result, a thyrotron may operate prematurely. To prevent this occurring, the circuits have been adjusted so that they are "saturated", i.e. the signals are so amplified that, in effect, the circuits are not sensitive to the varying maximum voltage but only to a lower voltage equivalent to the level B in fig. 4.3. and the signal thus obtained, shown in fig. 4.5. has a steady and continuous maximum voltage as far as the thyrotron is concerned.

At very low feed rates, the signals become intermittent and the method requires modification by increasing the length of the isolated section and thus decreasing the accuracy. However, the feed rates at which the 2" section was not suitable are so very small that measurements were not made in this range (less than 1 lb/min. for coal).

This method can operate successfully only if the solid velocity does not change as a result of introducing the break into the flow of the solids. From measurements made by stop-watch over the whole pipeline it has been shown that, at most velocities, the time of traverse is the same irrespective of whether the flow of solids is stopped completely, started or merely interrupted for a short period. However, at low velocities, when considerable saltation occurs, the

solids accelerate into the cyclone when the flow is stopped completely and the time of traverse is correspondingly less; this occurs only to a slight degree when the flow of solids is only interrupted.

With the 2" sections positioned at 60 ft. and 112 ft. from the feed point, up to 10 consecutive measurements can be obtained which vary by not more than 1%. Sometimes, however, a series of consecutive measurements show a progressive change of up to 5% overall because of slight changes in flow rates of the solids arising from the feed control shutter not re-opening to exactly the same aperture existing before the shutter was closed. Each measurement presented for coals A and B is the average of 5 consecutive measurements which do not vary by more than 1% or 10 consecutive measurements which do not vary by more than 5% overall. Unfortunately, the frequency counter was not available for measurements with other solids and the results for coals A and B have, therefore, been calibrated against stop-watch measurements of the time taken for the break in solids' flow to traverse the whole plant. These stop-watch measurements are reproduceable to within 0.1 sec. using a 10 sec. per revolution watch. The calibration, graph 4.1, has then been used for measuring the solid velocities of other solids. In graph 4.1. there is also given a calibration of the solid velocity, measured by the sonic method, against the time, similarly measured, taken by the solids to travel between 90 ft. and the cyclone. A comparison of the two calibrations shows how the effect of solid acceleration is greater in stop-watch measurements over the whole plant than in measurements over part of the plant excluding the acceleration region. Any error attributable to different times and distances in which particles are fully accelerated is small as all the solids, except lead, were fully accelerated at between 10 ft. and 20 ft. from the feed point. Lead was fully accelerated at 30 ft. to 40 ft. from the feed point and, in this case, the calibration may be slightly inaccurate.

4.5. Electrostatic charges

A Lindemann Electrometer proved to be far too sensitive for measuring charges on the insulated pipeline and was used in only a small number of experiments. An electrostatic voltmeter was suitable when the pipe was well insulated but atmospheric conditions were seldom

favourable for its use. In addition, an avo-meter could occasionally detect charges.

Most observations on charging were made visually by observing the behaviour of small particles being attracted to the external, and sometimes, the internal wall of the pipe.

4.6. Physical properties of the solids

During conveying, particles break up in different ways and to varying degrees according to the nature of the material. With most materials, the particles tend to become rounded but vegetable seeds disintegrate into oily matter, skins and broken seeds, and eventually agglomerate to form a "mash". The mode of break-down of the coals, which were initially graded, depends on the velocity. At high velocities, the particles apparently disintegrate into smaller particles of various sizes to give particles with a nearly uniform size distribution from dust upwards. The largest particles present, however, are much smaller than those in the original sample before conveying. At low velocities, apart from the formation of some dust, the particles do not disintegrate to a great extent; consequently, there is a discontinuity in the size distribution of the degraded material.

All the other materials used, tend to form some dust, but most of the particles do not break down to an appreciable extent. They, therefore, behave in a similar manner to coal conveyed at low velocities.

It has not been found possible to relate the conveying characteristics of the particles to their elementary physical properties, but the terminal falling velocity appears to be a good guide to their behaviour. The particles are, therefore, considered in terms of their terminal velocities but approximate sizes and densities are given in table 4.1. Particle shapes can be seen in plates 4.1.

The falling velocity is arbitrarily measured in the following way. Two samples, of equal volume, of the material are taken and one is kept as a reference. The other sample is dropped, a small quantity at a time, into the top of a vertical glass tube, 3 ft. long and 1" I.D., up which is passed a metered stream of air. The particles which are blown out of the tube are collected on a 2 ft. square horizontal board which surrounds the top of the tube. The volume of the solids collected on the board

is compared visually with that of the reference sample. This procedure is repeated at a number of air flow rates and the volumetric fraction of the sample which falls in the rising current of air is plotted against the air velocity as shown in graph 4.2. The falling velocity, S_o, is taken as the air velocity at which 50% of the sample is "elutriated". This value of S_o is somewhat arbitrary but it is difficult readily to give a more precise definition for a material containing particles with a wide range of size.

4.7. Experimental procedure

After the plant had been successfully developed to operate on a continuous recycling principle, the following measurements could be made concurrently:-

The flow rate and temperature of the air flowing through the transport pipe.

The pressure of the air at any of the twelve pressure tappings on the pipeline.

The pressure drop over each of the ten sections of pipeline between pressure tappings.

The feed rate of the solids.

The average bulk velocity of the solids over any length of pipe, but preferably longer than 20 ft.

The experimental investigation was comprised of the following phases:-

1. Each material was conveyed continuously for 30 minutes without altering any of the controls in order to discover whether measurements changed with the duration of conveying because of an electrostatic wall effect.

2. In the case of the materials which did not exhibit a time effect, the characteristics of the pressure gradient over the whole pipeline were studied in detail at various feed rates and solid velocities. From this investigation, the conditions necessary for the obtaining of reproduceable and significant results over the equilibrium region were defined.

3. Detailed measurements were then made on the conveying of each material over as wide a range in conditions as was possible within the capacity of the plant. Because the solid velocity can

be kept constant more easily than the air velocity or the feed rate, experimental runs were made at several constant solid velocities. At each solid velocity measurements were made at a number of feed rates under steady flow conditions. A few experiments were then made in which the feed rate was kept nearly constant whilst the solid velocity was varied.

4. Finally, sand and manganese dioxide, both of which exhibited a time effect due to an electrostatic wall effect, were conveyed in order to discover in what manner the measurements changed with the duration of conveying.

TABLE 4.1.

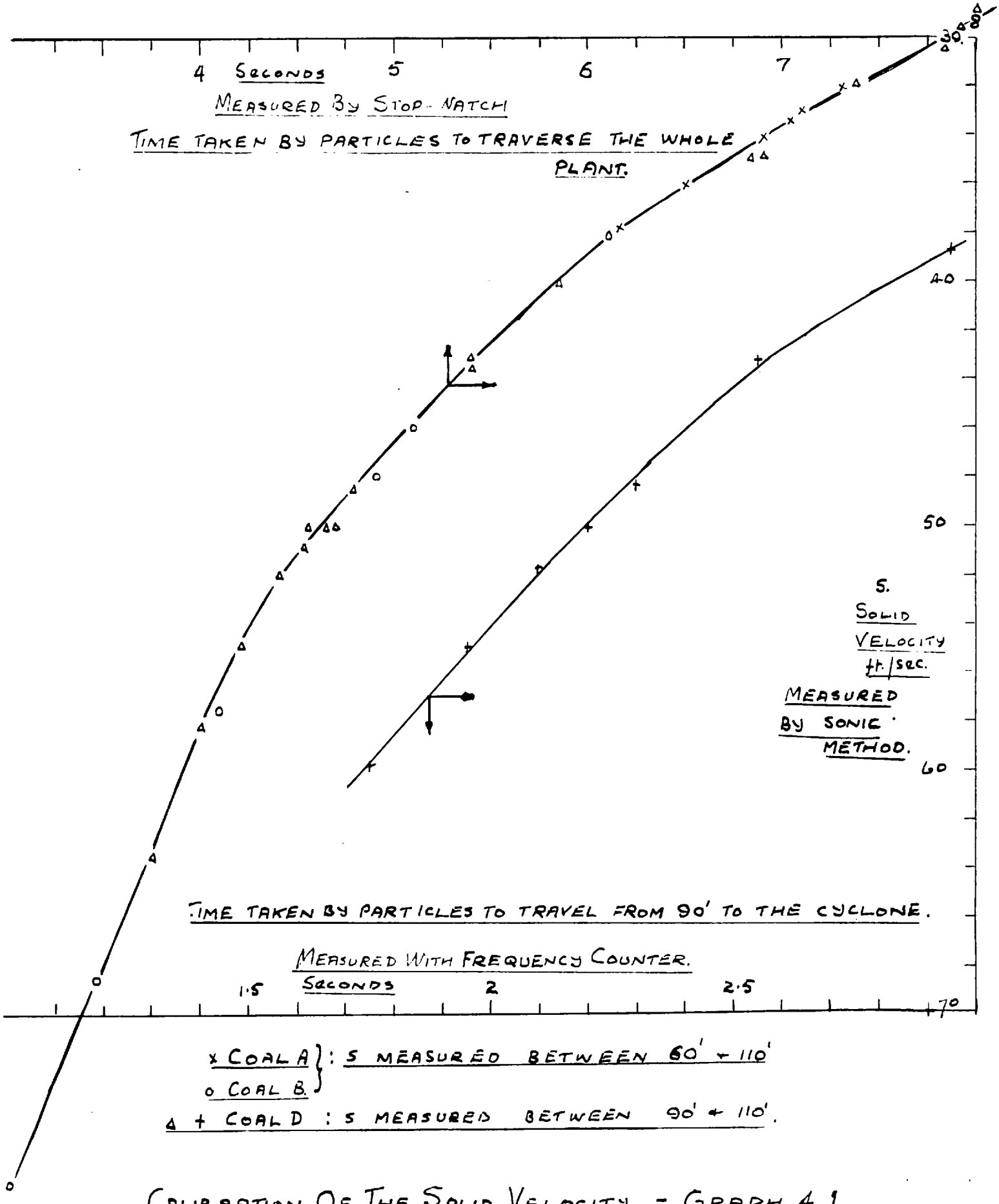
PHYSICAL PROPERTIES OF THE SOLIDS CONVEYED.

MATERIAL.	SHAPE.	PARTICLE SIZE.		DENSITY.	S_o
		RANGE.	MEAN.	lb./cu.ft.	ft./sec.
COAL. A.	ROUNDED.	·06" - DUST.	·03"	87·5.	9·2.
COAL. B.	ROUNDED.	·05" - DUST.	·025"		8·0.
COAL. C.	ROUNDED.	·04" - DUST.	·02"		7·0.
COAL D.	ROUNDED.	·08" - DUST.	·04"		10·7.
COAL. E.	ROUNDED.	·16" - DUST.	·08"		12·2.
PERSPEX A.	ANGULAR.	·08" - ·04"	·06"	74.	12·25.
PERSPEX B.	ANGULAR.	·2" - ·1"	·15"		16·4.
PERSPEX C.	SPHERICAL.	·04" - ·02"	·03"		7·7.
POLYSTYRENE.	SPHERICAL.	·016" - ·012"	·014"	67·5.	5·3.
LEAD.	SPHERICAL.	·04" - ·006"	·012"	692.	26·8
BRASS.	POROUS, FEATHERY FILINGS.	·023" - ·008"	·015"	527.	13·4.
ALUMINIUM.	ROUNDED.	·015" - ·004"	·009"	177.	9·9.
RAPE SEED.	SPHERICAL.	·08" - ·07"	·075"	67·5.	19·4.
RADISH SEED.	SPHERICAL.	·11" - ·09"	·1"	66·5.	21·25
SAND.	NEARLY SPHERICAL.	·06" - ·04"	·05"	163.	15·3
MANGANESE DIOXIDE.	ROUNDED.	·04" - ·01"	·03"	250.	17·3.

TABLE 5.1

THE FLOW PATTERNS EXHIBITED BY MATERIALS IN ORDER OF OCCURRENCE AS THE AIR VELOCITY IS DECREASED

	PERSPEX		COAL					BRASS	ALUMINIUM.	LEAD
	B	A	E	D	A	B	C			
(a) UNIFORM SUSPENDED.	1	1	1	1	1	1	1	1	1	(1)
(b) NON-UNIFORM SUSPENDED.	2	2	2	2	2	2	2	2	2	2
(c) SLUG	-	-	-	-	3	3	3	3	3	3
(d) PLUG	3	-	-	-	-	-	-	-	-	-
(e) DUNE	-	3	3	3	4	-	-	4	4	4
(f) MOVING BED	-	-	-	-	-	4	4	5	5	5
(f) STATIONARY BED.	-	-	-	-	-	-	-	6	6	6



CALIBRATION OF THE SOLID VELOCITY - GRAPH 4.1.

GRAPH 4.2.

MEASUREMENT OF TERMINAL FALLING VELOCITIES.

AIR VELOCITY ft/sec. IN TUBE INTO WHICH THE SAMPLE IS DROPPED.

30
25
20
15
10
5
0

S_o

LEAD.
RADISH.
RAPE.
MANGANESE DIOXIDE.
PERSPEX B.
SAND.
PERSPEX A.
BRASS.
ALUMINIUM.
PERSPEX C.

FRACTION (BULK VOLUME) OF SAMPLE ENTERING THE TUBE.

1/4. 1/2. 3/4. 1.

6

GRAPH 4.2.

TERMINAL FALLING VELOCITIES.

AIR VELOCITY ft/sec.

20
15
10
5
0

S_o

COAL D
COAL A
COAL E
COAL C
POLYSTYRENE
COAL B.

COAL	A	⊙
"	B	✱
"	C	△
"	D	×
"	E	⊙

0. 1/4. 1/2. 3/4. 1.

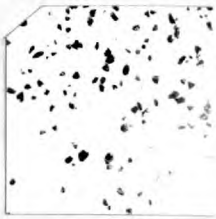
FRACTION OF SAMPLE.

COALS - Before Conveying

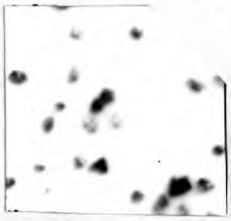
A - actual size



B - actual size



C - magnified 5 X



D - actual size

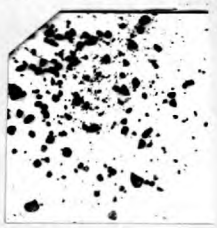


E - actual size

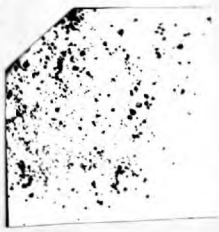


COALS - After Conveying

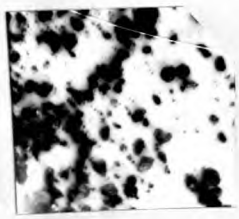
A - actual size



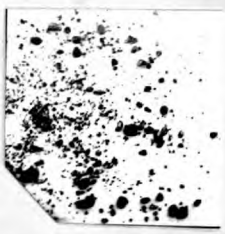
B - actual size



C - magnified 5 X



D - actual size



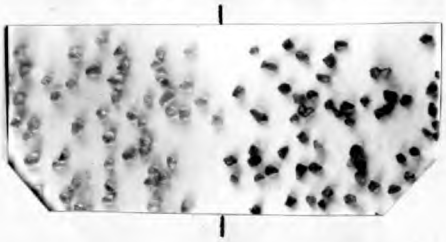
E - actual size



NOTE:- Coal A was conveyed at solid velocities of 30 to 40 ft./sec. only; the other coals were conveyed at 30 to 80 ft./sec.(see section 4.6)

PERSPEX A

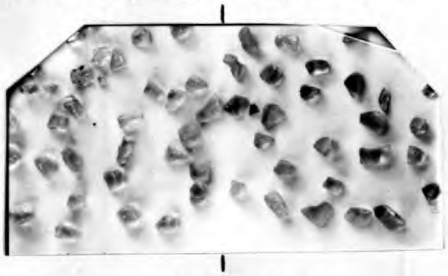
Before Conveying | After Conveying



Actual Sixe

PERSPEX B

Before Conveying | After Conveying



Actual Size

PERSPEX C

After Conveying



Magnified 5 X

POLYSTYRENE

After Conveying



Magnified 5 X

RAPE

Before Conveying



Actual Size

RADISH

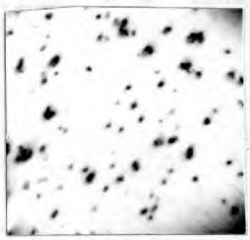
Before Conveying



Actual Size

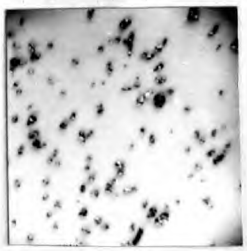
NOTE:- Polystyrene and Perspex A, B and C were very similar in size and size distribution, both before and after conveying.

BRASS
After Conveying



Magnified 5 X

ALUMINIUM
After Conveying



Magnified 5 X

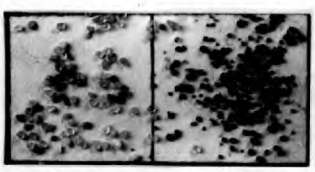
LEAD
After Conveying



Magnified 5 X

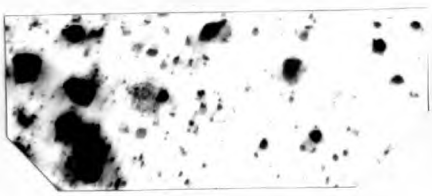
SAND

Before Conveying | After Conveying



Actual Size

MANGANESE DIOXIDE
After Conveying



Magnified 5 X

NOTE:- Brass, Lead, Aluminium and Manganese Dioxide were similar in particle size and size distribution, both before and after conveying.

Chapter 5.

Experimental Observations

5.1. Introduction

It has been found that the characteristics of the pressure gradient in the pipeline are closely associated with the flow pattern of the solids and that both vary with operating conditions. In this chapter, a description is given of the way in which the flow pattern is influenced by the acceleration region, the flow rates of the air and of the solids, the physical properties of the solids and by electrostatic charging. Further, the relationship between the flow pattern and the pressure gradient is discussed with the object of outlining the conditions necessary for obtaining reproduceable and generally significant results.

5.2. Flow patterns

The flow patterns observed in the course of the work are described below. They are classified according to whether or not saltation flow occurs. In the text, "saltation" is used to denote that some particles settle out and come to rest in the pipeline.

The following patterns (a) and (b) are observed when the particles are suspended in the air stream and saltation is absent.

(a) Uniform suspended flow

After entering the air stream, the particles immediately follow trajectories which appear to be parallel to the axis of the pipe. The particles are evenly distributed over the cross-section.

(b) Non-uniform suspended flow

After the particles enter the air stream, their initial trajectories deviate downwards so that the particles hit and bounce off the bottom of the pipe at some point in the acceleration region. Thereafter, the particles become and remain suspended throughout the pipeline and follow trajectories almost parallel to the axis of the

pipe. However, the concentration of the particles is higher at the bottom than at the top of the pipe.

The following four patterns, (c), (d), (e) and (f), are observed when saltation occurs.

(c) Slug flow

Particles settle out in the bottom of the pipe and agglomerate to form dunes which build up until their height is equal to about one half of the pipe diameter; they are then swept downstream en masse.

(d) Plug flow

This may be regarded as a special case of slug flow. It was observed only with large size (0.15") perspex. The particles settle out and agglomerate until they completely block the pipeline. The plug of solids is then swept downstream. The slugs and plugs formed during the conveying of perspex always exhibited intense electrostatic charges.

(e) Dune flow

Stationary dunes build up to a height equal to about one third of the pipe diameter. As a result, the air velocity above the dunes is artificially increased and suspended flow occurs there. The dunes are in a state of dynamic equilibrium with particles continually settling out whilst others are ejected into the air stream in which they are conveyed in suspension.

(f) Bed flow

A dense bed of solids, about one third of the pipe diameter in height, is formed on the bottom of the pipe. In a shallow layer at the free surface of the bed, particles oscillate vigorously as if in a fluidised state. Some particles bounce out of this layer into the air stream above. The particles are there conveyed in suspension because the air velocity is increased as a result of the partial constriction of the bore of the pipe. The bed, when first formed, moves slowly along the pipe, the velocity of the particles increasing from almost zero at the walls to a maximum at the free surface. If the air velocity is decreased sufficiently, the bed becomes stationary, although bouncing continues at the surface and conveying continues above the bed.

5.3. The influence of the acceleration region on the flow pattern in the whole of the pipeline

Suspended flow patterns (a) and (b) can be obtained with all solids provided the air velocity is sufficiently high. The flow pattern persists throughout the whole of the pipeline.

The flow patterns (c), (d), (e) and (f), obtained in saltation flow, are not exhibited by all the solids. Each pattern is initiated at a point in the acceleration region, close to the feed point, where the particles first hit the bottom of the pipe. Whereas pattern (f) develops throughout the whole of the pipeline, patterns (c), (d) and (e) were at no time observed in the equilibrium region. Each of these three patterns in the acceleration region was accompanied by a modified type of the flow pattern (b) in the equilibrium region. The flow of the particles was uneven, however, and they tended to travel in groups of alternately high and low solids' concentration.

5.4. The influence of the flow pattern on the pressure in the pipeline

With the suspended flow patterns (a) and (b) the air pressure at each point along the pipeline remains steady. With the saltation flow patterns (c), (d) and (e) in the acceleration region, the pressure is unsteady throughout the whole length of the pipe. The pressure fluctuations increase in magnitude as the degree of saltation increases. Pressure fluctuations also occur with flow pattern (f) but are much smaller than with the other saltation flow patterns.

5.5. The relationship between the flow pattern and the physical properties of the solids

All solids exhibit the two flow patterns (a) and (b) and the minimum air velocity required to achieve the same degree of suspension increases with the terminal falling velocity of the particle. (A uniform suspended flow pattern was not observed with lead as a sufficiently high air velocity could not be attained in the plant.)

The saltation flow patterns exhibited by each solid are given in table 5.1., which also shows the order in which these patterns set in as the air velocity is decreased. (Table 5.1. is given beside table 4.1.

for convonience in comparing both tables.)

In general, it can be said of the solids investigated that, as the air velocity is decreased after saltation starts thon:-

1. Small particles of high density e.g. aluminium, brass and lead, exhibit slug, dune and bed flow successively.

2. Small particles of low density, e.g. the coals A, B and C, exhibit slug flow and bed flow in turn before blockage occurs.

3. Large particles of low density, e.g. perspex A and B and the coals D and E, exhibit slug and dune flow in turn.

Zenz and Segler both observed that the minimum air velocity required to prevent blockage increased as the feed rate was increased. A similar behaviour is observed in the present work in that, as the feed rate is decreased, each saltation flow pattern sets in at a lower air velocity; this effect is especially noticeable at low air velocities.

5.6. Electrostatic phenomena

In the conveying of sand and manganese dioxide, the flow characteristics change with the duration of conveying. For a given solid's feed rate and air flow rate the pressure drop gradually increases and the solid velocity decreases with time. This behaviour has not been observed with any other material conveyed (although a similar behaviour exists with vegetable seeds due to breakage of the particles). It is attributed to an electrostatic phenomenon which is peculiar to sand and manganese dioxide.

Charges could be detected and measured on the particles and the pipeline during the conveying of all materials. In this respect, sand and manganese dioxide do not appear to be significantly different from other materials. Further, with no material could the magnitude of the charges be related to the measured pressure gradient nor the solid velocity. For all solids, the measurements were independent of whether the pipeline was earthed, insulated or charged from an external source.

Thus, although the measurements and the flow pattern for sand and manganese dioxide change with time as a result of some electrostatic phenomenon, the results presented in appendix 4 for the conveying of other materials do not change with time. Nevertheless, perspex and

polystyrene do exhibit an unusual behaviour which is described in chapter 9 together with the observations on the conveying of sand.

5.7. The characteristics of the pressure gradient in the pipeline

In graph 5.1. are shown some typical results obtained for coal C (average particle size .02"). The pressure gradient measured over each pipe section is plotted against the distance of the mid-point of the section from the feed point for a variety of flow conditions. Close to the feed point, the pressure gradient decreases rapidly with distance in what corresponds to the acceleration region. At greater distances, the behaviour is different at high and low air velocities. At high air velocities, the pressure gradient increases slowly in an approximately linear manner. At low velocities, the pressure gradient follows a wave pattern which is not readily apparent if the results are plotted as the total pressure, or the total pressure drop from the feed point, against distance. This wave behaviour increases in degree with increase in both the feed rate and in the term $\frac{F}{s}$, which is the concentration of particles in the pipeline. Straight lines have been drawn to replace the wave-type curves for low velocities in graph 5.1. These lines are similar to those obtained at high velocities and give the average rate of increase of the pressure gradient throughout the pipeline.

At high feed rates and low air velocities, the pressure gradient for given flow conditions is not accurately reproduceable. Measurements for coal C conveyed at a solid velocity of 49 ft./sec. and feed rates of 19 and 24 lb./min. are shown in graph 5.2. On repeating the experiments, the "amplitude" of the wave-type curve obtained will lie anywhere between the limits shown, although, the mean straight lines are reproduceable within the limits of experimental accuracy for given flow conditions.

The pressure distribution follows a similar pattern for all the materials conveyed and can be directly related to the flow pattern of the solids. In general, the wave behaviour and the pressure fluctuations are not exhibited in suspended flow but set in and increase in magnitude as the degree of saltation increases. Saltation flow and the wave behaviour of the pressure gradient are observed over a wide range of velocities for small particles but over a much narrower range for large particles.

GRAPH 5.1

S = 30.
F = 20.

GRAPH 5.1

S = 70 ; F = 10·4.

S = 60 ; F = 8·4.

GRAPH 5.1.

S = 70 ; F = 20.

S = 60 ; F = 22.

S = 40 ; F = 17·5

S = 30 ; F = 12·2.

S = 40 ; F = 7·12.

GRAPH 5.2.

S = 49 ; F = 24

S = 49 F = 19.

THE MEASURED PRESSURE DROP OVER EACH PIPE SECTION IN CMS. WATER.

DISTANCE FROM THE FEED POINT OF THE MID-POINT OF EACH SECTION.

5.8. The influence of plant defects on the pressure gradient and flow pattern

In the initial stages of the work, an inspection of the "Ermeto" couplings showed that slight eccentricities in the sleeves caused ridges at the shoulders of the couplings and at the ends of the pipe sections between which there were also gaps of up to $\frac{1}{32}$". These gaps were taken up and sand was conveyed continuously for several hours to remove the ridges; the pipe bore was thus well "run in".

Experiments with the 2" pipe sections, used for the purpose of measuring the solid velocity as outlined in section 4.4. showed that, provided these sections are correctly lined up according to the eye, their incorporation in the pipeline had no effect on the measured pressures or on the observed flow patterns, even when the gaps between the ends of the pipe sections were as great as $\frac{1}{8}$". A wave behaviour of the pressure gradient distribution could be induced and the flow pattern changed by deliberately misaligning the 2" sections to an abnormally large degree.

The pressure tubing and tappings were regularly cleaned, blown out and checked for leakages. The manometers and pressure tubing were used in several combinations without effect on the measurements obtained.

It was shown experimentally, that the use of the rotary valve under the conditions outlined in section 3.6. had no influence on the behaviour of the solids or the pressure gradient.

Thus, it can be said that the experimental observations and measurements in the present work are neither caused nor influenced by any defects in the plant nor in the experimental technique.

5.9. Experimental conditions necessary for obtaining generally significant results

The apparently contradictory results in the literature for pressure gradients in pneumatic conveying refer to short sections of pipelines of diameters of 2" or less and have been determined under conditions where the particles entering the pipeline have no initial horizontal velocity component.

The results of the present work for identical conditions in a 1"I.D.

pipeline show that the results for such conditions are likely to be significant only when uniform suspended flow is obtained and when the pipe sections are in the equilibrium region. Otherwise, the results can be expected to be unreliable and non-reproduceable. However, the effect of systematic fluctuations of the pressure gradient in the equilibrium region can be largely eliminated in the present work by measuring over a section of pipe in the equilibrium region of not less than 40 ft. in length. The extent of the acceleration region is best determined by a graphical examination of the pressure distribution as shown in graph 5.1. However, in the present work, the exact length of the acceleration region cannot be determined accurately because relatively few pressure measurements were made close to the feed point. Nevertheless, it is never more than 20 ft. long except for lead in which case it is between 30 ft. and 40 ft. long.

In pipelines with diameters of less than 2" it is considered necessary to make pressure drop measurements over at least 40 ft. of pipeline in the equilibrium region, as indicated above. However, it is probable that these precautions are not so important in pipes of larger diameters or when the solids enter the pipeline with an appreciable velocity component in the direction of flow.

5.10. Presentation of results

The pressure drop over a given section of pipe can be conveniently regarded as being made up of two components, one attributable to the flow of air alone and the other to the presence of solids. The excess pressure drops (Δp_x) presented in appendix 4 have all been determined for the section of pipe between 40 ft. and 110 ft. from the feed point. The pressure drop attributable to the flow of air itself during conveying is calculated using the Fanning friction equation 2.9. and the pressure measured at the mid-point of the section. The pressure in the pipe fluctuates at low velocities, especially at high feed rates, but the effect in the calculation of the air friction pressure drop and the air velocity is small because the maximum variation, as seen in graph 5.1, is only 5 cm. of water on a total pressure of between 80 and 120 cm. of mercury, that is about 0.4%.

If the calculated pressure gradient for air flow during conveying

is plotted on graph 5.1., then it gives a straight line with a slope equal to that of the corresponding line for the total measured pressure gradient. This indicates that within the limits of experimental accuracy the excess pressure gradient (the difference between the total measured and the calculated air pressure gradients) is constant over the equilibrium region for any given flow conditions.

Details of the experimental results and data are presented in appendix 4.

In the conveying of all the materials, the accuracy and reproduceability of the data are not significantly influenced by defects in either the experimental technique or the construction of the plant which is operating on a continuous recycling process. However, as further discussed in chapter 9, electrostatic effects influence the measurements in the conveying of sand and manganese dioxide and of perspex and polystyrene at the lowest conveying velocities.

The experimental data have been used to obtain the best correlation between the variables. In addition, the flow pattern of the solids, the effect of attrition on the size of the particles and the physical properties of the particles have been taken into account.

The best correlation found for the solid velocity and the pressure drop during conveying are outlined in chapters 6 and 7 respectively. Other methods of correlation are discussed in chapter 8. The characteristics of the electrostatic phenomenon in the conveying of sand and manganese dioxide are then discussed in chapter 9.

Chapter 6.

Solid Velocities

The measured solid velocities are presented in appendix 4 and are shown plotted against the air velocity for various feed rates in graphs 6.1 to 6.15, in appendix 5. The solid velocities of sand and manganese dioxide decreased with time and are discussed, in more detail, in chapter 9; the text of this chapter does not refer, in general, to these materials, except where specified.

6.1. The general behaviour of the velocity ratio

The variations in both the velocity of the air relative to the particles and the ratio of the particle velocity to the air velocity have been examined and it has been found that the former is easier to interpret and is more useful for classifying the solids and for correlating the measurements of solid velocities.

For all materials, the velocity ratio increases with air velocity and, except for lead, becomes constant at high air velocities; it is probable that the same behaviour would have been observed with lead if higher air velocities could have been used. For a given material, the variation of the velocity ratio over the range in air velocity used is a function of the falling velocity of the solid. For instance, it increases from 0.87 to 0.89 in the case of polystyrene (falling velocity = 5.3ft./sec.) and increases from 0.5 to 0.75 for lead (falling velocity = 26.8ft./sec.).

Although it is, theoretically, impossible for both the relative velocity and the velocity ratio to remain constant as the air velocity is changed, they are approximately so, for most solids at high air velocities, within the limits of experimental error.

6.2. Classification of the solids in terms of the relative velocity

From graphs 6.1 to 6.15, it can be seen that at high air velocities the relative velocity of each solid is constant and is independent of the air velocity and the feed rate.

At low air velocities the various solids behave in different ways and they can be classified, depending on the behaviour of the relative velocity, in the following manner.

Class A

The relative velocity of the solids in Class A, viz., lead, polystyrene, perspex B and C, unbroken rape and radish seeds and brass, remains constant and equal to the value obtained at high air velocities. Therefore, the relative velocity of solids in Class A remains constant for all flow conditions. This behaviour applies to vegetable seeds only before they break up and to sand only before the wall effect builds up (ref. chapter 9). The results for materials in Class A are shown in graphs 6.1 to 6.8.

Class B

For the solids in Class B, viz., coals D and E and perspex A, the relative velocity (graphs 6.9 to 6.11) is constant at low velocities and is independent of the air velocity and the feed rate. It is, however, between 2 and 4 ft./sec. higher than the constant value of the relative velocity at high air velocities. Thus, the relative velocity changes in an apparently abrupt manner, at some air or solid velocity but the critical values cannot be exactly determined from the present results.

Class C

The solids in Class C, viz., coals A, B and C and aluminium, behave similarly to those in Class A only at very low feed rates i.e. the relative velocity is constant. At higher feed rates, the relative velocity, at constant solid velocity, increases with the feed rate. As the solid velocity increases, the difference between the relative velocity at high and low feed rates progressively diminishes as can be seen in graphs 6.12 to 6.15. It would appear that the relative velocity depends in some manner on the volume of solids or the number of particles per unit volume of the pipe.

6.3. The effects of breakdown of particles

After the first experiments on the conveying of rape and radish seeds, the particles began to break up as described in section 4.6, and the relative velocity increased with the duration of conveying as a result of the change in the physical properties of the material.

However, the first experiments with the seeds were carried out at low air velocities, at which a feed rate effect would be most noticeable, and the results are seen to be independent of the feed rate; this indicates that unbroken rape and radish seeds fall into Class A.

Coals also broke up quickly during conveying but in a different manner from vegetable seeds (see section 4.6.). No definite effect on the relative velocity could be detected, although, some results indicate that the relative velocity decreases slightly as the particles break down. This behaviour is to be expected from the correlation given later in this chapter (graph 6.16) which predicts that the relative velocity increases with the falling velocity of particles.

6.4. Effect of physical properties of particles on the relative velocity

It has been shown that the solids can be divided into three groups according to the behaviour of the relative velocity. This classification of the solids can be related approximately to the physical properties of the particles. With the exception of perspex A and lead, the following generalisations apply.

Class A

Each solid in Class A has a size distribution factor of less than 3 (the ratio of the largest to the smallest size of the particles) if the existence of a very small amount of dust is neglected.

Class B

Coals D and E in Class B have a large size distribution from dust upwards and an average particle size of .04" or more.

Class C

Each solid in Class C has a large size distribution from dust upwards and an average particle size of .03" or less.

Lead and perspex A have, so far, been excluded from the classification. The lead shot used has a seven-fold size range but the smaller particles are relatively few in number and, if these are ignored, the effective size distribution would be two-fold and it is thus reasonable to include lead in Class A.

It is not unreasonable to expect the behaviour of solids in Class B to be intermediate between that of the solids in Classes A and C i.e.

the variation of the relative velocity with feed rate should be smaller than that for solids in Class C; however, any such variations would be small and difficult to detect from the present results. The results for perspex A appear to be anomalous; judged on the behaviour of the relative velocity, perspex A falls into Class B, but, judged on its size distribution factor of 2, it would be expected to fall into Class A. From the correlation of results described in the following section, it is found that only coals D and E fall into Class B; perspex A falls into Class A but its behaviour is influenced by electrostatic charges.

Thus, in the absence of electrostatic effects the behaviour of the relative velocity depends on the size and size distribution of particles. For solids with a size distribution ratio of 3 or less (ignoring up to 5% of the smallest particles) the relative velocity is constant for all flow conditions (Class A). For solids with a wide size distribution from dust upwards, the relative velocity changes with the concentration of particles in the pipeline, the change being marked for solids with an average particle size of less than 0.04" (Class C), but very small for larger particles (Class B).

6.5. Correlation of the solid velocity

A number of attempts were made to relate the relative velocity to the properties of particles; the most satisfactory procedure is outlined below. The relative velocities are, unfortunately, much less accurate than the solid and air velocities and are the limiting factors affecting the reliability of the correlation.

Solids in Class A

The relative velocity of solids in Class A is approximately proportional to the falling velocity and may be correlated by the equation

$$(u - s) = 1.3 s_o \qquad 6.1.$$

but the constant of proportionality in the above equation varies between 1 and 1.6 according to the properties of the solid.

The results are better correlated by plotting the ratio of the falling velocity to the relative velocity against the square root of the ratio of the falling velocity to the density of particles, as shown

in graph 6.16. It is seen that all the solids in Class A, except brass, are well correlated on the graph and their relative velocity can be calculated from the equation

$$(u - s) = \frac{s_o}{.468 + \sqrt{s_o/w}} \qquad 6.2.$$

to within ± 5% using measured values of the falling velocity, So, and the density, w. However, individual measurements of the relative velocity vary by ± 3ft./sec. from this calculated value.

The results for brass do not agree well with equation 6.2, probably, because of the feather-like shape of the particles. No effect of particle shape on the relative velocity has been detected with the other materials.

Solids in Class C

All the results for solids in Class C can be correlated by plotting the relative velocity against the term $\frac{F}{s}$ as shown in graph 6.17. It is found that the value of the relative velocity, extrapolated to $\frac{F}{s} = 0$, can be calculated by means of equation 6.2. The points shown on graph 6.16 for solids in Class C have been determined by using the values of the relative velocity for $\frac{F}{s} = 0$.

Thus, the relative velocity of solids in Class C, for all flow conditions, can be calculated from the equation

$$(u - s) = \frac{s_o}{.468 + \sqrt{s_o/w}} + \frac{1770}{s_o}\frac{F}{s} \qquad 6.3.$$

to within 5ft./sec. of individual measured values. It is seen that equation 6.3 reduces to equation 6.2 for $\frac{F}{s} = 0$.

Solids in Class B

It is seen from graphs 6.9, 6.10 and 6.11 that the relative velocity of solids in Class B apparently changes abruptly at some air velocity; the average of the values at low and high air velocities is 12 and 15 ft./sec. for coals D and E, respectively.

The relative velocity of coals D and E is apparently independent of $\frac{F}{s}$ and has an arithmetic mean value of 13. and 15ft./sec. for coals D and E, respectively; these values of the relative velocity have been used to determine the points for coals D and E shown in graph 6.16.

It is considered that the characteristics of coals D and E are intermediate between those of solids in Classes A and C but the difference between the relative velocity at low and high loadings cannot be detected in the present results because it is of the same

order as the experimental error. In the absence of more accurate measurements, the relative velocity of coals D and E may be calculated using equation 6.2 to within $\pm$ 4ft./sec.

Although the characteristics of perspex A are apparently identical to those of solids in Class B i.e. coals D and E, it is shown below that this is not the case and that perspex A does not fall into Class B.

Porspex A

Judged on their size distribution ratio of 2, perspex C (average size .03"), perspex A (.06") and perspex B (.15") should fall into Class A and thus their relative velocity should be constant and independent of flow conditions.

It is found that the relative velocity of large sized perspex (B) is independent of $\frac{F}{S}$; that of intermediate sized perspex (A) depends on $\frac{F}{S}$ (graph 6.18) but in a different manner from that of solids in Class C; there are insufficient measurements of the feed rate for small sized perspex (C) to determine the relationship between $\frac{F}{S}$ and its relative velocity.

It is seen from graph 6.18 that, for values of $\frac{F}{S}$ above .007 lb/ft, the relative velocity of perspex A is constant and may be calculated using equation 6.2 i.e. as for solids in Class A; this value of the relative velocity has been used to determine the point for perspex A in graph 6.16. For smaller values of $\frac{F}{S}$ the relative velocity may be calculated from the equation

$$(u - s) = 10 - 675 \frac{F}{S} \quad \text{in f.p.s. units.} \qquad 6.4.$$

to within $\pm$ 5ft./sec.

It will be seen in the following chapter that this variation of the relative velocity of perspex is associated with anomalous values of the pressure drop in the pipeline.

It is suggested that the anomalous behaviour of perspex A is due to an electrostatic effect which is fundamentally different from that exhibited by sand and manganese dioxide (described in chapter 9). Judged by their size distribution, both perspex A and sand fall into Class A. The relative velocity of perspex A is the same as the predicted value only at high loadings and decreases with the loading but is independent of the time of conveying. That of sand is the same as the predicted value only at the start of conveying and increases with the time of conveying; when steady values are obtained, it increases as

the loading decreases.

Although polystyrene is similar in structure to perspex, it does not exhibit a similar behaviour. However, Hinkle's measurements of the relative velocity of polystyrene (similar in size to that used in the present work) conveyed in a glass pipeline are several times greater than those made in the present work using a brass pipeline. The possibility that Hinkle's measurements were made in the acceleration region, close to the equilibrium region, cannot, alone, explain such large differences in measurements. Therefore, the relative velocity can be influenced by electrostatic charges and may depend on the nature of the solids and the pipeline.

6.6. Conclusions

The relative velocity during conveying depends, primarily, on the size and size distribution of the particles and, probably to a lesser extent, on the electrical properties of the particles and the pipeline.

In the absence of electrostatic effects, solids can be classified and the relative velocity can be predicted as follows.

Solids in Class A have a size distribution ratio of 3 or less and the relative velocity of such solids is constant for all flow conditions and can be calculated from equation 6.2 using measurements of the falling velocity and the density of particles.

Solids in Class C have a large size distribution from dust upwards and an average particle size of less than .04". The relative velocity depends on the particle concentration and can be calculated from equation 6.3. For loadings less than about .015 cu.ft.solids/cu.ft.pipe the relative velocity is constant and equal to the value given by equation 6.2 for Class A solids.

The solids in Class B have a large size distribution from dust upwards and an average particle size of .04" or more. The relative velocity is about 1 ft./sec. greater than the value determined from equation 6.2 for high loadings and about 1 ft./sec. less for low loadings.

Particle Shape

The value but not the behaviour of the relative velocity of brass appears to depend on the unusual shape of the particles.

Electrostatic Effects

The relative velocity for perspex A in a brass pipeline is given by the relation for Class A solids at high loadings. At low loadings, however, it decreases with particle concentration and may be calculated from equation 6.4.

The influence of electrostatic charges on the relative velocity when conveying sand is fundamentally different from that in the conveying of perspex A and is discussed in detail in chapter 9.

A greater accuracy in measuring the relative velocity is required in order to determine the influence of electrostatic effects on the relation between the relative velocity and the size, shape, density, size distribution and falling velocity of the particles.

Chapter 7.

Correlation of Pressure Drops

Attempts have been made to correlate the measured pressure drops obtained during conveying using various methods suggested in the literature. In addition, a number of equations were developed on the basis of both theoretical and empirical considerations and their usefulness was examined. The most satisfactory correlation obtained is of an empirical nature and is outlined in this chapter. The experimental results used in the correlation are those obtained over a relatively long section of pipe remote from the feed point (the section between 40 ft. and 110 ft. from the feed point) in order that the effects of solid acceleration and pressure variations along the pipeline are minimised. Details of the less satisfactory correlations which were obtained are omitted.

The text of this chapter does not, generally, refer to the results for sand, which change with the time of conveying; however, where specifically mentioned, the results obtained at the start of conveying sand have been included.

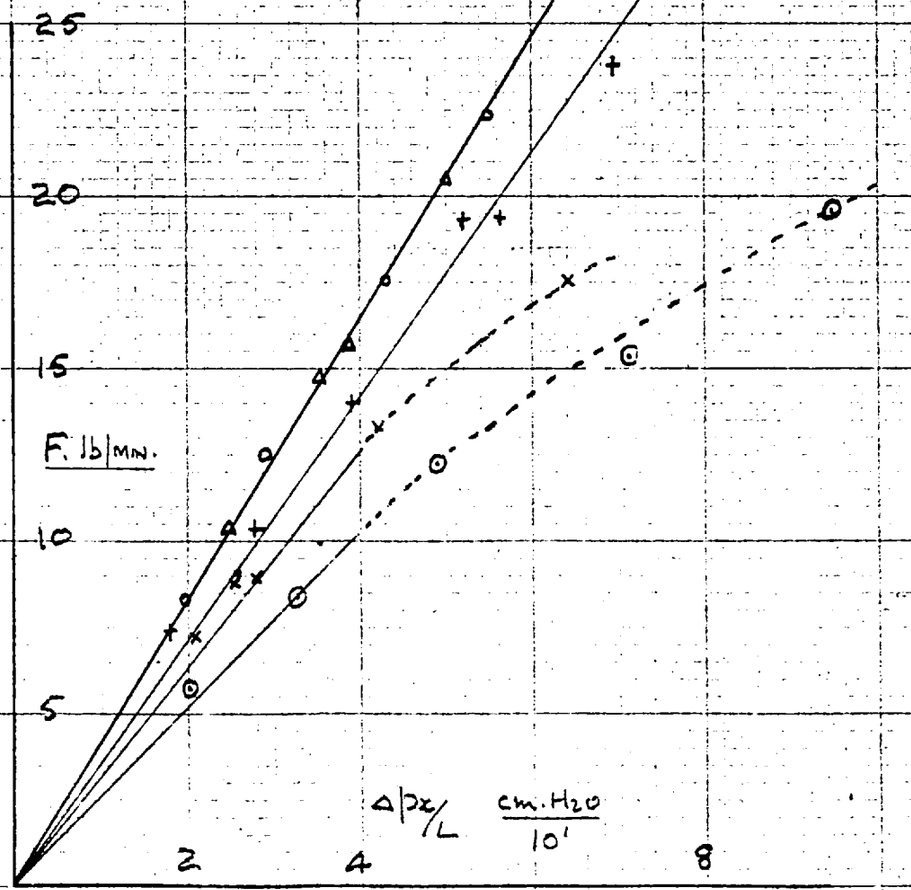
The experimental results are most conveniently expressed in terms of the excess pressure drop, Δp_x, which is determined by subtracting the air pressure drop during conveying, Δp, calculated by means of the Fanning equation 2.9, from the measured pressure drop, ΔP, (sections 4.3 and 5.10).

A typical relationship between the excess pressure drop and the feed rate, F, is as shown in graph 7.1, which refers to coal C. It is seen that the relationship for each solid velocity is linear except that at low solid velocities there is a divergence from the linear relationship at high feed rates. The extent of this divergence varies from material to material; in general, it is largest with materials which have a wide size distribution and which contain a large quantity of dust and when the solid velocity is near to the minimum conveying velocity (i.e. near blockage conditions).

RESULTS FOR COAL C.

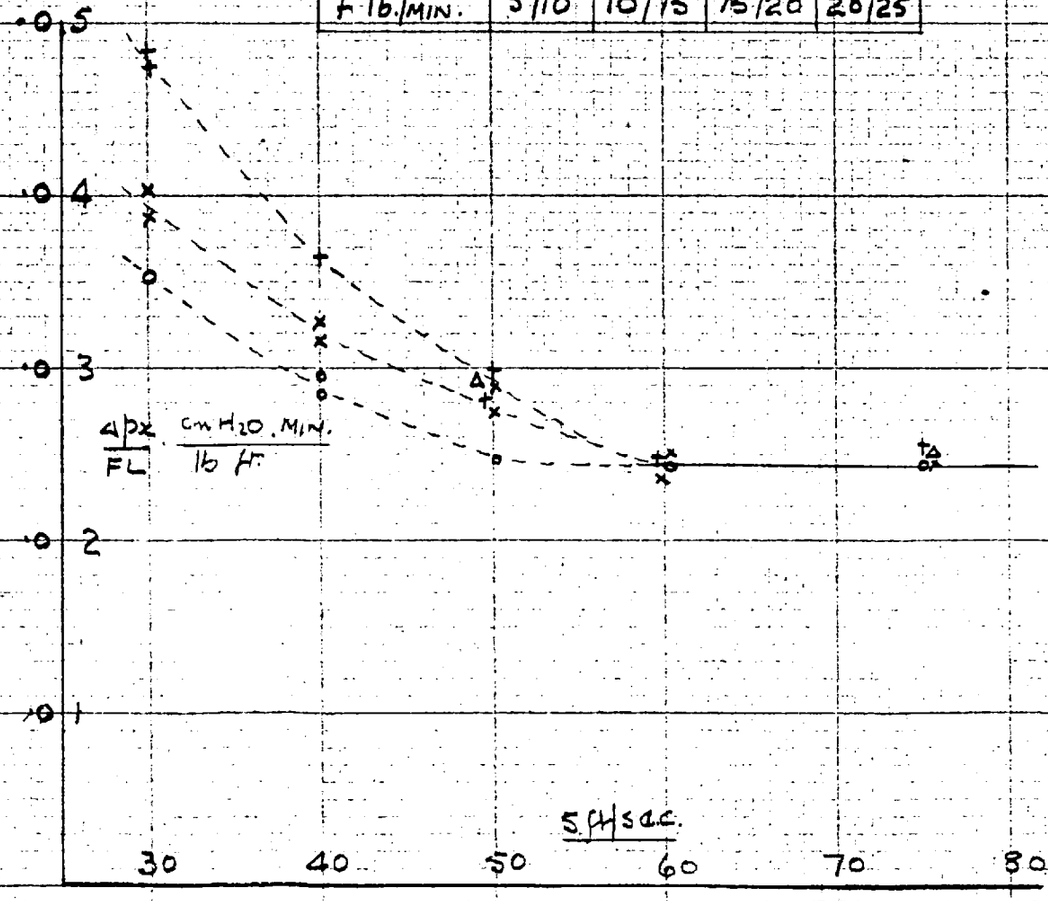
GRAPH 7.1

	⊙	×	+	○	△
S ft./sec.	30	40	50	60	75



GRAPH 7.2.

	○	×	+	△
F lb./min.	5/10	10/15	15/20	20/25



The relationship between the term, $\frac{\Delta p_x}{FL}$, and the solid velocity for coal C can be seen in graph 7.2. The term $\frac{\Delta p_x}{FL}$ increases with the feed rate at low solid velocities but to a progressively smaller extent as the velocity increases; at high velocities, $\frac{\Delta p_x}{FL}$, becomes constant and independent of the feed rate. In general, it can be said that $\frac{\Delta p_x}{FL}$ decreases as the particles become more uniformly suspended and approaches a constant value for a given material at high solid velocities; at low solid velocities, $\frac{\Delta p_x}{FL}$ increases with feed rate for solids in Class C and, to a smaller extent, for solids in Classes A and B. A comparison of graph 7.2 with similar graphs obtained for coals by Mitlin shows the advantage of the experimental technique used in the present investigation. The behaviour of the term $\frac{\Delta p_x}{FL}$ cannot be easily determined from Mitlin's results because of experimental error; his pressure drops were measured over only 10 ft. of pipeline and the effect of the cyclic behaviour of the pressure gradient in the pipeline was, therefore, apparent; furthermore, the feed rate could not be progressively increased at a constant solid or air velocity during the experiments.

An examination of the manner in which $\frac{\Delta p_x}{FL}$ varies with the other parameters shows that $\frac{\Delta p_x}{\Delta p F}$ is inversely proportional to the square of the solid velocity. No other linear relationship between the parameters and Δp_x or the measured pressure drop was obtained.

The relationship between $\frac{\Delta p_x \, s}{\Delta p}$ and $\frac{F}{s}$ is shown for each material, including seeds before disintegration occurred, in graphs 7.3 to 7.16. This method of plotting is most convenient because for each material, the plot should pass through the origin since $\Delta p_x = 0$ when $F = 0$. In each of graphs 7.3 to 7.16, all but a few points fall on a straight line to within $\pm 15\%$ (of the same order as experimental error). For all materials, except perspex, the lines pass through the origin showing that $\frac{\Delta p_x \, s}{\Delta p}$ is directly proportional to $\frac{F}{s}$; the results can be correlated by plotting the mean value of $\frac{\Delta p_x \, s^2}{\Delta p \, F}$ for each material against the reciprocal of the falling velocity as shown in graph 7.19.

The results for all materials except sand, perspex and broken vegetable seeds can thus be expressed by the equation obtained from graph 7.19, i.e.

$$\frac{\Delta p_x \, s^2}{\Delta p \, F} = \frac{45{,}000}{s_0} \qquad \text{in f.p.s. units} \qquad 7.1.$$

Sand

The results obtained for sand at the start of conveying give an average value of 66 for the term $\frac{\Delta px}{\Delta p}\frac{s^2}{F}$ and this value has been used in plotting the point on graph 7.19. This point lies close to the line for other materials and, therefore, equation 7.1 is also applicable to sand at the start of conveying before the measurements have been appreciably affected by electrostatic charges which build up with the time of conveying.

Perspex

The results for perspex, which are plotted on graphs 7.5, 7.15 and 7.16, show that when $\frac{\Delta px}{\Delta p}$ s = 0, the term $\frac{F}{s}$ appears to have a finite value which increases as the size of perspex decreases.

The results for the three sizes of perspex are expressed by the equation

$$\frac{\Delta px}{\Delta p}\frac{s^2}{F} = \frac{45000}{s_o} - \frac{37.7}{s_o}\frac{s}{F} \text{ in f.p.s. units} \qquad 7.2.$$

to within ± 15%. The points for perspex, shown on graph 7.19, are those obtained using the slope of the lines in graphs 7.5, 7.15 and 7.16 (represented by equation 7.2). If the slopes of the best lines passing through the origin are used, the points obtained do not fall close to those obtained for the other materials indicated in graph 7.19.

It has been shown in chapter 6 that anomalous values of relative velocity are obtained for perspex A; these, together with the anomalous values of pressure drops, are considered to be caused by an electrostatic effect fundamentally different from that exhibited by sand (discussed in chapter 9).

At high loadings (i.e. large values of $\frac{F}{s}$) equation 7.2 reduces to equation 7.1; therefore, under those conditions, the pressure drop for perspex is the same as for materials which do not exhibit electrostatic effects. As $\frac{F}{s}$ decreases, the measured pressure drop for perspex becomes smaller than the expected value by an amount which is proportional to $\frac{s}{F}\frac{1}{s_o}$, (equation 7.2).

The behaviour of the relative velocity for perspex A follows a similar pattern; the results shown in graph 6.18 can be represented by the equation

$$(u - s) = \frac{s_o}{.468\sqrt{s_o/w}} - \frac{.092}{s_o}\frac{s}{F} \text{ in f.p.s. units} \qquad 7.3.$$

for the range in $\frac{F}{s}$ investigated just as well as by equation 6.4.

Thus, at high values of $\frac{F}{s}$ equation 7.3 reduces to equation 6.2 (i.e. that for solids in Class A which do not exhibit electrostatic effects). As $\frac{F}{s}$ decreases, the measured value of the relative velocity for perspex A becomes less than would be predicted from equation 6.2 by an amount proportional to $\frac{s}{F\ s_0}$.

Equation 7.3 predicts that the effect becomes smaller as the falling velocity increases; no effect on the relative velocity can be detected with perspex B which has a higher falling velocity than perspex A. Insufficient measurements have been obtained with perspex C, which has a smaller falling velocity than perspex A, to assess the applicability of equation 7.3.

The results of Segler and Gasterstadt

The data of Segler and Gasterstadt, obtained for the conveying of wheat, have been used to investigate the general usefulness of equation 7.1. Unfortunately, the solid velocities measured by Segler are considered to be rather inaccurate, for reasons already given, (section 1.3) and those measured using a photographic method, by Gastestadt, refer to only one air velocity but a number of feed rates. Gasterstadt's results show that the relative veloicty for wheat is 15 ft./sec and is constant over the range of feed rates investigated.

This value of the relative velocity of wheat has been used, together with the data of Segler and Gasterstadt, to determine the values of $\frac{\Delta p_x\ s}{\Delta p}$ and $\frac{F}{s}$ which are shown plotted in graphs 7.17 & 7.18.

The data of Segler are consistent with equation 7.1, provided that a different value of the numerical constant is used for each pipe diameter (2", 4", 12", 16" diameters); in this work, pressure drops were measured over a long length of pipeline remote from the feed point. Gasterstadt made his measurements over the whole plant, which consisted of two 150 ft. lengths of pipelines of internal diameters 3.5" and 3.75" respectively, connected by a return pipe bend. The results include effects due to acceleration of air and solids, a pipe bend and a change in pipe diameter. This, no doubt, explains why the results of Gasterstadt do not agree well with equation 7.1; his results, shown in graph 7.18, show that $\frac{\Delta p_x\ s^2}{\Delta p\ F}$ increases with the velocity and suggest that $\frac{\Delta p_x\ s^{1.5}}{\Delta p\ F}$ is constant.

GRAPH 7.19.

CORRELATION

$$\frac{\Delta p_x \, S^2}{\Delta p \, F} = \frac{750}{S_0}$$

$\frac{\Delta p_x \, S^2}{\Delta p \, F}$ $\frac{ft^3 \ min.}{Sec^2 \ lb}$

120
100
80
60
40
20
0

SAND.

POLYSTYRENE.
COAL C.
PERSPEX C
COAL B.
COAL A
COAL D
ALUMINIUM
COAL E
PERSPEX A
BRASS
RADISH
PERSPEX B
RAPE
LEAD

$1/S_0$ Sec/ft.

0 · 04 · 08 · 12 · 16 · 2

SEGLER'S DATA - WHEAT GRAPH 7.20.

x - SEGLER

o - CALCULATED FOR WHEAT IN 1" I.D. PIPELINE

$\frac{\Delta p_x \, S^2 \, S_0}{\Delta p \, F}$ $\frac{ft^3 \ min.}{Sec^2 \ lb}$

700
600
500
400
300
100

PIPE DIAMETER INCHES.

0 4 8 12 16

BRITISH MADE

Other data in the literature cannot be expressed as a plot of $\frac{p_x s}{\Delta p}$ versus $\frac{F}{s}$ either because solid velocity measurements are not given or because the effects of acceleration of the particles are significant. The data of Mitlin and other workers in this department show approximate agreement with equation 7.1; a wide scatter is obtained when $\frac{\Delta p_x s}{\Delta p}$ is plotted versus $\frac{F}{s}$, using their results because the measurements of solid velocity are insufficiently accurate and the pressure gradient was determined over only a 10 ft. length of pipe. The usefulness of the other methods of correlation which have been used is discussed in chapter 8.

Pipe diamter

The effect of pipe diameter has not been investigated in the present work. However, the results of Segler have been plotted in graph 7.20 to show the effect of pipe diameter. Since wheat has a size distribution of less than 2, and probably does not give rise to electrostatic effects in a steel pipeline, the relative velocity should be given by the equation for solids in Class A, i.e. $(u - s) = \frac{s_o}{.468 - \sqrt{s_o/w}}$

Using the relative velocity of 15 ft./sec. for wheat, as obtained by Gasterstadt, the falling velocity is found to be 13.5 ft./sec. Using this value and Segler's data plotted in graph 7.17, the term $\frac{\Delta p_x s^2 s_o}{\Delta p \ F}$ has been calculated and plotted against the pipe diameter in graph 7.20. Equation 7.1 predicts that the above term should be constant for all materials in a given pipeline in the absence of electrostatic effects. The value obtained in the present work for a 1" I.D. pipeline is also plotted in graph 7.20.

Conclusions

In the absence of electrostatic effects, the experimental results for pressure drop during conveying can be correlated by equation 7.1 to within $\pm$ 15%.

The results of Segler indicate that an equation of the form of 7.1 is applicable for pipes of different sizes and that the constant in equation 7.1 decreases as the pipe diameter increases, in the manner shown in graph 7.20.

Two different effects have been observed which have been attributed

to electrostatic charges.

1. With perspex, both the pressure drop and the relative velocity are smaller than the values predicted by equations 7.1 and 6.2 and the divergence becomes more marked as the particle concentration decreases. The measurements are reproducible and apparently independent of the time of conveying and can be correlated by equations 7.2 and 7.3.

2. With sand and manganese dioxide, the pressure drop and the relative velocity both increase with the time of conveying, and the values predicted by equations 7.1 and 6.2 are obtained only at the start of conveying of these materials; the effect increases as the particle concentration decreases. This behaviour is quite different from that of perspex and is discussed in detail in chapter 9.

The correlations given in this chapter apply to the conveying of solids in the equilibrium region over a wide range in flow conditions, including saltation flow, but they are not applicable to bed flow.

Chapter 8.

Comparison of Correlation Methods used in the Literature.

8.1. Introduction

It is very difficult to compare most of the results presented in the literature with those from the present work because,

(a) some results are significantly influenced by effects due to solid acceleration;

(b) others refer to very short sections of pipeline and are not generally significant because of the cyclic behaviour of the pressure gradient;

(c) the pressure drop due to air flow has been calculated in different ways;

(d) few measurements of the solid velocity have been presented and they have usually been measured in separate experiments from those in which pressure drops were measured.

However, a comparison of results and methods of correlation is given in this chapter primarily to emphasise the importance of observing the experimental conditions outlined in chapter 5 which are regarded as necessary for obtaining significant measurements. Furthermore, the pressure and velocity of the air existing during conveying must be used for calculating the pressure drop attributable to air friction.

8.2. Calculation of the excess pressure drop

In addition to the method used in chapter 7, two other methods, outlined in section 2.2, have been used in the literature for calculating the pressure drop due to air flow (and hence the excess pressure drop) during conveying. These two pressure drops are those which would exist if the air flow during conveying were to pass through the same pipeline in the absence of solids at either the same velocity or at the same mass flow rate as that existing during conveying. They are denoted by the symbols $\Delta p'$ and Δp^{+} , respectively, to differentiate them from

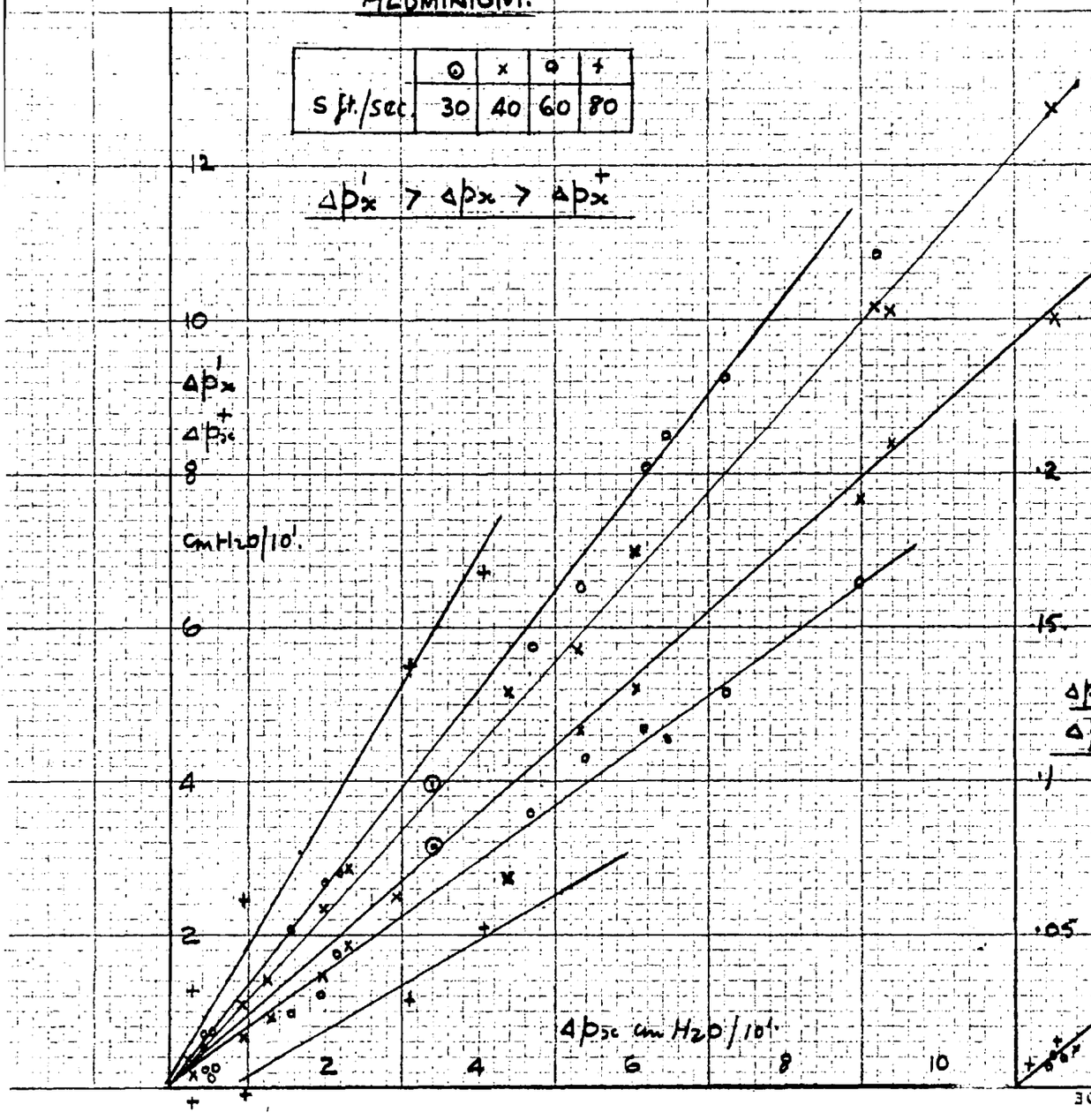
Results For Aluminium.

Graph 8.1

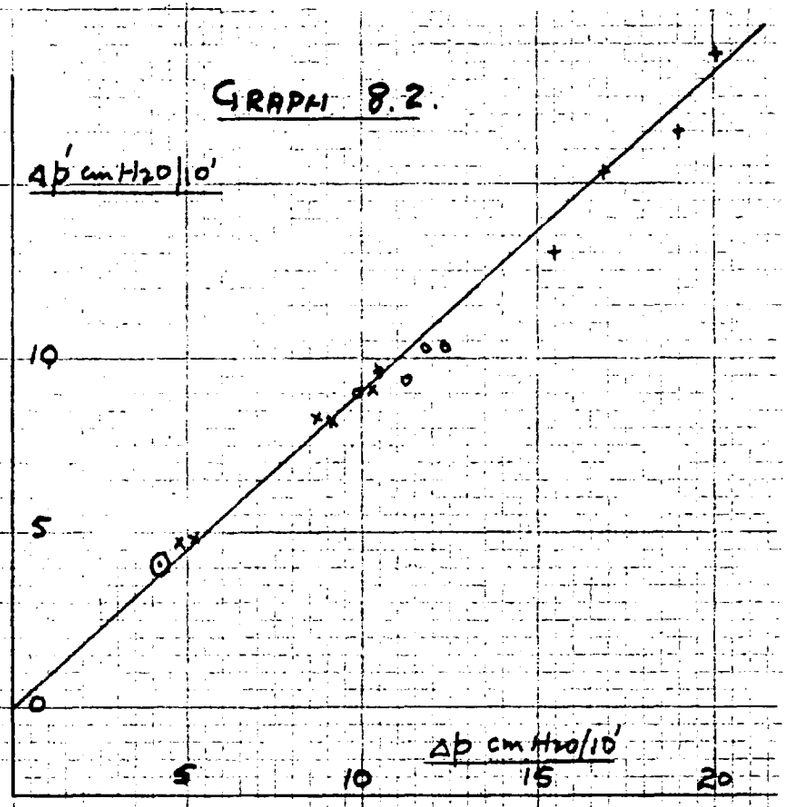
Aluminium.

	⊙	×	○	+
s ft./sec.	30	40	60	80

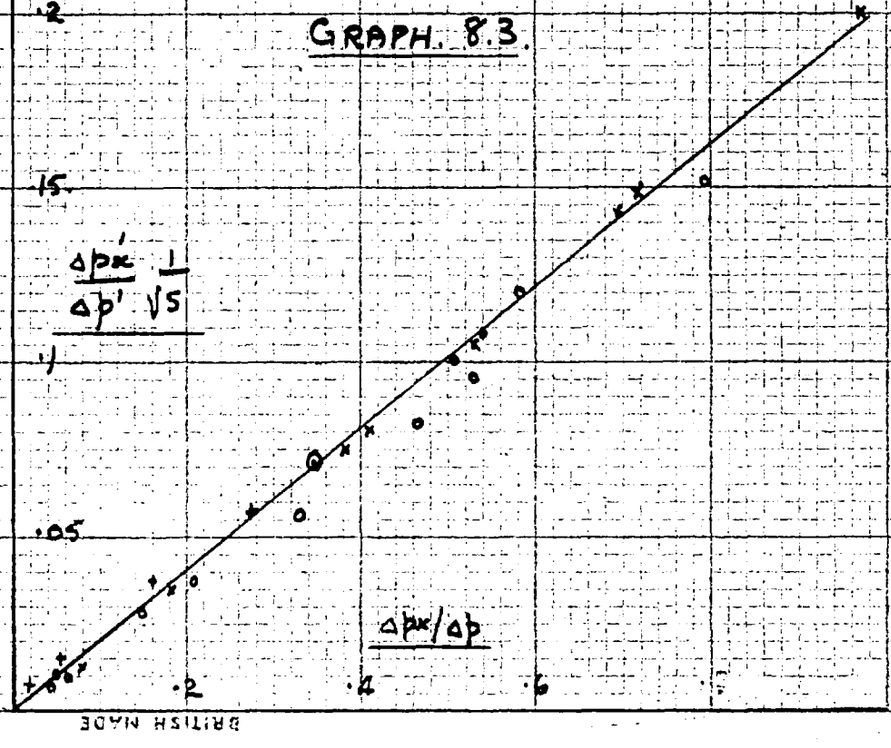
$\Delta p'_x > \Delta p_x > \Delta p^+_x$



Graph 8.2.



Graph. 8.3.



BRITISH MADE

Δp , the air pressure drop during conveying calculated from the Fanning equation 2.9, which is used in the correlations presented in chapter 7. The symbols $\Delta p_x^!$ and Δp_x^+ are used to denote the corresponding values of the excess pressure drop. However, to avoid confusion, no such differentiation in symbols was made in chapter 2, where the equations used by various authors are presented.

The results from the present work have been used to calculate $\Delta p^!$, Δp^+, $\Delta p_x^!$, Δp_x^+, $\frac{\Delta p_x^!}{\Delta p^!}$, $\frac{\Delta p_x^+}{\Delta p^+}$.
In general, it has been found that, approximately,

$$\Delta p^! \propto \Delta p \propto \Delta p^+ \qquad 8.1.$$

$$\Delta p_x^! \geq \Delta p_x \geq \Delta p_x^+ \qquad 8.2.$$

$$\frac{\Delta p_x^!}{s^n} \propto \Delta p_x \propto \Delta p_x^+ . s^n \qquad 8.3.$$

$$\frac{\Delta p_x^!}{\Delta p^! s^n} \propto \frac{\Delta p_x}{\Delta p} \propto \frac{\Delta p_x^+ s^n}{\Delta p^+} \qquad 8.4.$$

for all flow conditions, where n varies between 0.5 and 1.5, according to the properties of the solids.

For example, the results for aluminium have been plotted as

$\Delta p_x^!$ and Δp_x^+ against Δp_x in graph 8.1,

as Δp against $\Delta p^!$ in graph 8.2

and as $\frac{\Delta p_x^!}{\Delta p^! \sqrt{s}}$ against $\frac{\Delta p_x}{\Delta p}$ in graph 8.3.

No satisfactory general correlation of pressure drops in the present work was obtained using either $\Delta p_x^!$ or Δp_x^+ instead of Δp_x and without incorporating the solid velocity. Although such correlations may be very convenient for practical design purposes, they have no general significance in a positive pressure plant; a comparison of Gasterstadt's results indicates that the behaviour of $\Delta p_x^!$ and Δp_x^+ also depends on the type of plant used.

8.3. Gasterstadt's correlation

Gasterstadt measured pressure drops over the whole of the pipeline which consisted of two 150 ft. lengths of 3.5" and 3.75" I.D. pipes; therefore, his results contain acceleration and other effects and are not precisely comparable with the present results. However, a qualitative comparison shows that $\frac{\Delta p_x}{\Delta p}$ does not depend on the type of plant, whereas, $\frac{\Delta p_x^!}{\Delta p^!}$ and $\frac{\Delta p_x^+}{\Delta p^+}$ do.

The present results show that in a positive pressure plant, $\Delta p' < \Delta p < \Delta p^+$; however, Gasterstadt's results for a reduced pressure plant show that $\Delta p' > \Delta p > \Delta p^+$ In the former case, the total pressure is atmospheric at the downstream end of the plant and, in the latter case, at the upstream end. This relation exists because, when solids are added to an air stream, the mass rate of which is maintained constant, the pressure is increased at all points in a positive pressure plant but is decreased in a reduced pressure plant.

Gasterstadt's correlation equation 2.7 shows that, in a suction plant,

$$\frac{\Delta p_x^+}{\Delta p^+} = r \tan\theta \qquad 8.5.$$

$$\propto \frac{F}{\rho u} \tan\theta \qquad 8.6.$$

where $\tan\theta$ decreases as the velocity increases and becomes constant at high velocities. As the air velocity, u, is approximately proportional to the solid velocity, s , then $\frac{\Delta p_x^+}{\Delta p^+} \propto \frac{F}{s}$ at high velocities. On the other hand, an examination of his results plotted on graph 7.18 shows that, approximately, for all flow conditions,

$$\frac{\Delta p_x}{\Delta p} \propto \frac{F}{s^{1.5}} \qquad 8.7.$$

The present results show (equation 7.1) that in a positive pressure plant

$$\frac{\Delta p_x}{\Delta p} \propto \frac{F}{s^2} \qquad 8.8.$$

From relationship 8.4, for a positive pressure plant,

$$\frac{\Delta p_x^+}{\Delta p^+} \propto \frac{\Delta p_x}{\Delta p\, s} \qquad 8.9.$$

assuming an average value of n = 1.

Therefore, from 8.9 and 8.8,

$$\frac{\Delta p_x^+}{\Delta p^+} \propto \frac{F}{s^3} \qquad 8.10.$$

Therefore, it can be seen, approximately, from 8.8 and 8.7 that $\frac{\Delta p_x}{\Delta p\, F}$ is inversely proportional to the velocity squared, irrespective of the type of plant. On the other hand, 8.6 and 8.10 show that $\frac{\Delta p_x^+}{\Delta p^+ F}$ is

inversely proportional to the velocity in a reduced pressure plant but to the velocity cubed in a positive pressure plant.

Similarly, it can be shown that $\frac{\Delta p'_x}{\Delta p\ F}$ is inversely proportional to the velocity cubed in a reduced pressure plant but to the velocity in a positive pressure plant.

Therefore, a comparison of the excess pressure drop in a positive pressure plant with that in a reduced pressure plant is significant, only when the air pressure drop has been calculated as Δp and not as $\Delta p'$ or $\Delta p^{\dagger}$.

8.4. The correlation of Pattantyus and Papai

Pattantyus and Papai expressed their measurements of pressure drops for the conveying of wheat, obtained over a wide range in feed rates and air velocity in a positive pressure plant with pipes of large diameters, by the equation

$$\frac{\Delta p'_x}{F\ L} = \frac{k\ u}{A} \qquad 8.11.$$

where k is a constant for wheat for all flow conditions.

They determined the total pressure gradient by using a graphical plot of the pressure against distance; it has been shown (section 1.7), using the results of Gasterstadt, that such a method does not necessarily give accurate values of the excess pressure drop. Their data are not presented in the literature and the accuracy of equation 8.11 is not assessed. Pattantyus and Papai, however, observe that the results obtained at high velocities by Gasterstadt agree with equation 8.11.

It has been shown in relationship 8.3 that for the present results,

$$\Delta p'_x \propto \Delta p_x\ s^n$$

Therefore, from equation 7.1, for a given pipe diameter

$$\Delta p'_x \propto \frac{\Delta p\ F\ s^n}{s^2} \propto \frac{F\ L\ \rho\ u^2\ s^n}{s^2},$$

therefore, $$\frac{\Delta p'_x}{F\ L} \propto \frac{\rho\ u^2}{s^{(2-n)}} \qquad 8.12.$$

Thus, from a qualitative point of view, 8.12 shows that for high velocities, when $\frac{s}{u}$ is constant, the present results can be expressed by equation 8.11 only for solids for which $n = 1$.

8.5. Analogies to the Fanning equation

Several investigators expressed their results by a form of Fanning equation. Equation 7.1 is also of similar form and when compared with the other equations used in the literature, a complicated relation is found to exist between the friction factors. For example, Mehta's equation 2.6 gives the expression,

$$\frac{f_c}{f} = \frac{1 + \frac{45{,}000\ F}{s^2\ s_o}}{1 + (\bar{v}\ s^2/\rho u^2)^b} \quad \text{for D = 1".}$$

where b is an experimental constant which depends on the properties of the material, for the friction factor, f_c, used by Mehta.

The total pressure drop in the equilibrium region for a 1" I.D. pipeline may be expressed as follows, using equation 7.1,

$$\Delta P = \Delta p + \Delta p_x = \Delta p\left(1 + \frac{45{,}000\ F}{s_o\ s^2}\right)$$

$$= f\left(1 + \frac{45{,}000\ F}{s_o\ s^2}\right)\frac{\rho u^2\ L}{2\ D} \quad \text{in f.p.s. units} \qquad 8.13.$$

Equation 8.13 is similar in form to Segler's equation 2.4 and provides a means of calculating the friction factor, ft, used by Segler. For example, for a 1" I.D. pipeline,

$$f_t = f\left(1 + \frac{45{,}000\ F}{s_o\ s^2}\right)$$

8.6. Drag equations

An examination of the usefulness of equations derived using the drag equation 2.1 has shown that this approach to the problem is not very promising. By substituting the expression for Δp_x given by equation 7.1 into equation 2.2, then C, the drag coefficient for conveying conditions, is found to be directly proportional to the air velocity at high air velocities, i.e. when particles are fully suspended. No general, simple correlation was obtained using equations based on the drag equation.

8.7. Correlations of previous workers in this Department

Hillyar-Russ, Charles, Clark and Mitlin all measured their pressure drops over pipe lengths which were too short to permit reproduceable results to be obtained, and their measurements of the solid velocity

were rather inaccurate. Thus, they found it difficult to find a basic pattern in their results.

These authors all used the term $\frac{\Delta p_x}{F L}$ to express their results. As already observed in chapter 7, the term $\frac{\Delta p_x}{F L}$ behaved in apparently different ways for each material, especially at low air velocities, because of experimental error and the cyclic behaviour of the pressure gradient.

In general, the correlations of the above authors are somewhat similar to equation 7.1, but they include a constant or an index whose value depended on the properties of the material. The plots given show a wide scatter of points.

Mitlin used the equation $\frac{\Delta p_x'}{\Delta p'} = \left(\frac{F}{s}\right)^{1.6}$ to express his results for coals. The use of $\frac{\Delta p_x'}{\Delta p'}$ was slightly preferable to $\frac{\Delta p_x}{\Delta p}$ for correlation purposes and the power of $\frac{F}{s}$ was different for each of the other materials conveyed.

Although Clark did not use pipes of different diameters, his equation for perspex, $\frac{\Delta p_x A}{F L} = \frac{.45}{s}$

may be re-written as $\frac{\Delta p_x}{\Delta p} \propto \frac{F}{s D \rho f u^2}$

In this form, the expression takes account of the effect of pipe diameter in a manner similar to that shown in graph 7.20 for Segler's results in pipes of large diameter. However, the velocity terms are different from those in equation 7.1.

The results from the present work do not agree very well with the above correlations of Mitlin and Clark.

8.8. Conclusions

The results of the present work are correlated by equation 7.1 better than by any expression found in the literature. Segler's results for wheat conveyed in larger pipes can also be expressed by an equation identical to 7.1 but with a modified constant for each pipe diameter. Gasterstadt's results in a reduced pressure plant can be correlated by equation 8.7 for all flow conditions whereas they are correlated by his own equation (8.5) only for high velocities. It is probable that Gasterstadt's results are correlated by equation 8.7, and not by equation 7.1 (or 8.8), which has been obtained from the present work, because

acceleration and other effects contributed to the pressure drops which he obtained. These factors, together with the cyclic behaviour of the pressure gradient in the pipeline, can explain why the results of other workers do not agree with equation 7.1.

It is considered that the pressure drop due to air flow during conveying is properly assessed only when it is calculated using the actual pressure in the pipeline; some workers have overlooked this point.

Furthermore, before results can be compared, it is essential to determine whether they are influenced in any way by wall effects due to electrostatic charges.

Chapter 9.

The Wall Effect and Frictional Electrification

9.1. Introduction

As already indicated, the characteristics of sand and manganese dioxide during conveying are considerably different from those of the other materials used and the observations and correlations described in chapters 6 and 7 are applicable to these two materials only for a limited range of flow conditions as described later. Only sand and manganese dioxide exhibit this wall effect, which was first observed by Charles and Mitlin in the conveying of granite, carborundum and various grades of sand and which they attributed to the presence of electrostatic charges on the wall of the pipeline.

The main characteristic of the wall effect, already referred to in section 1.9, is that as the time of conveying increases, the wall effect builds up from a minimum at the start of conveying to an equilibrium value; the measurements change progressively and the resistance to flow in the pipeline increases correspondingly until steady values are obtained.

Because of the change in resistance to flow, it is found with the present plant that a solid velocity in excess of 50 ft./sec. cannot be attained at equilibrium conditions, although velocities of up to 80 ft./sec. can be obtained when the wall effect is at a minimum. In order to investigate the wall effect over a wider range of solid velocities, the air supply system would require modification. However, because the experimental technique developed is satisfactory for studying the wall effect, it was decided to investigate, in detail, only one grade of sand and to deduce the pattern of behaviour of the effect. A plant for a more detailed study of the effect in the future can then be designed on the basis of the results obtained and an experimental programme can be planned.

In this chapter, the results of observations and experiments on the conveying of one grade of sand are presented in order to demonstrate

the pattern of behaviour of the wall effect. Then follows a method of correlating the results and a general discussion of the nature of the effect and of frictional electrification.

9.2. The characteristics of the wall effect

Graph 9.1 (graphs 9.1 to 9.10 are in appendix 5) shows the results from the first experiment in which sand was conveyed continuously without altering the control settings; a low feed rate was used so that samples could be withdrawn without exhausting the feed hopper.

During the experiment, the feed rate and the air mass flow rate decreased to a small extent; the air pressure, the excess pressure drop and the relative velocity increased; whilst the air and solid velocity decreased until steady values were obtained after 60 minutes of conveying, when the wall effect reached equilibrium.

Removal of wall effect

At any time after the wall effect has appeared it can be reduced to a minimum value by conveying coal or perspex at a very low feed rate for as little as three minutes. It can also be partly reduced by allowing the plant to stand idle for several weeks and, as shown by Mitlin, by wetting and then drying the inside of the pipeline. When the sand which has been conveyed is replaced by a fresh sample of the same type of sand, the same measurements are obtained immediately and the wall effect is unaltered. Thus, it appears that the effect resides on the plant and not on the solids; however, it is not affected by removing some of the dust from the pipe walls by pulling clean rags through the pipeline several times.

Reproduceability of measurements

When sand is conveyed immediately after the wall effect has been reduced to a minimum, the measurements are reasonably reproduceable, for given flow rates, and the initial rate of build-up of the wall effect appears to be approximately constant for the same starting conditions. After equilibrium is reached, the excess pressure drop for given flow rates remains constant for up to at least 85 minutes of

continuous conveying. However, the equilibrium value changes from day to day for the same flow rates as is shown in graphs 9.4 and 9.5. As the feed rate is increased, the measurements at equilibrium become more reproduceable and the percentage increase in the excess pressure drop over the minimum value becomes smaller.

The effect of the feed rate

It is found that the wall effect depends, to a great extent, on the feed rate.

At a constant solid velocity, the time required to reach equilibrium becomes smaller as the feed rate is increased. Graphs 9.2 and 9.3 show that when sand is conveyed at 42 ft./sec., equilibrium is reached after 45 and 135 minutes for feed rates of 15 and 4.5 lb./min., respectively.

The relationship between the feed rate and the excess pressure drop depends on whether the feed rate is greater or smaller than about 7 lb./min. Graphs 9.4 and 9.5 show that, for a constant solid velocity, the excess pressure drop at equilibrium is directly proportional to the feed rate for feed rates between zero and 7 lb./min, but the constant of proportionality varies from day to day; graph 9.5, however, shows that, for higher feed rates, the relationship is still linear but the proportionality constant is different from that at feed rates less than 7 lb./min.

The change in the relationship between the feed rate and the excess pressure drop, shown in graph 9.5, occurs between 5 and 7 lb./min. It is found that an abrupt change in the flow pattern of the solids occurs at a feed rate of 6.5 lb./min; this change is independent of the time of conveying but becomes more marked as the time increases.

If the feed rate is gradually increased from zero, the flow of solids is, at first, smooth and continuous as with other materials. At a feed rate of 6.5 lb./min., reproduceable to within $\pm 3\%$, the flow is suddenly heard to become discontinuous and the solids travel in regular pulses. This behaviour does not originate at the feed point where the flow remains continuous. A comparison of the manometer readings indicates that pulsing exists throughout almost the whole of the pipeline from the acceleration region onwards and, therefore, it must develop quite close to the feed point. As the feed rate is

further increased above 6.5 lb./min., the "staccatto" rhythm of the flow persists but the pulses of solids progressively merge, and, at feed rates above 25 to 30 lb./min., the flow again becomes continuous.

This behaviour and the value of this critical feed rate are reproduceable over the whole range of velocities used and are not dependent on whether the feed rate is being increased or decreased. Furthermore, it can be seen from the results that the equilibrium value of the excess pressure drop is very sensitive to small changes in both the feed rate at values below 10 lb./min. and in the solid velocity at low values around 40 ft./sec. Thus, a high degree of accuracy is required for measurements under these conditions of flow.

Relative velocity

It is found that the increase in the excess pressure drop is accompanied by corresponding changes in the relative velocity. The latter increases with time by up to 24 ft./sec. over minimum values at a feed rate of about 1 lb./min., but the increase becomes smaller as the feed rate increases. The relative velocity at equilibrium decreases very rapidly, at first, as the feed rate is increased from zero, and then more slowly when the feed rate is increased above 7 lb./min.; this behaviour can be seen in graph 9.8, which shows results at equilibrium for a range in solid velocity of 38 to 48 ft./sec. The same results are used in the plot of $\frac{F}{s}$ against the relative velocity in graph 9.9, but the scatter of the points in graphs 9.8 and 9.9 is such that it is not possible to decide whether the feed rate or the ratio of $\frac{F}{s}$ gives the better correlation of the relative velocity at equilibrium.

The initial values of the relative velocity at all feed rates are of the same order as the equilibrium values at the highest feed rates and are shown plotted on graph 6.8. The average of these initial values has been used to obtain the point for sand shown in graph 6.16 which shows that at the start of conveying the relative velocity can be correlated in the same way as that for other materials which do not exhibit electrostatic effects, i.e. by using the equation 6.2,

$$(u - s) = \frac{s_o}{.468 + \sqrt{s_o/w}}$$

which is applicable to solids in Class A into which sand falls (having

a size distribution ratio of less than 3).

9.3 The pattern of the wall effect

The pattern of the wall effect deduced from the results is represented in graphs 9.7 and 9.8 and is described below for three different conditions.

1. The wall effect reduced to a minimum

Immediately after the wall effect has been reduced to a minimum, the ratio, $\frac{\Delta p_x}{F\,L}$ (line A, graph 9.7) at a constant solid velocity, and the relative velocity (graph 6.8) are constant and independent of the feed rate; the behaviour is similar to that with materials which do not exhibit the wall effect.

2. The wall effect at equilibrium

The equilibrium values of the ratio, $\frac{\Delta p_x}{F\,L}$ at constant solid velocity, vary from day to day, depending on atmospheric conditions, and fall in the dotted zone F, in graph 9.7, for a solid velocity of about 40 ft./sec. They may be represented by the two lines B and C in graph 9.7 depending on whether the feed rate is above or below 6.5 lb./min. Similarly, the relative velocity at equilibrium may be represented by the two lines D and E in graph 9.8 according to whether the feed rate is above or below 6.5 lb./min. The results at equilibrium for a solid velocity of 48 ft./sec. (graph 9.6) indicate that $\frac{\Delta p_x}{F\,L}$ decreases as the velocity increases, as for materials which do not exhibit electrostatic effects.

Thus, at equilibrium, the term $\frac{\Delta p_x}{F\,L}$ for a given solid velocity is constant for feed rates up to 6.5 lb./min. but decreases as the feed rate is increased above this value. At high feed rates, it approaches the minimum value and the wall effect can then be disregarded. The relative velocity decreases rapidly as the feed rate is increased up to 6.5 lb./min. and then more slowly as the feed rate is further increased.

3. The wall effect building-up

The relationship between the feed rate and the excess pressure drop or the relative velocity at any time during the build-up of the wall effect may be represented by curves such as H in graph 9.7 and K in graph 9.8.

A wider range in solid velocity must be investigated to decide conclusively the relationship between the solid velocity and the wall effect.

It has been reported in chapter 6 that, for materials which do not exhibit electrostatic effects, the relative velocity is approximately proportional to the falling velocity. Further, it has been shown, in chapter 7, that the term $\frac{\Delta p_x\, s^2}{\Delta p\ F}$ is inversely proportional to the falling velocity. Thus, when the values of $\frac{\Delta p_x\, s^2}{\Delta p\ F}$ and the relative velocity, determined for the above materials from individual experiments, are plotted against each other, it is found that the points are represented by a single curve; this is shown in graph 9.10 in which curve C represents all the data to within $\pm$ 30%. In order to avoid confusion, only the average values of $\frac{\Delta p_x\, s^2}{\Delta p\ F}$ and the relative velocity for materials other than sand have been used in graph 9.10.

The best method found for correlating the results for sand appears to be to use a plot of $\frac{\Delta p_x\, s^2}{\Delta p\ F}$ against the relative velocity. All the results for sand, for feed rates of 1 to 30 lb./min. and solid velocities of 38 to 48 ft./sec. have been plotted on graph 9.10, irrespective of the time of conveying. It is seen that all the points are represented by the straight line D. The results obtained immediately after the wall effect has been reduced to a minimum lie very close to the curve C. This confirms that $\frac{\Delta p_x\, s^2}{\Delta p\ F}$ and the relative velocity, for these conditions, are given by the general correlations (equations 7.1 and 6.2, respectively) obtained for materials which do not exhibit wall effects. As the time of conveying increases, the value of $\frac{\Delta p_x\, s^2}{\Delta p\ F}$ increases from the curve C along the line D. The equilibrium value of $\frac{\Delta p_x\, s^2}{\Delta p\ F}$ is greatest for the lowest feed rates and progressively decreases along the line D as the feed rate is increased and approaches the curve C at the highest feed rates.

The scatter of the points for sand in graph 9.10 is understandable

because the percentage error in the relative velocity is large, and any error in measuring the air flow rate or the solid velocity is magnified in graph 9.10 and tends to spread the results in a direction at right angles to that of the line D, especially at low feed rates.

Thus, it can be said that the relative velocity is a measure of the influence of the wall effect on the pressure drop and, if the relative velocity is known, the term $\frac{\Delta p_x \, s^2}{\Delta p \quad F}$ can be determined from graph 9.10 or the equation

$$\frac{\Delta p_x \, s^2}{\Delta p \quad F} - \frac{45{,}000}{s_o} = 655 \left[(u - s) - \frac{s_o}{.468 + \sqrt{s_o/w}} \right] \quad \text{in f.p.s. units} \quad 9.1.$$

The relative velocity at equilibrium can be predicted from graph 9.8 or 9.9 for any feed rate and solid velocity. In general, the values of the relative velocity at equilibrium during wet weather are lower than those during dry weather.

Further work is required so that the relative velocity may be predicted at any time as the wall effect builds up, and so that the precise effect of the solid velocity on the wall effect may be determined. The feed rate, and probably the solid velocity, affect the rate at which the wall effect builds up.

9.5. Materials which exhibit the wall effect

A change in measurements, with time, has been observed only in the conveying of sand, manganese dioxide and vegetable seeds. The change in measurements with vegetable seeds was also observed by Mitlin and is not attributable to electrostatic effects but to the breakdown of particles and the deposition of oily material on the walls of the pipe; furthermore, the effect is not reversible.

Manganese dioxide behaves in an identical manner to sand and the magnitude of the wall effect is similar. The effect can be minimised in the same way and the flow pattern changes at a reproduceable feed rate of 5 lb./min. as compared to 6.5 lb./min. for sand.

A more detailed study of the behaviour of manganese dioxide was not carried out but the few points for manganese dioxide, on graph 9.10, suggest that its behaviour is qualitatively similar to that of sand.

From experiments with sand and manganese dioxide, it can be concluded that during the conveying of any similar material the wall

effect builds up progressively with time irrespective of the material being conveyed. If manganese dioxide, for instance, is conveyed sufficiently long to reach equilibrium and it is then replaced by sand, the equilibrium values for sand will be obtained immediately. Therefore, the effect is entirely a property residing on the pipeline and is independent of the solids being conveyed provided the solid is capable of producing the wall effect.

9.6. Frictional electrification

A considerable amount of research has been carried out in the past on the subject of frictional electrification and a summary of the relevant references is given in appendix 3. There appears to be no agreed theory which can be applied in order to predict the charges which are likely to be developed in any particular instance, and only recently has any satisfactory theoretical explanation of some of the various associated phenomena been put forward (Harper).

The process of electrification between two bodies depends on a variety of factors, such as the heaviness, duration and velocity at contact, surface films and impurities, surface strains, the nature and pressure of surrounding gases and the capacitance of each body. When considering the electrification produced by dust clouds, the size and composition of the particles are important.

Where conditions are similar to those encountered in pneumatic conveying, the velocity and feed rate of the solids and the temperature and humidity of the air will be important. An interesting investigation related to conveying is that of Vollrath, who conveyed particles through a bank of copper tubes for the purpose of generating electric current.

Several authors have previously referred to the presence of electrostatic charges during conveying e.g. Farbar, Mehta, Chudjakov and Tshuchanov, Mitlin and Charles. In the present study, charges were measured on an insulated section of pipeline during the conveying of all materials, and the particles were also found to be charged. Voltages of up to 200 were measured on the insulated pipeline but the value depended upon atmospheric conditions; in wet weather, no charges could be measured on the pipeline. The charges remained on the

pipeline after conveying and slowly leaked to earth at a rate depending on the insulation; they disappeared immediately on earthing the pipeline. Similarly, the charges on particles withdrawn from the plant leaked to earth at different rates depending on the insulating properties of the material.

However, for given flow conditions in the conveying of any material, the measurements at any time were independent of whether the pipeline was earthed, insulated or charged from an external source.

9.7. Observations of electrostatic charging

Observations were made of electrostatic charging in the transparent perspex tube at the feed point by noting the size and number of "test" particles attracted to the tube. These test particles consisted of a selection of all the materials conveyed and were placed on a tray situated 1" below the perspex tube. Although conditions in the brass pipeline are unlikely to be identical to those in the perspex tube, the following observations provide a means of comparing the charges generated during the conveying of different materials.

Test particles usually became attracted to the tube after a short period of conveying of each material. The attraction varied in intensity from day to day and sometimes disappeared. The forces of attraction originated both in the perspex tube and the conveyed particles. These two sources appeared to have charges of opposite sign because the test particles were often attracted to the tube, then suddenly repelled and immediately attracted back again to the tube. This phenomenon usually occurred at a small feed rate when the feed rate was being reduced.

The intensity of the charges was strongest when conveying sand and manganese dioxide, somewhat weaker with perspex, polystyrene and coal, and weakest with the remaining materials.

In some experiments, particles of sand which had been conveyed through the pipeline were introduced into the tube from the feed hopper after the air supply had been shut off. The particles were seen to "leap" up to 6" along the tube both downstream and upstream from the feed point and they then adhered strongly to the wall of the tube. This behaviour was not observed with other materials.

After conveying sand, the perspex tube retained a residual charge which persisted for several days unless removed by wiping with a cloth; however, a residual charge was never detected in dismantled sections of the brass pipeline.

During the conveying of perspex, the formation of slugs (see chapter 5) was accompanied by intense attraction of test particles to that part of the tube where the slugs formed. It cannot be confirmed whether or not the charges on the conveyed particles caused the formation of slugs.

In one experiment, the air velocity was progressively reduced when conveying polystyrene at 1 lb./min. When the velocity had fallen to 15 ft./sec. the particles were seen to form a layer on the walls of the sight glass at 110 ft. from the feed point. At the same time, the pressure drop over the 100 ft. to 110 ft. section rapidly increased four-fold. The pressure drop over each succeeding pipe section increased similarly in turn indicating that the layer of particles on the pipe wall developed upstream along the pipeline to the feed point where the layer was eventually seen to form; conveying then stopped.

This increase in the pressure drop is not comparable with the wall effect in that it occurs very rapidly at an air velocity of 15 ft./sec. and does not increase with the time of conveying; it must be caused by artificial roughening of the pipe wall and by reducing the effective area for flow.

It may be that the increase in the total pressure drop due to the wall effect, which for sand at low feed rates and velocities is as much as three-fold, is caused by a similar mechanism. It is suggested that in the case of sand, the particles are retarded and held close to the pipe wall by electrostatic forces but do not form a layer which adheres to the pipe; thus, both the relative velocity and the pressure drop increase and the slow increase with time indicate a correspondingly slow build-up of electrostatic charges.

The results for perspex, already discussed, indicate that they are influenced by a wall effect whose nature is quite different from that observed with sand. Because the pressure drop and the relative velocity are lower than would be expected, it is considered that the perspex particles are repelled from the pipe walls; furthermore, the effect with perspex is apparently independent of the time of conveying.

The results for polystyrene, however, do not indicate the presence of any wall effect except in the experiment described above.

9.8. Conclusions

The nature of the wall effect obtained with sand and manganese dioxide may be seen in the following conclusions from the present study.

The wall effect is due to the formation on the pipe wall of an insulated layer of charged dust particles which retain their charges over a long period of time. Conveyed particles are then retarded and held close to the wall by these charges and, thus, the frictional resistance to the flow of air is increased.

At very low feed rates there is sufficient space for all the particles to travel near the wall and the effect of increasing the feed rate is to increase the air friction until the region near the wall is saturated at the critical feed rate or particle concentration. Any additional particles must travel in the central core, remote from the pipe wall; further, slugs then form and a change takes place in the flow pattern of the solids. As the feed rate is further increased, the proportion of the particles in the pipeline which are very close to the wall becomes smaller and, thus, the effect of the electrostatic charges or the wall effect becomes less. At very high feed rates, the distribution of particles over the cross-section of the pipe is more or less the same as for other materials which do not exhibit the wall effect and the air friction is modified in the same way in both cases.

The results for the excess pressure drop may be correlated as shown in graph 9.10 in terms of the relative velocity. For equilibrium conditions, the relative velocity may be predicted from either graph 9.8 or 9.9 and for initial conditions, from the general correlation (equation 6.2). It would not appear to be possible to predict the relative velocity for intermediate stages of the wall effect until further studies have been made.

One important feature of the wall effects which remains unexplained is the nature and formation of the electrostatic charges. Charges in frictional electrification are usually associated with the transfer of electrons between bodies but, in some cases, ions act as charge carriers (with some liquids, even more complex charge carriers have been suggested).

It is suggested that two types of charges are produced during conveying.

1. Charges produced by the transfer of electrons in the process of frictional electrification are generated very rapidly on the pipeline, the conveyed particles and dust particles.

When the pipeline is conducting, the charges on it apparently have no effect on conveying and can be removed by earthing the pipeline. When the particles are non-conducting, they can induce opposite charges on to the pipeline and become attracted to it; this effect is observed with polystyrene at very low velocities in the present work.

Charged dust particles adhere to the wall of the pipeline and also retain their charges if they are non-conducting. If the conveyed particles have charges (generated by the process of frictional electrification) similar in sign to those on the dust layer, the conveyed particles are repelled from the wall of the pipe. This mechanism may, possibly, explain the behaviour of perspex.

2. The second type of charges are produced by attrition during conveying and may explain the wall effect exhibited by sand. The dust particles carry ionic charges and adhere to the wall of the pipeline; if they are non-conducting, they retain their charges over a considerable period of time. The development of these charges depends on the rate of particle attrition and is, therefore, a relatively slow process. The layer can be discharged very quickly, as a result of electrostatic attraction, when materials of a different nature are conveyed. It is difficult to remove the dust layer mechanically and pulling cloths through the pipeline is not very effective because sufficiently intimate contact cannot be made. After the dust particles have lost their charges, they no longer exert any effect on the conveying process. The wall effect then builds up anew at a rate depending on particle attrition.

It may be significant that the only materials observed, in the present study, to exhibit this effect are dioxides, both of which have a similar crystal structure with ionic bonds.

Thus, with sand, the dust layer is charged by a process of particle attrition and attracts the conveyed particles which, probably, are rapidly and oppositely charged by frictional electrification, irrespective of their electrical condition, when they enter the conveying line. On the other hand, with perspex, both the dust layer and the conveyed particles are rapidly and similarly charged by frictional electrification and the

conveyed particles are repelled from the wall.

Chapter 10.

Conclusions.

A plant has been constructed so that the pneumatic conveying of a range of solid particles in a horizontal pipeline, 1" in diameter, could be studied. Measurements have been made of the pressure drop and the velocity of the particles relative to the gas stream and the results have been correlated in terms of the physical properties of the particles and the flow rate of air.

In order to permit measurements to be made over a prolonged period, a continuous recycling of solids was effected by incorporating a rotary valve to transfer the solids from the downstream separator to the feed hopper. By this means, it was possible to ensure that stable conditions of flow had been attained and to study the progressive increase in pressure drop and relative velocity which takes place during the conveying of some materials such as sand and manganese dioxide.

A large number of experimental results are required before any form of generalised correlation can be attempted. The experimental methods used previously for the determination of the velocities of the solid particles were either inaccurate or tedious and consequently were not capable of giving accurate results in sufficient quantity in a reasonable time. An entirely new method of measurement was, therefore, developed in which a pulse of air was introduced into the conveying line by interrupting the flow of solids for a short period. The time taken for the pulse to travel between any two points in the pipeline could then be determined by an electronic method. Accurate results with errors of less than 1% could be rapidly obtained.

The flow pattern within the pipe was observed visually and it was found that the degree of uniformity of dispersion of the particles in the pipe increased with the velocity of flow. In general, the velocity required to produce a given flow pattern is found to be inversely proportional to the terminal falling velocity of the particles. At high velocities, the pressure gradient in the pipeline is approximately

uniform and measurements can, therefore, be taken over comparatively short lengths. At lower velocities, however, conditions become far less uniform and a cyclic variation of the pressure gradient becomes apparent; consistent readings can be obtained only by measuring the pressure difference over a much longer length of pipe. It has been established that, in order to obtain consistent and reproduceable results, pressure gradients should be measured over pipe sections of at least 40 ft. in length and situated sufficiently far from the feed point of the solids for the effect of the acceleration of the particles to be negligible. The lack of consistency of the results of previous workers is frequently attributable to the fact that these considerations have been ignored, and to the inaccuracies inherent in measuring techniques. Furthermore, with some solids, electrostatic charges build up on the walls of the pipeline and influence measurements.

In the absence of electrostatic charging, the additional pressure drop attributable to the presence of solids in the air stream can be expressed to within ± 15% by the relation:-

$$\frac{\Delta p_x \, s^2}{\Delta p \; F} = \frac{45{,}000}{s_o} \qquad \text{in f.p.s. units} \qquad 7.1.$$

The solid velocity, s, is a function of the physical properties of the solids and the air velocity.

For the purpose of calculation of the solid velocity, the particles can be divided into three classes as follows. Class A solids have a narrow size range with the ratio of the linear dimensions of the largest particles to that of the smallest not exceeding about 3. For these solids, the relative velocity is given to within ± 3 ft./sec. by the equation

$$(u - s) = \frac{s_o}{.468 + \sqrt{s_o/w}} \qquad \text{in f.p.s. units} \qquad 6.2.$$

For solids with a wider size range and a mean particle size of 0.04" or more (Class B), the relative velocity will be up to 1 ft./sec. greater at solid loadings greater than .01 cu.ft. solids per cu.ft. of pipe and about 1 ft./sec. less at lower loadings.

When the size range is larger and the particles are smaller than 0.04" (Class C), the relative velocity varies with the solids' loading

and is given to within $\pm$ 5 ft./sec. by:-

$$(u - s) = \frac{s_o}{.468 + \sqrt{s_o/w}} + \frac{1770\ F}{s_o\ \ s} \quad \text{in f.p.s. units} \quad 6.3.$$

The results for all the materials examined, except brass, are expressed by the appropriate equations, given above, which are applicable whether the particles are fully suspended in the air stream or if saltation flow is occurring. The effects of acceleration of the particles are not included and, therefore, the equations are not applicable close to the feed point. The anomalous value of the relative velocity of the brass particles used is probably attributable to the unusual feathery shape of the particles.

When perspex particles are conveyed, an insulated dust layer forms on the wall of the pipe and becomes charged by frictional electrification. The particles themselves aquire a like charge and are repelled from the walls with the result that the pressure gradient is reduced. The effect is established almost instantaneously and is most marked at low solid loadings and with fine particles.

As previously reported by Charles and Mitlin, with a number of materials, including sand and manganese dioxide, the pressure gradient in the pipeline increases progressively with the time of conveying and eventually reaches a limiting value after a prolonged period. It is suggested that a charged dust layer is built up on the walls by a process of particle attrition, and that the dust layer and the particles aquire opposite charges. The particles are consequently attracted to the walls and are retarded; there exists a critical flow rate at which the space near the walls becomes saturated with particles which then form slugs. The resulting change in the flow pattern causes a change in the behaviour of both the relative velocity and the pressure gradient in the pipeline. At the start of conveying, the pressure gradient and the relative velocity are similar to those for materials which do not exhibit effects due to electrostatic charges. As conveying proceeds, the pressure gradient and the relative velocity both increase simultaneously and throughout are related, irrespective of the solids' loading and probably the velocity of flow, to within $\pm$ 30% by the equation

$$\frac{\Delta p_x\ s^2}{\Delta p\ \ F} = \frac{45{,}000}{s_o} + 655\left[(u - s) - \frac{s_o}{.468 + \sqrt{s_o/w}}\right] \quad \text{in f.p.s. units} \quad 9.1.$$

The increases in pressure gradient and relative velocity are greatest at low solids' loadings and the effect takes the greatest time to build up to a state of equilibrium. At any stage during the development of the charged layer, it can be electrically discharged by passing solids, such as perspex or coal, through the pipeline for a very short time.

The correlations obtained in the present work permit the calculation of the pressure drop during conveying in a 1"I.D. pipeline provided that the particles do not give rise to electrostatic charging. Some indication of the effect of pipe diameter on pressure drop has been obtained from considerations of Segler's work, but clearly a considerably extended investigation is required. Furthermore, the opportunity should be taken to extend the ranges of velocities and feed rates used in the present investigation and further solids should be used in order to verify the validity of the classification which has been devised for the particles and to determine the effect of particle shape. The problem of electrostatic charging also warrants a thorough exploration with particular regard to the nature of the material and the size of the pipeline and to determine the applicability and improve upon the appropriate correlations obtained in the present work.

Application to design problems

The correlations obtained from the present work and the results of Segler may be used for the design of a conveying plant knowing the feed rate, the physical properties of the solids and the distance over which they are to be conveyed.

By assuming a given pipe diameter and solid velocity, then the relative velocity and, hence, the required air velocity, may be determined from the correlations given in Chapter 6 and the value of the term, $\frac{(P_1 - P_2)}{f(P_1 + P_2)}$ may be determined using graph 7.20. P_1 and P_2 are the pressures at the inlet and discharge ends of the conveying line and are equal to atmospheric pressure in a reduced pressure and a positive pressure plant, respectively. The value of f for the flow of air alone in the same pipeline at the velocity existing during conveying can be determined. A small safety factor is introduced by using this value of f to determine P_2 in a reduced pressure plant and P_1 in a positive pressure plant. Thus, the power requirements can be calculated for the assumed values of pipe diameter and solid velocity.

By repeating the calculation for a series of pipe diameters and solid velocities, the most economic design may be determined.

However, the above method for design requires to be further developed in order to account, quantitatively, for particle acceleration, pipe bends, end and inlet effects and electrostatic charging.

Theoretical considerations

From the results of the investigation, it is not possible to give a completely satisfactory quantitative analysis of the fundamental mechanisms which govern the process of pneumatic conveying. However, the effects of the important variables can be clearly seen from the correlations outlined in Chapters 6 and 7.

When air flows alone through a pipe, a pressure gradient is set up to balance the forces arising from the shear stress set up at the walls of the pipe. Close to the walls, the flow is laminar and consequently the shear stress is given by the product of the viscosity and the velocity gradient at the walls. When particles are present in the pipeline, the flow pattern is modified and energy is transferred from the air to the particles with the result that the velocity gradient, and, hence, the shear stress, at the walls is increased. The pressure drop is thus increased in the same proportion as the velocity gradient.

The increase in pressure drop can be expressed in terms of the velocities of the air and the solids and the terminal falling velocity of the solids. The ratio of the velocity of a particle to its terminal falling velocity gives a measure of the degree of suspension of the particles and, thus, affects the average distance of the particles from the walls. When the particles are poorly suspended and their average distance from the wall is small, the velocity gradient in the air near the walls is increased to a large extent and the excess pressure drop is correspondingly high. If the average distribution of the particles is unaffected by the solids' concentration, the excess pressure drop would be directly proportional to the feed rate of the solids; this is borne out in practise.

Electrostatic charging appears to cause particles either to be attracted towards the walls or repelled. In the former case, the

particles are retarded and the velocity gradient in the air is increased with the result that the pressure drop increases progressively as the charges build up; in the latter case, the pressure drop is reduced.

Appendix 1.

Nomenclature

a effective cross - sectional area of a particle

A cross - sectional area of the pipeline

b an experimental constant used by Mehta

C the drag coefficient during conveying

Co " " " for falling velocity conditions

d the "equivalent" diameter of a particle

D the diameter of the pipeline

f the Fanning friction factor

fc a friction factor used by Mehta

fd " " " " " "

ft " " " " " Segler

F the feed rate of the solids into the pipeline

$\bar{F}$ the drag force on a particle

k an experimental constant used by Pattantyus

L the length of a test section of the pipeline

n the weight of a particle

p the arithmetic mean pressure in the test section of length L

po the pressure at the orifice meter

Δp the pressure drop attributable to air friction calculated by the Fanning equation

$\Delta p'$ " " " " " " " which would exist if air flowed alone at the same velocity as in conveying

Δp^{+} the pressure drop attributable to air friction which would exist if air flowed alone at the same mass rate as in conveying

Δpo the pressure drop across the orifice plate

$\Delta pacc.$ the contribution to the total pressure drop of solid acceleration

$\Delta px = (\Delta P - \Delta p)$ the excess pressure drop attributable to the presence of the solids in the air stream

$\Delta p_x'$ & Δp_x^+ the excess pressure drops corresponding to $\Delta p'$ & Δp^+

ΔP the total, measured pressure drop during conveying

Q the air flow rate through the pipeline in stand. cu.ft./min.

Q_o " " " " " " orifice " " "

r the specific loading - the mass ratio of the flow rate of the solids to that of the air

Re $= \frac{\rho u D}{\mu}$ - the Reynolds Number

s the bulk average solid velocity

s_o the falling velocity of a particle

t time in seconds

T^oK the air temperature in degrees Kelvin

T^oC " " " " " Centigrade

u the nominal air velocity

V voltage

w the density of a particle

$\bar{w}$ $= \frac{F}{s A}$ the disperse density

α $= \frac{\Delta P}{\Delta p}$ the specific pressure drop

ρ the density of the air in the pipeline

$\tan \theta$ a function used by Gasterstadt

μ the viscosity of the air

Appendix 2.

Bibliography - Pneumatic Conveying.

Adam

Chem. Ing. Tech. 29 151 1957

Albright, Holden, Simons, Schmidt.

Ind. Eng. Chem. 43 1837 1951

Ambrose

Physics 4 265 1933

Bagnold

Proc. Inst. Civil Eng. April III 174; 205 1955

Belden and Kassel

Ind. Eng . Chem. 41 1174 1949

Chudjakov and Tshuchanov

Dokladi Akademi Nauk. U.S.S.R. 78 681 1951

Charles

Thesis Univ. of London 1953

Charles, Clark, Newitt, and Richardson

Trans. Inst. Chem. Eng. 209 1952

Clark

Thesis Univ. of London 1951

Coulson and Richardson

"Chemical Engineering" Vol. I Pergamon Press

Cramp and Priestley

"The Engineer" 137 34; 64; 89; 112. 1924

Davis

Engineering 140 1; 124. 1935

Farbar

Ind. Eng. Chem. 44 2947 1952

ibid. 41 1184 1949

Gasterstadt

V. D. I. Forshungsarbeiten No. 265 1924

Hariu and Molstad

Ind. Eng. Chem. 41 1149 1949

Hillyar - Russ

Thesis Univ. of London 1950

Hinkle

Thesis Georgia Inst. of Tech. 1953

Hitchcock and Jones

Brit. J. Applied Physics June 1958

Jones and Hermges

- ibid .- 3 283 1952

Korn

Chemical Engineering. March, Vol. 57, 108 1950

Lapple and Shepherd

Ind. Eng. Chem. 32 605 1940

Mehta

Thesis Univ. of Purduo 1955

Ind. Eng. Chem. June 986 1957

Mitlin

Thesis Univ. of London 1954

Pattantyus and Papai

Acta Tech. Acad. Sci. Hung. 8 129 1954

Pinkus

J. Applied Mechanics 19 425 1952

Segler

"Pneumatic grain conveying" N.I.A.F. Brunswick 1951

Uspenski

Za Ekonomiu Topliva No. 3,1951: No.12, 1950

Vogt and White

Ind. Eng. Chem. 40 1731 1948

Wagon

Z. V. D. I. 92 577 1950

Wood and Bailey

J. Inst. Mech. Eng. 142 No. 2 149 1939

Zenz

Ind. Eng. Chem. 41 2801 1949

Appendix 3.

Bibliography - Frictional Electrification

Controlled rubbing experiments

Cardani	N. Cimento	Vol.123	199	1922
French	Physics Review	9	151	1917
Hess	Z. Phys.	78	430	1932
Harper	Proc. Roy. Soc.	A205	83	1951
	- ibid -	A218	111	1953
Jamieson	Nature- London	83	189	1910
Kluge	Ann. Phys. Lpz.	1	1	1929
Martin	Proc. Phys. Soc. -London	53	186	1941
Mc Clelland	Proc. Roy. Irish Acad.	34	40	1917
Morris-Jones	Phil. Mag.	29	261	1915
Owen	- ibid -	17	457	1909
Peclet	Ann. Chem. (Phys.)	57	337	1834
Prati	Atti Acad. Lincei	Vol.31(2)	478	1922
Richards	Phys. Rev.	16	290	1920
	- ibid -	22	122	1923
Rimarski	Congress Int. de l'Acetylene	Vol.4		1936
Rudge	Phil. Mag.	25	481	1913
Shaw	Proc. Roy. Soc.	A118	97; 108.	1928
		A111	339	1926
		A122	49	1929
Wolf	Ann. Phys. Lpz.	1	260	.929

Experiments simulating pneumatic conveying.

Blactin	Safety in mines research board paper No.71			1931
Nuckolls	Underwriters laboratories Inc. Bull. of Research No.8			1939
Vollrath	Phys. Rev.	42	298	1932
Walther	Braunkohle	28	789	1929
Whitman	Phys. Rov.	28	1287	1926

Experiments with dust clouds

Boning	Z. Tech. Physik	8	385	1927
Deodhar	Proc. Phys. Soc.	39	243	1927
Kunkel	J. Appl. Phys.	21	820	1950

General experiments and theory

Cochn	Z. Phys.	29	186	1924
	-ibid-	5	242	1921
Frenkel	Phys. Review	36	1604	1930
	J. Phys. U.S.S.R.	5	25	1941
Froudlich	"Colloid & Capillary Chemistry"	Methuen Lond. 3rd. Edit.	284	1926
Helmholtz	Ann. Phys. Leipzig.	7	337	1879
Knoblauch	Z. Phys. Chem.	39	225	1902
Macky	Proc. Roy. Soc.	A119	107	1928
Mrozowski	Phys. Review	85	609	1952
Perucca	Z. Phys.	51	268	1928
Richardson	Phil. Mag.	23	263	1912
Tamm	Z. Sowjet.	1	733	1932
Vick	Brit. J. Applied Phys.	Supplement No.2 p.s1		1953
Vieweg	J. Phys. Chem.	30	265	1926

Discharge in experiments

Almy	Phil. Mag.	16	456	1908
Earhart	Phys. Review	23	358	1906
Hobbs	Phil. Mag.	10	617	1905
Kinsley	Phil. Mag.	9	692	1905

Surface effects

Cabrera	Rep. Phys. Soc. Progr. Phys.	12	163	1949
Evans	"Metallic corrosion, passivity & protection"	Arnold,Lond.		1937
Thomson	General Electric Review	25	418	1922

Appendix 4.

Results.

A selection of the data obtained in the conveying of the solids used in the present work, is given in this appendix; the symbols used are explained below.

Measured data .

Q ; cu.ft./min. @ 15°C & 76 cm. Hg. The air flow rate through the pipeline, corrected for air leakage through the rotary valve.

F : lb./min. The feed rate i.e. the flow rate of the solids into the pipeline.

p : cm. Hg. The pressure in the pipeline at 75ft. from the feed point, determined by measuring the pressure at 80 ft. and the pressure drop between 80ft. and 70ft. from the feed point.

s : ft./sec. The average bulk velocity of the solids measured between 60' and 90'.

T°C The temperature of the airflowing through the pipeline in degrees contigrade.

Calculated data.

Δ p : cm. water/10' The pressure drop attributable to air friction calculated using the Fanning equation for the pipe section between 40' and 110'.

Δp_x : cm. water/10' The excess pressure drop attributable to the presence of the solids, $=(\Delta P - \Delta p)$, where,

Δ P : cm. water/10' The pressure drop during conveying measured between 40' and 110' (divided by 7).

u : ft./sec. The air velocity determined at 75'

The range in flow conditions used in the present work is as follows :-

s - solid velocity	-	30 to 80 ft./sec.
u - air velocity	-	40 to 120 ft./sec.
F - feed rate	-	1 to 40 lb./ min.
	-	0 to 0.40 cu.ft. solids/min
Q - air flow rate	-	15 to 50 stand. cu.ft./min.
- Loading	-	0 to 0.02 cu.ft. solids/cu.ft.pipe
p - pressure	-	80 to 135 cm.Hg. abs.

The lower solid velocity which can be used varies with the material and the feed rate and is determined by the onset of blockage.

Coal. A T = 15°C.

F	Q	Δp	Δpx	u	s	p
2.4	15.4	3.1	.75	43	32.1	82.5
3	15.5	3.1	1	43	32	83.1
4.4	16	3.3	1.4	44	32	84.2
5.34	16.6	3.5	1.6	45	33	85
6.3	16.8	3.55	2	45.4	32.6	85.6
6.5	17.2	3.7	1.95	45.8	35.3	86.5
7.05	17.2	3.65	2.65	45.5	33.2	87.5
9.69	17.6	3.8	3.25	45.8	33.8	88.7
9.34	17.5	3.7	3.25	45.8	32.8	88.5
11.7	17.7	3.75	4.15	45.6	33	89.7
13.3	18.3	3.9	4.8	46.2	32.8	91.1
14.8	18.7	4.05	5.23	47	32.8	92.1
16.7	19.1	4.1	6.15	47.2	32.8	93.5
19.3	19.6	4.25	6.75	48	33.4	95
20.7	20.2	4.35	7.65	48.7	34.1	96.3
22.5	20.4	4.35	8.65	48.3	35	97.8
22.5	19.8	4.2	8.6	47.2	33.4	97.2
17.6	19.6	4.25	6.6	47.9	33.2	94.5
12.2	18.8	4.1	4.3	47.9	33	90.8
10.3	18	3.9	3.95	47.6	32.7	89.6
8.9	17.9	3.9	3.1	47	33.9	88.7
5.7	17.2	3.7	1.9	46.1	34.1	86.4
2.7	15.9	3.25	1	43.6	34.1	84.2
3.6	27.4	8.03	.55	70.2	59.5	90.1
6.2	28.2	8.15	1.31	70.2	59.5	92.8
6.8	17.5	3.92	1.72	48.8	35.6	83.6
7.4	17.8	4.06	1.85	49.3	35.6	84.3
8.5	18.5	4.3	2.18	50.8	36.3	85.3
10	18.7	4.4	2.5	50.7	36.3	86.2
12.4	19.4	4.54	3.28	51.9	36	87.6
15.3	19.8	4.62	4.28	51.9	35.5	89.4
18.4	20.2	4.64	5.67	51.6	35.3	91.2
21.4	21.3	4.6	6.98	53.4	35.3	93.4
19.6	21.1	4.96	6.05	53.4	35.8	92.6
14.1	19.9	4.64	3.98	52.1	35.8	89.1
6.05	18.6	4.39	1.17	51.5	36.2	84.2
5.5	18.1	4.22	1.08	50.9	36.6	83.6
4.8	17.7	4.1	1.07	49.8	-	83.4
3.9	17.1	3.88	.87	48.4	-	82.5
2.9	17.2	3.92	.55	49.1	-	81.8
1.65	17.1	3.97	.24	49.5	-	80.8
7.6	18.9	4.44	2	51.3	37.3	85.5
8.65	18.9	4.43	2.16	51.3	37.3	85.8
10.6	19.5	4.58	2.76	51.9	37.3	87.2
11.5	19.5	4.56	3.11	51.6	37.6	87.8
13.6	20.2	4.77	3.66	52.6	37.6	89
13.9	20.5	4.9	3.5	53.5	37.6	89
15.2	20.7	4.94	4,08	53.4	37.5	90
7.7	19.2	4.54	1.59	52	36.5	85.5
7.25	19.3	4.57	1.73	52.4	37.2	85.7
6.35	19.2	4.6	1.26	52.4	37.4	84.8
4.9	18.5	4.38	.95	51.3	37.8	83.6
3.75	17.6	4.09	.59	49.8	37.1	82.4
2.6	16.8	3.8	.43	48.1	37.3	81.2

Coal B. T = 17°C.

F	Q	Δp	Δpx	u	s	p
6.95	18.3	2	1.81	50.2	37.6	84.6
1.95	16.8	3.71	.5	47	37.9	82.4
3.05	17	3.78	.75	47	37	83.2
3.87	17.5	3.81	1.13	47.8	37.6	83.9
5.2	18.3	4.17	1.5	49.4	37.7	85.2
6.23	18.7	4.3	2	50.1	37.8	85.9
8.62	18.9	4.29	2.6	49.8	37.2	87.2
10.4	19.8	4.59	3.1	51.3	37.6	88.6
12.7	20.8	4.87	3.9	52.8	37.6	90.5
14.9	21.6	5.15	4.75	53.8	37.6	92.3
16.8	21.9	5.2	5.7	54	38	932
16.6	21.5	5.13	5.4	53.4	37.8	93.7
16.6	21	4.8	5.84	52	36	94
16.1	21	4.8	5.6	52.1	35.4	94.1
16.2	21.2	4.88	5.97	52.6	35.2	94.2
18.5	22.4	5.35	6.5	55	36.7	95.3
20.5	23.6	5.67	7.53	56.2	36.5	97.9
24	24.6	5.95	8.52	57.3	38.2	100
10.3	20.1	4.61	3.24	51.4	37.8	89.3
11.3	23.9	6.05	3.11	59	46.1	92.2
14	25.1	6.45	3.73	60.5	46	94.4
15.2	25.5	6.55	4.43	60.6	46.5	95.6
18.2	26.7	6.95	5.17	62.3	45.6	97.8
19.8	27.4	7.13	5.81	62.6	46	99.6
22.6	27.6	7.1	7.17	61.9	45.5	101.5
24.5	27.4	6.95	8.8	60.7	-	102.8
9.1	22.2	5.4	2.38	55,7	45.4	90.6
9.1	23	5.8	2.47	57.9	45.2	90.7
9.25	23.2	5.85	2.33	58.3	45	90.6
7.9	23.4	5.97	2.09	59	46	90.4
6.5	23	5.9	1.46	59	46	89.1
4.64	22.3	5.65	.97	58	46	87.8
3.42	22	5.53	.7	58	45.5	86.7
2.33	21.7	5.5	.24	57.9	46	85.7
10.9	23.4	5.86	2.92	58.1	46	91.8
9.94	20.7	4.8	3.17	52.5	37.5	89.8
12.6	29	8.2	2.63	68.5	57	96.6
13.1	27.6	7.45	3.46	64.5	57.4	96.6
12.7	27.6	7.4	3.63	64.5	56.3	96.6
25	27.3	6.83	8.14	59.7	45.6	103.4
20.2	25.2	6.23	6.78	58.3	44.6	98.6
20.4	25.1	6.2	6.85	58	45.6	98.7
23.3	30.7	8.36	6.6	67.1	56.7	104.9
25.1	32	8.75	7.34	68.4	55.4	107.4
20.5	31	8.6	5.83	68.5	56	103.6
17.9	30.4	8.45	5.13	68.4	57.3	101.9
15.3	30.2	8.45	4.16	69.5	58	100.3
13.5	29.5	8.25	3.66	68.5	58	98.8
11.5	29.2	8.17	3.23	68.4	58	97.7
9.65	28.3	7.9	2.52	67.5	58	95.7
7.45	27.6	7.7	1.9	67.5	58.7	93.8
5.8	26.8	7.43	1.51	66.5	58	92.3
4.25	27	7.6	1.09	67.8	59.4	91.4

Coal B (cont'd.)

F	Q	Δp	Δpx	u	s	p
2.94	26.3	7.35	.79	67	58	90
I.9I	26.7	7.6	.42	68.5	-	89.2
2.2	3I	9.6	.7	76.5	69	92.9
3.44	3I.5	9.8	I.02	77	68	93.9
5.3	32.4	9.85	I.44	77.6	69	96
7.5	32.4	9.8	I.94	76.I	69	97.6
8.87	33.2	I0.I	2.48	76.6	69	99.4
I0.5	33.8	I0.3	2.92	76.8	68.5	I0I
I3.I	34.6	I0.5	3.47	76.9	67.8	I03.2
I5.3	36	II	4.02	78.2	68.5	I05.7
I8.6	36.8	II.2	4.82	78	68	I08
2I.8	37.9	II.5	5.49	78	65.5	III.3
23.5	37.4	II.3	5.25	77.6	64.5	II0.5
2I	38.2	II.7	4.87	80.3	66.5	I09.7
24.2	38.9	II.8	5.68	79.4	66	II2.8
I8.I	37.2	II.5	4.27	79.4	67.3	I08
I6	36.5	II.3	3.78	78.6	67.3	I06.7
I3.8	35.2	I0.7	3.2	77.7	65.9	I04.2
8.3	33	I0.I	I.97	77.I	66.5	98.5
5.I	32	9.75	I.29	76.5	67	96.4
.88	30.4	9.5	.I6	77	-	90.8
I9.9	44.4	I4.6	4.72	87.7	75.8	II6.8
I8.2	43	I4.I	3.97	87	76.2	II3.8
I4.5	42.2	I3.8	3.63	86.5	77.5	II2.5
I3.4	4I.4	I3.7	3.07	87	77.4	I09.2
II.I	40.6	I3.5	2.5I	87	76.5	I07.3
8.4	40	I3.4	2.09	87.2	76.5	I05.2
6.3	39.4	I3.3	I.64	87.6	77.5	I03.3
4.27	39.5	I3.5	I.I5	89.2	76.7	I0I.9
2.64	39.5	I3.7	.67	90.7	-	I00
I.2	39.2	I3.8	.22	9I.7	-	98.I

Coal C T = I2°C

F	Q	Δp	Δpx	u	s	p
5.7	I6.5	3.47	2.0I	44.8	30.I	84.2
8.4	I6.9	3.46	3.27	43.7	30	88.9
I2.2	I7.5	3.75	4.88	45.8	30.I	88.8
I5.3	I .2	3.85	7.23	45.8	30	92.I
I9.9	I9.I	4.07	9.49	46.8	30	94.7
7.I2	I9.7	4.62	2.I3	5I.7	39.I	86.9
8.75	20.4	4.86	2.5	53.I	38.5	87.7
8.94	I9.5	4.5	2.86	5I	39.I	87.8
I3.3	20.9	4.86	4.2	52.6	39.I	9I
I7.5	2I.I	4.8	6.44	5I.4	39.I	93.8
7.44	24.8	6.6	I.85	62.3	50.5	9I.2
I0.4	24.I	6.27	2.83	60.6	48.5	92.3
I4	24.7	6.4	3.96	60.9	48.5	94.4
I9.4	26.2	6.8	5.68	6I.7	48.5	98.8
I9.3	26.9	7.I7	5.I7	6I.9	48.7	98.6
23.9	28.8	7.8	6.94	63.5	48,7	I03.2
8.44	30.I	8.8	2.04	7I	60.5	96.9

Coal C (cont'd.)

F	Q	Δp	Δpx	u	s	p
I2.5	30.7	8.87	2.98	70.7	60.5	99.3
I7.6	32.I	9.25	4.28	7I.6	60.5	I02.6
22.3	32.I	9.I	5.54	70	59	I05
I0.4	37.5	I2	2.55	8I.8	75.5	I05.4
I4.7	39.9	I2.8	3.6	83	75.5	II0.4
I5.6	40.5	I3.I	3.97	83.8	75.5	III
20.4	4I	I3.I	5.I3	82.5	75.5	II4.2

Coal D T = I6°C.

2.97	I5.4	3.08	.94	42.4	30	82.6
3.8I	I5.6	3.I7	I.I2	42.7	30.2	83.3
5.2I	I5.9	3.74	I.68	43	30.5	84.3
6.75	I5.9	3.2I	2.I4	42.6	30	85.I
7.97	I6.I	3.24	2.67	42.6	28.5	85.8
9.34	I6.I	3.32	3.I5	42.2	29	86.8
I0.9	I6.5	3.33	3.5I	42.9	3I	87.7
I2.6	I6.5	3.3	4.I	42.5	30	88.4
I4.2	I6.9	3.4	4.67	42.9	30	89.5
I6.I	I6.6	3.28	5.67	4I.8	28.7	90.4
I7.8	I7.2	3.43	6.26	42.6	30	9I.8
I9.I	I7.4	3.48	6.7	42.6	30.3	92.7
I.25	I5.7	3.26	.43	44	32	8I.6
2.5	I7.2	3.8	.55	47.3	35	83.I
3.3	I7.6	3.9	.83	47.7	35.4	84
4.2	I7.7	3.9	I.I4	47.6	35	84.7
7.32	I8.2	4	I.88	47.9	34	86.5
6.2	I8.3	4.06	I.68	48	34.5	86.I
II	I8.7	4.I2	3.22	47.9	35.5	88.7
I4.I	I8.8	4.06	4.06	47.2	36	90.2
I7.4	I9.3	4.I8	5.I2	47.4	35	92.4
2I.2	20	4.3	6.46	48	35	94.8
2.I	20.7	5.08	.5I	55	4I.5	85.3
5.72	20.9	5	I.4	54	40	87.8
8.8	2I.4	5.I	2.05	54	40.5	89.9
I2.2	2I.7	5.I	2.97	53.8	39.8	9I.7
I5.5	2I.4	4.9	4.04	52	4I.4	93.2
I9.4	22	5.05	5.I8	52.4	40	95.4
22.6	22.I	5	6.I8	5I.9	40.2	96.8
3.65	26.I	7.2	.79	65.5	5I	90.2
7	26.5	7.I7	I.47	64.8	49.5	92.5
II.I	26.9	7.I7	2.5	63.7	5I	95.7
I5.4	27.6	7.3	3.7	63.5	50.5	98.6
20.4	28	7.3I	4.57	63	50	I0I
24.8	28.4	7.34	5.76	62.2	50	I03.2
28.3	29.5	7.74	6.64	62.7	50	I06.2
II.3	27	7.I6	2.56	63.7	50.5	96
I3	27.7	7.4	2.89	64.4	50.5	97.4
I5.5	28.3	7.54	3.5	64.6	5I	99.2
I7.6	29.2	7.85	3.89	65.7	5I	I00.9
23.I	29.7	7.87	5.32	64.8	50.5	I03.9
27.8	30.5	8	6	64.5	50.5	I06.9

Coal D (cont'd.)

F	Q	Δp	Δpx	u	s	p
12.2	31.7	9.17	2.07	71.8	61	100.6
17.2	33.6	9.7	3.32	72.5	61	105.6
24.6	37.2	11	4.8	75.1	62.5	112.6
23.7	37.6	10.9	6.01	74.4	64	115
6.44	40.3	13.6	1.44	88.2	77	104.8
11.4	42.1	14.1	1.92	88.2	77	109.9
17.1	45.4	15.2	3.24	88.8	77	117.5
22.7	47.2	15.5	4.17	88.2	77	123.4
27.9	47.5	15.2	5.14	86	77	127.4
11.1	16	3.14	3.9	42	27.5	87.6

Coal E T= 15°C.

3.42	16.3	3.42	.91	45	29.9	83.6
4.65	17	3.65	1.02	46.2	29.7	84.5
5.77	17.1	3.67	1.22	46.2	29.2	85.2
7.71	17.3	3.68	1.96	46	29.7	86.7
9.04	17.5	3.74	2.18	46	29.7	87.5
10.8	17.7	3.77	2.65	46.1	29.7	88.4
14	17.8	3.77	3.71	45.7	29.7	89.9
16.3	18	3.78	4.54	45.4	30.1	91.4
4.4	21.4	5,3	.81	56.5	39.8	87.2
6.84	21.6	5.24	1.22	55.6	39.8	89.3
10.3	22.1	5.42	1.89	56.2	39.8	90.9
13.7	22.5	5.46	2.66	55.7	39.8	92.7
16.9	22.4	5.34	3.46	54.8	39.8	94.1
19.1	22.6	5.34	4.2	54.7	39.8	95.6
21.1	22.7	5.34	4.69	54.3	39.8	96.7
3	27.1	7.8	.44	69.4	51	90
6	27.1	7.58	.94	67.5	51	92.2
9.44	27.9	7.8	1.52	68	51	94.7
13.6	27.9	7.58	2.52	66.2	51	97.2
17.8	28.5	7.67	3.35	65.6	51	100.2
22.7	29.7	8.02	4.3	66	51	103.7
26.9	30.1	8.05	5.2	65	51	105.7
4.5	32	9.6	.65	76.8	63	95.5
7.4	33.4	10	1.1	77	63	98.9
12.5	33.8	10	1.75	76.5	63	101
15.8	35.1	10.3	2.3	76.2	63	105.2
18	35.8	10.8	2.9	76.5	63	106.7
22.7	37	11.1	3.1	76.2	63	110.9
28.1	37.8	11	4.9	74.6	63	115.3
9.56	25.4	7.02	1.81	64.5	51.8	91.8
14.7	26.5	7.27	2.97	64.7	52.2	95.3
19.3	27.4	7.53	4.1	65	52.2	98.4
24.4	29.1	8.06	5.07	66.5	52.2	102.3
7.62	31.6	9.83	1.77	76.5	63.3	96.9
11.8	31.9	9.8	2.22	75	63.3	99.3
17.5	33	9.98	3.62	74.5	63.3	103.6
23.4	34.9	10.6	4.51	75.4	63.3	108.2
10.9	26	7.15	2.33	64.2	52.2	94.2
14.5	26.9	7.4	3.16	65	52.2	96.8

Coal E (cont'd.)

F	Q	Δp	Δpx	u	s	p
19.5	27.6	7.53	4.17	64.5	52.2	99.6
24.8	28.2	7.63	5.35	64.3	52.2	102.7
15.7	33	10.1	2.8	75	63.3	103.2
21.8	33.5	9.95	4.4	73	63.3	107.2
7	26.7	7.7	1.22	68.5	52.2	91.7
11.1	26.8	7.53	2.14	66.5	52.2	94.7
15.7	27.5	7.63	3.12	65.8	53	98
20.7	27.9	7.6	4.15	64.8	52.2	101.1
25.1	29	7.9	5.25	65.5	52.2	104.2
10.1	31.6	9.75	1.98	75.4	63.3	98.4
15.6	33.2	10.2	2.99	76	63.3	102.9
21.1	34.1	10.3	4.19	74.3	63.3	107.5
25.6	35.3	10 5	5.04	74.5	63.3	111.1
10.1	40.7	14.1	1.74	88.7	75.4	107.5
18.8	41.5	13.8	3.43	88.5	75.4	113.7
25.7	42.8	13.9	4.9	84	75.4	119.5

Radish T= 22°C

-	19.9	4.91	.99	54.7	32	85.7
3.7	20.5	5.16	.68	56.4	33.5	85.7
5.03	18.9	4.51	.83	52	31	85.3
7.3	19.2	4.46	1.27	52	31.5	87
9.37	19.6	4.61	1.93	52	31	88.8
11.4	20	4.73	2.39	52.5	31.5	90
12.2	20.4	4.86	2.8	53	32.5	90.3
10.2	19	4.4	2.37	50.6	30	88.2
7.8	19.0	4.38	1.72	50.7	30	86.8
5.81	19	4.55	1.2	52.2	31	85.7
5.3	23.1	6.22	.88	62	40	87.9
7.4	22.6	5.92	1.53	59.7	39	89
9.5	22.6	5.85	2.3	59	38.5	90.6
11.6	23.4	6.04	3.05	59.3	38.5	92.9
12.3	23.2	5.86	3.92	58	39	94.1
9.8	23.1	5.89	3.46	58.3	38	92.5
8.2	23.2	6.02	3.28	59.6	38.5	92
6.5	24.1	6.48	2.56	62.5	39	91
-	23.1	6.32	2.28	62	39	90
-	23	6.28	2.42	61.8	39	89.9
-	23.1	6.3	2.54	61.9	39	89.9
-	22.9	6.21	2.81	61.3	38.5	90.1
5.94	22.9	6.21	2.83	61.3	38.5	90.1
-	22.8	6.19	2.84	61.2	38.5	90.1
-	22.8	6.17	2.87	61.1	39	90.1
5.75	22.7	6.15	2.99	61	38.5	90.1
5	28.6	8.71	2.47	73	47.5	94.1
-	28.1	8.24	3.54	70	47.5	96.2
-	28.8	8.53	3.79	71.1	47	97.3
7.5	28.7	8.54	4.03	70.6	47	97.6
9.56	28.5	8.18	5.22	69	46.5	99.4
11.9	29.4	8.35	6.79	68.5	46.5	102.7
13.4	30.2	8.59	8.79	69	46.5	105.2
11.1	11	8.64	8.16	70	46.5	103.3
8.9	30.6	9.13	6.85	72.3	46	101.7
13.4	34.6	10.3	10.8	74.6	50.5	111.4
11.7	35.2	10.8	9.95	76.5	50.5	110.4

Perspex B. T = 20°C.

F	Q	Δp	Δpx	u	s	p
2.9	I6	3.48	.I0	46.7	29.5	8I.8
3.05	I6.5	3.65	.58	47	30	82.8
6.95	I6.7	3.7	.76	47	3I	83.7
9.2	I7.I	3.9	I.I	48.8	3I	83.9
II.4	I7.I	3.85	I.7	48	30	84
I3.6	I7.5	3.97	I.98	48.7	30	84.9
IC.9	I7.3	3.95	I.4	48.8	30	83.4
7.9I	I6.8	3.7I	I.04	47	30	84.3
5.45	I6.3	3.54	.64	46.2	29.5	83
5.57	I9.9	4.96	.29	55.3	39	85.2
7.9	20.9	5.33	.42	57.2	40	86.6
IC.4	2I.8	5.69	.74	58.8	40.5	87.7
I2.C	2I.3	5.34	I.25	57	39	88.5
I5.5	2I.5	5.4I	I.65	56.7	39	89.7
I5.3	2I.6	5.45	I.6I	57	39.5	89.4
II.7	2I.I	5.3I	I.I3	56.6	39.5	88
8.3	20.9	5.28	.79	56.8	39	87
5.86	20.5	5.I3	.48	56	40	86.I
7.4	3I.4	IC.I	.32	76.6	59.5	94.6
IC.4	3I.8	IO I	.88	77.6	6I	97
I3.6	32	IO.2	I.I7	77.2	60.5	98.3
I6.9	32.5	IO.2	I.57	77	6I	IOO.I
I9.4	33.2	IC.5	I.66	77.3	62	IOI.I
I4.9	32	I0.I	I.2I	77	60.5	98.6
I2.I	3I.I	9.76	.82	76.5	59	96.4
8.7	3I.3	9.95	.57	77.7	60.5	95.4
9.3	40.6	I4.6	.7	92.4	76.5	IO4.I
I3.I	42.8	I5.6	.87	93.7	77	IO8.2
I3.4	43.5	I5.7	I.22	93.2	76.5	IIO.7
2I.4	45.4	I6.3	I.75	94	78	II4.8
23.6	47.3	I7	2.05	95.5	77	II7.6
I7.5	44.6	I5.8	I.77	92.5	77	II4.6
I5.3	43.8	I5.9	I.02	94	77	IIO.I
II.I	42.8	I5.7	.65	95	77	I07.I
I4.8	33.3	IO.6	I.I2	79.5	6I	99.3
I2.2	2I.I	5.35	.95	57	40	88
II.8	I6.8	3.7I	I.6	46.7	30	85.3
II.4	2I.8	5.75	.63	59	40	87.7

Rape T = 2I°C.

F	Q	Δp	Δpx	u	s	p
4.9	I6.9	3.79	.82	47.8	30	83.2
5.9	I7.5	4	I.0	49	30	84
6.8	I7.4	3.92	I.I5	48.4	30	84.4
8.I	I7.6	3.94	I.59	48.2	30	85.2
9.3	I7.9	4.05	I.9	48.9	30	86
I0.4	I2.9	4.0	2.5	48.4	30	86.7
I4.5	I8.I	4.06	3	48.7	30	87.7
I3.2	I8.8	4.2	3.7	49	30	89.I
I4.6	I8.7	4.I4	4.42	48.6	30	90
II.3	I8.2	4.06	3.46	48.6	30	88.3
8.8	I8.2	4.I4	2.43	49.2	30	86.7
6.36	I7.7	3.97	I.7	48.8	30	85.I
3.69	2I.7	5.67	.75	59.4	40	86
5.0	2I.9	5.67	I.07	59.2	40	86.9
6.2	22	5.67	I.43	59	40	87.9
7.3	22.5	5.83	I.79	59.5	40	88.9
8.8	23.2	6.04	2.2	60.2	40	90.3
I0.I	23.4	6.04	2.8	59.8	40	9I.8
II.4	23.5	6.0	3.5	59.5	40	92.7
I2.6	23.7	6	4.57	59	40	94.3
I7	24.2	6.04	6.I6	58.5	40	97
3.5	I8.3	4.33	I.82	50.7	29.5	85.2
5.3	I8.2	4.2	2.57	49.7	29.5	86.4
8.2	I8.7	4.3I	3.34	50.I	3I	88
I0.3	I8.3	4.II	4.I3	48.3	30.5	89.2
I4.I	I8.9	4.26	4.84	49.2	30.5	9I
I6.2	I8.8	4.I6	6.29	48.2	29.5	92.2
I5	I8.9	4.25	4.85	49	30	9I
II.9	I8.6	4.22	3.78	49.2	30	9I
8.4	I8.3	4.23	2.43	49.4	30.5	86.8
5.3	I7.8	4.II	I.6	49.6	30	84.8
8.8	I8.4	4.24	2.59	49.8	30.5	87.I
I3.I	I8.8	4.28	4.22	49.4	30.5	89.8
4.5	22.3	5.94	I.26	60	39	87.6
6.3	22.3	5.85	2.0	59.I	39	89.I
9.8	22.8	5.8I	3.I4	58.4	39	92.I
I0	23.I	5.83	4.37	57.8	39	94.3
II.9	23.4	5.93	4.55	58.4	39	94.7
-	29.9	9.I2	I.98	74	50	95.4
-	29.8	8.82	3.46	7I.7	50	98.3
-	29.6	8.7I	4.09	7I	50	98.9
-	29.4	8.52	5.08	70.4	50	99.4
-	29.3	8.5	5.6	70.7	50	98.8
-	29.I	8.3	6.8	69	42.5	I00
-	3I.2	9.I	8.I5	7I.7	46.5	I03.4
-	32	9.4	8.05	72.5	45	I04.I

NOTE: Results are given in chronological order; the seeds break up with time of conveying.

Polystyrene T = 10°C

F	Q	Δp	Δpx	u	s	p
5.50	31.1	8.6	I.I	71	59	99.8
5	30.9	9.06	I.44	71.3	62	101.7
-	30.9	6.9	2	70	60.5	103.8
[illegible]	31.1	9.05	I.65	71.2	62	102.7
[illegible]	31.4	8.81	3	66.7	62	107.5
[illegible]	30.4	9	I.05	71.8	62	99
2.85	16.9	3.88	.37	46.4	39	85.4
.45	18.3	4.1	I.14	48.5	39	88.8
4.44	19	4.1	2.08	48.4	40.5	92.6
9.	19.7	4.27	3.23	47.6	40	97.1
-	21	5	2	53.4	46.5	92.1
8	21.6	4.91	I.93	53.3	46.5	91.8
3	14.6	2.86	I.16	41.5	34.2	83.6
.9	15.1	2.94	I.33	41.2	35.2	85.1
3.46	14.7	2.74	2.07	39.7	34	86.8
3.5	15	22.73	3.41	36.7	34.2	90.5
[illegible]	26.5	7.3	I.59	65.6	59	94.5
3.45	27.6	7.6	I.6	67.5	59	96.6
8.45	28.5	8.03	2.27	67.7	60.5	98.3
10.6	28.7	7.96	2.9	67.1	89.5	100.1
2.7	17.2	3.82	I.13	47.1	39.5	85.3
5.55	17.2	3.71	I.85	46.2	39.5	86.9
.9	17.6	3.76	2.81	45.5	40	90.3
11.4	17	3.48	3.86	43.6	40	91.4

Perspex A T = 23°C

F	Q	Δp	Δpx	u	s	p
I.9	14.8	2.99	.27	43	30	81.3
3.65	15	3.05	.63	43	30	82.3
5	15.3	3.15	.99	43.3	30	83.2
8.5	15.9	3.31	I.71	44	30	84.9
12	16.2	3.41	2.79	44.3	30	86.4
14.3	16.4	3.44	3.73	44	29.5	87.6
17	16.5	3.45	4.58	43.7	29.5	88.7
13.6	16.5	3.49	3.23	44.6	29.5	87.2
7.1	15	2.99	I.67	42.2	29.5	84
13	14.9	3.04	.89	43	29	81.7
15.6	16.5	3.47	4.15	44.3	29.5	88.1
13.1	15	3.06	.46	43	29.5	82
15.6	16.3	3.4	4.04	44	29.5	87.9
6.2	19.4	4.78	.59	53.5	38.5	85.7
13.1	20.6	5.06	I.7	55	40	88.9
18	20.3	4.9	2.53	53.5	39	89.8
18.1	20.8	5.05	3.02	54	39	91
9.6	19.5	4.77	I.16	53.3	39	87
6	15.1	3.06	I.25	43	28.9	83
11	15.7	3.26	2.53	43.5	29	85.3
16.3	16.7	3.53	4.14	44.9	29.8	88.1
11.5	16.1	3.32	2.69	44.4	29.8	85.7

Perspex A (cont'd.)

F	Q	Δp	Δpx	u	s	p
5.1	15	3.06	I.22	42.9	29.8	82.8
6	19.2	4.7	.69	53.4	39	85.3
11.5	19.7	4.76	I.79	53	39	87.7
17.5	20.6	4.97	3.02	53.7	40.5	90.7
13.1	20.5	5.03	I.99	54.9	40	88.9
6	19.2	4.71	.75	53.4	39.5	85.1
8	28.4	8.65	.65	73	60.5	92.5
12.4	28.5	8.5	I.21	71.5	60.5	94.5
16	28.4	8.34	I.59	70	59.5	95.9
20.5	28.8	8.37	2.33	69.5	59	98.1
23.7	29.4	8.46	3.04	69.5	58	100.3
18.6	28.6	8.31	2.14	69.5	59	97.5
11	27.9	8.24	I.13	70.5	59	94
10.78	36.8	12.6	.87	85.6	77	101.9
16.6	36.8	12.2	I.75	83.5	77	105.3
23.3	44.9	15.7	2.5	91	81	117.7
28.3	47.8	16.6	3.4	91.5	81	124.1
32	50.3	17.4	4	93.7	84	128.2
21.9	40.3	13.6	2.6	86.2	77	111.3
13.2	41	14.4	I.45	90	77	108.4
5.15	15.1	3.09	I.3	43.3	29.5	82.9
6.15	18.7	4.53	.99	52	39	85.3
8.1	27.5	8.2	.83	70.9	59	92.5
11.1	38.3	13.1	I.45	87.3	77	104.3
8.5	28.3	8.52	.84	71.8	59	93.5
6.1	18.9	4.62	.83	52.6	39	85.3
5.4	15.5	3.26	I.27	44.4	29.8	83.1
11.81	16.4	3.52	3.08	45.2	30	86.4
13.1	19.8	4.77	2.47	53	39	89.1
17.6	29.7	8.89	2.2	71.5	59	98.9
21.5	39.4	13.1	2.4	85	76	110.1
14.0	20.5	5.01	2.6	54.1	40	90.2
12.4	17.1	3.76	3.14	46.3	29.5	87.3
18.6	31.2	9.39	2.09	73.5	59.9	100.5

Perspex C. T = 24°C.

F	Q	Δp	Δpx	u	s	p
3.2	28.4	8.66	.14	74.3	62	90.7
4	28	8.61	.34	72.8	61	91.2
7.5	28.2	8.55	.9	72	63	93.2
-	28.4	8.67	.83	72.5	64	93.2
5.5	28.6	8.8	.68	73.2	63	92.7
-	35	11.9	.67	84.4	77	98.6
-	29.6	9.27	.67	75.3	64	93.8
-	18.9	4.66	.35	53	41	84.7
-	27.2	8.14	.55	70.7	59	91.3
-	13.8	2.55	.84	40	31	81.9
-	36.2	12.5	.54	86.4	76.5	99.7

Lead. T = 17°C.

F	Q	Δp	Δpx	u	s	p
13.8	34.9	11.1	2.55	80	43	103
13.5	35.6	11.5	2.41	81	45	103.6
13.9	36.6	11.9	2.3	82.5	46	104.5
14.1	37.7	12.5	2.22	84.5	48	105.3
16.1	45.9	16.5	1.95	95	57.5	114.2
16.6	48.1	17.5	2.16	97	60.5	117
17.5	52	19.3	2.25	101	65.5	121.6
18.4	54.1	20.2	2	103	68	124.2
17.3	50.5	18.7	2.1	99.5	60.5	119.6
15.9	37.6	12.5	2.26	84.6	48	104.7
14.3	36.3	12	1.84	83.4	45	102.8
13	31.3	9.68	1.92	75.7	40	97.6
13.6	36.9	12.3	1.68	85	47	102.8
15.9	53.7	20	2.2	103.	68	123.6
12.1	38.5	13.1	1.55	87.8	47.5	103.2
32	36.6	11.2	5	77.2	38.5	111.6
34.6	49.5	16.9	5	91.5	51.5	127.5
32.1	52.5	18.2	5.1	94.6	57.5	130.8
8.9	56.6	22.7	.8	112	72.5	120
13.4	55.2	21.2	2.1	107	68.5	122.1
15.6	54	20.6	1.65	105	65	121.7
20.7	52.2	19.1	2.6	100	59	123.5
42.8	49.8	16.5	6.5	89	51.5	132
10.3	49.1	18.9	.6	103	62	112.8
15.4	47.1	17.2	1.7	97	55.5	114.6
25.4	45.6	15.6	3.5	90.5	51.5	119
33.3	43.6	13.9	6.2	83.5	45	123.3
42.3	43.4	13.7	6.55	82.5	44	124.3
32.2	44.2	14.6	5	86.5	46.5	120.5
8.3	39.9	14.2	.55	91.9	53	102.5
11.9	38.3	12.5	2.5	84.4	46.5	107
23.8	50.9	18	2	95	52	126.5

Aluminium. T = 20°C.

9.1	30	9.22	2.02	74.1	62	95.6
13.7	31.8	9.82	3.28	75.8	62	99.4
20	32.8	10	5.3	75	60.5	103.7
31	38.6	12.2	7.2	80.6	62	113.2
22.1	37.6	12	6.2	80.5	62	110.6
6.8	32.3	10.4	1.54	79.1	65.5	96.5
3.26	16.5	3.66	1.27	47	-	83.3
12.5	19.1	4.77	3.4	51	-	88.9
23.5	24.2	6.26	6.09	59.5	-	96.2
2.05	17.6	4.24	.3	50.7	40	82.5
3.6	19.3	4.84	.9	54.3	41.5	84.6
6.7	20.2	5.07	1.93	55	41	86.9
11.6	21.5	5.49	2.94	57	40.5	89.6
3.5	28.6	8.77	.47	73.8	60.5	91
3.25	28.7	8.81	.44	74.3	60.5	90.9
4.5	28.7	8.78	.52	74	60.5	91.3

Aluminium. (cont'd.)

F	Q	Δp	Δpx	u	s	p
9	30.3	9.25	1.95	74.4	60.5	95.8
17.4	32.8	9.93	4.69	75.2	59.5	102.6
25.2	39	12.3	6.5	81	64	112.2
31.3	38.1	11.4	9.08	78	60.5	114.8
17	44.7	15.5	4.1	91	77	115.5
15	51.3	19	3.1	101	84	119.9
8.4	52.1	20.2	1.0	106	87	116.1
5.7	44.8	16.7	.25	98	82.5	106.9
33.5	28.6	7.49	11.6	62.8	40	107
28	28	7.45	9.05	63.8	40	103
20.5	25.7	6.78	5.02	62	40.5	97.4
15.4	23.9	6.2	4.34	60	40	93.5
9.1	22.2	5.7	2.32	88.6	41	89.3
9	16.6	3.03	3.91	45.3	27.1	86.5
12.9	18.1	3.94	5.26	47.1	28	90
21.6	22.2	5.22	9.38	53.4	33	97.7

Brass. T = 18°C.

13.6	21.2	5.22	2.94	55.4	40.5	90.1
23.6	24.7	6.3	5.8	59.5	42.5	97.6
22.3	25.4	6.6	5.1	60.7	47.5	98.1
22.9	30.3	8.64	4.81	69.4	59	103
12	32	9.9	1.7	76	63	98.9
4.63	32	10.4	.5	79.5	63	94.7
5.6	47.7	18	.5	101	82.5	110.8
18	45	15.5	2.7	90.5	78	117
25.3	44.5	14.8	4.5	87	78	120.4
43.5	48.5	15.7	7.85	86	73.5	132.6
3.13	23.4	6.4	.44	62.5	48.5	87.1
5.1	23.7	6.45	.69	62.4	48.5	88.6
8.25	24.1	6.41	1.49	61.8	48.5	90.9
10.9	25.8	7.05	1.91	64.5	48.5	93.4
18.1	25.9	6.9	3.52	62.9	48.5	96.6
23.6	27.7	7.48	4.42	64.7	48.5	100.2
34.1	30.5	8.35	6.8	66.5	48.5	107.3
46.5	29.8	7.67	11.8	62.4	48.5	112.2
26.8	28.2	7.6	4.9	64.7	46.5	102
5.06	44.1	16.1	.7	95.3	78	108
8.44	45.2	16.1	1.55	93.6	78	113.2
13.6	46.7	16.1	2.55	91.5	78	119.4
19.5	47.4	16.1	3.35	90	78	123.5
27.5	48.6	15.9	5.95	87	73	130.5

Sand (selection of results.)

t	F	Q	Δp	Δpx	u	s	p
First experiment. 30-9-58 T-17°C. New sand-control settings constant,							
5	6.5	34.3	10.7	1.4	78	59	102.6
10	-	33.2	10.1	1.88	75	52	103.2
15	-	33.4	10	2.7	75	50	104.6
2[illegible]	-	32.9	9.75	3.05	74	49	104.7
22	-	32.8	9.7	3.6	73	46	104.7
25	-	32.5	9.48	4.57	72	45	105.2
27	-	32.7	9.6	4.65	73	44	104.9
30	-	32.2	9.32	5.58	72	43	105.4
33	-	32.2	9.3	5.7	71	42	105.5
37	-	32.1	9.3	5.96	71	-	105.4
40	6.1	32	9.17	6.33	71	40	105.7
50	6.3	31.5	8.85	7.15	69	40	106.6
60	6.1	31.4	8.83	7.37	69	40	106.6
- equilibrium reached -							
cont'd 1-10-58 - at equilibrium.							
5	6.9	32.6	9.3	7.4	71	44	108
20	6.3	32.5	9.35	7.25	71	40	106.7
30	7.6	32.5	9.37	8.18	72	41	106.5
45	6.4	31.1	8.71	7.74	69	41	106.6
50	6.7	31.2	8.72	7.78	69	40	106.9
continued 2-10-58- at equilibrium.							
10	5.8	32.7	9.27	8.33	71	39	108.3
30	5.4	32.4	9.19	8.01	71	38	107.2
60	4.9	32.3	9.24	7.36	72	38	106
85	4.8	32.5	9.5	6.78	73	38	104.7
100	4.8	33.6	10.1	6.56	74	40	105.2
110	1.5	32	10.4	2.19	80	41	93.8
130	3.9	35	11	5.45	79	41	103.8
140	1.1	33.2	10.6	2.12	84	39	93
150	1.1	37.5	13.3	1.58	90	45	96.6
continued 3-10-58- at equilibrium.							
5	2.9	33.4	10.4	6.25	77	39	101.2
25	3	32.9	10.1	4.63	77	38	100.5
40	4.9	31.2	9.05	6.5	71	37	104.8
60	7.6	33.3	9.9	6.72	74	42	105.5
80	2.8	32.6	9.7	5.5	74	40	103.5
continued 7-10-58- at equilibrium.							
15	2.8	32	9.82	3.33	76	43	98.8
30	4.1	31	9.12	4.38	72	39	101.2
45	12	31	8.55	5.9	71	43	104.5
80	25	32.6	8.65	9.05	66	44	115.7
100	135	32.7	9.32	6.33	71	44	108
110	3.6	33.5	10.2	4.85	76	41	102.7

t = Duration of continuous conveying after any interval.

t	F	Q	Δp	Δpx	s	u	p
14-10-58 at equilibrium. each set of readings taken at 10 minute intervals.							
10	1.3	34	11.5	.72	48	84	94.2
20	2.07	33.2	10.7	1.78	48	80	96.4
30	3.03	33.2	10.5	2.56	48	79	98.6
40	4.03	33.9	10.6	3.25	47	78	101
50	6.44	37	11.7	4.8	52	81	107.9
60	6.3	31.7	9.27	5.33	47	72	102.8
70	4.87	32.3	9.67	3.83	46	74	101.8
80	7.28	32.7	9.77	5.23	48	74	103
90	9.56	33.4	10	5.4	48	74	104.7
100	13.7	33.6	9.85	6	48	73	107.3
110	15.7	33.5	9.65	6.75	47	72	109
120	18.2	34	9.73	7.22	48	72	111.2
130	20.4	35	10.1	7.85	48	72	113.6
140	25.6	34.5	9.62	8.18	48	70	115.8
150	31.2	34	9.24	8.66	47	68	117.6
160	22.1	33.5	9.37	7.83	47	69	112.5
170	16.4	33.2	9.55	6.6	47	71	108.7
180	11	33.5	10	5.66	47	74	105.8
190	6.3	35	10.8	5.96	48	78	105.2
200	4.63	36.1	11.4	5.15	47	80	105.9
210	3.28	37	12.2	3.97	47	84	103.4
interval of 20 minutes conveyed sand replaced by new sample.							
5	4.05	36.4	11.6	5.3	46	81	105.2
25	4.37	36.2	11.5	5.15	46	81	105.3
35	5.25	38.9	12.4	6.6	46	82	110.2
60	5.5	38.4	12.2	6.25	45	82	109.4
new sample replaced by previous sample interval of 20 minutes.							
5	4.56	38	12.3	5.35	48	83	107.5
15	4.53	38	12.3	5.5	48	83	107.3
Perspex conveyed for 5 mins.@10 lb/min							
5	4.8	33.2	10.8	1.71	61.81		96.6
35	4.37	33.1	10.5	2.3	48	79	98.3
40	4.62	32.8	10.2	3.27	48	77	99.8
continued 16-10-58.							
5	4.2	32.5	9.65	5.85	41	74	102.1
20	3.95	32.4	9.68	5.62	39	74	101.3
30	3.89	32.3	9.6	5.8	40	74	101.3
perspex conveyed for 25 min.@10lb/min							
1	5.28	34.4	11.3	1.6	64	82	96.9
25	4.81	33.4	10.5	2.05	52	78	99.3
40	4.81	32.7	9.9	4.35	47	75	100.8
65	4.44	32.2	9.52	6.68	39	73	102.1

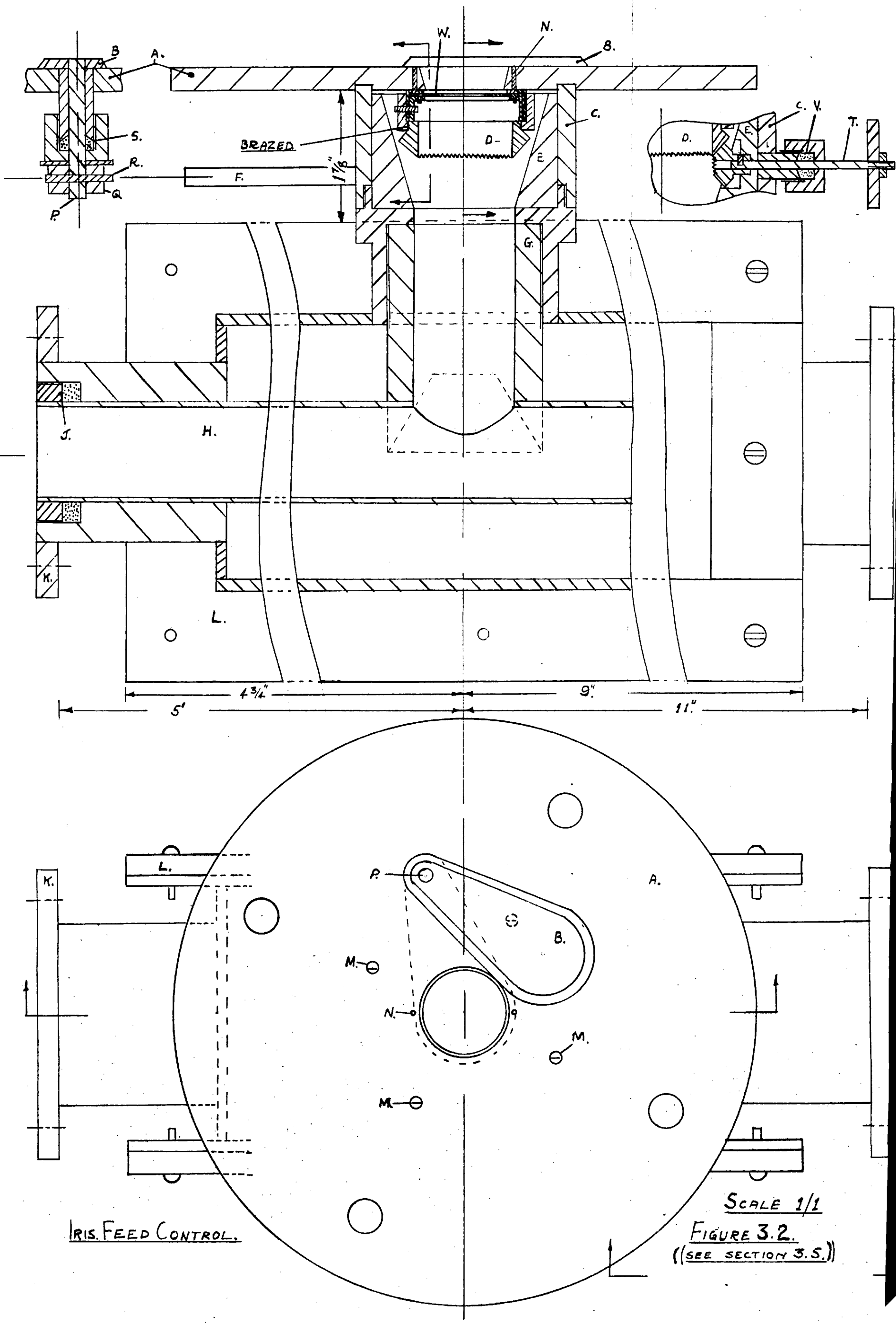
Sand and Manganese Dioxide. T-12°C.

t	F	Q	Δp	Δpx	u	s	p
4-11-58 at equilibrium T-15°C.							
15	4.81	35	10.7	7.82	77	43	105.4
perspex conveyed for 60 min.@11 lb/min							
6-11-58 continued T-18°C.							
5	3.56	22	5.76	.84	60	43	86
30	4.55	24.6	6.74	1.58	64	42	89.7
55	4.25	27.3	7.74	3.41	68	41	93.8
70	4.2	27.3	7.65	4.5	67	39	95
85	4.55	30	8.75	6.1	71	40	99
100	4.62	32	9.47	7.48	74	43	101.7
130	4.62	31.8	9.4	7.6	73	39	101.9
150	4.9	33.5	10.1	8.1	75	42	104.3
160	4.7	33.8	10.3	7.9	76	43	104.1
7-11-58 continued							
cloths pulled through the pipeline.							
15	4.5	33.7	10.2	8.5	75	42	104.6
10-11-58 at equilibrium.							
10	4.5	36.5	11.4	8.5	79	43	106
perspex conveyed for 40min.@10 lb/min.							
10	4.25	22	5.65	.96	59	42	86.6
cloths pulled through the pipeline.							
10	5.2	22.6	5.82	1.18	59	43	87.4
continued 11-11-28							
10	5	23	6.5	.8	61	44	87.8
interval of 20 minutes.							
Sand replaced by Manganese Dioxide.							
controls kept constant.							
1	4.3	22	5.55	2.25	58	39	88
3	-	22	5.52	3.08	58	37	88.5
7	-	22	5.5	3.8	58	35	89
20	-	20	4.52	5.43	52	-	89.4
control settings altered.							
25	3.05	29	8.6	5	72	38	94
30	-	29.1	8.4	7.3	70	39	96.8
35	-	29.2	8.45	7.65	70	39	96.5
50	3.5	29	8.35	8	70	39	96.8
equilibrium reached.							
interval of 20 minutes							
Manganese Dioxide replaced by sand.							
10	4.55	30.1	8.7	6.4	71	43	98.9

Appendix 5.

Graphs and Drawings.

Fig.	3.2	- Page	120
"	3.3	- "	121
"	3.4 & 3.5	- "	122
"	3.6, 3.6,a,b,c., & 3.7	- "	123
Graph	6.1 to 6.18	- "	124
"	7.3 to 7.18	- "	125
"	9.1 to 9.10	- "	126

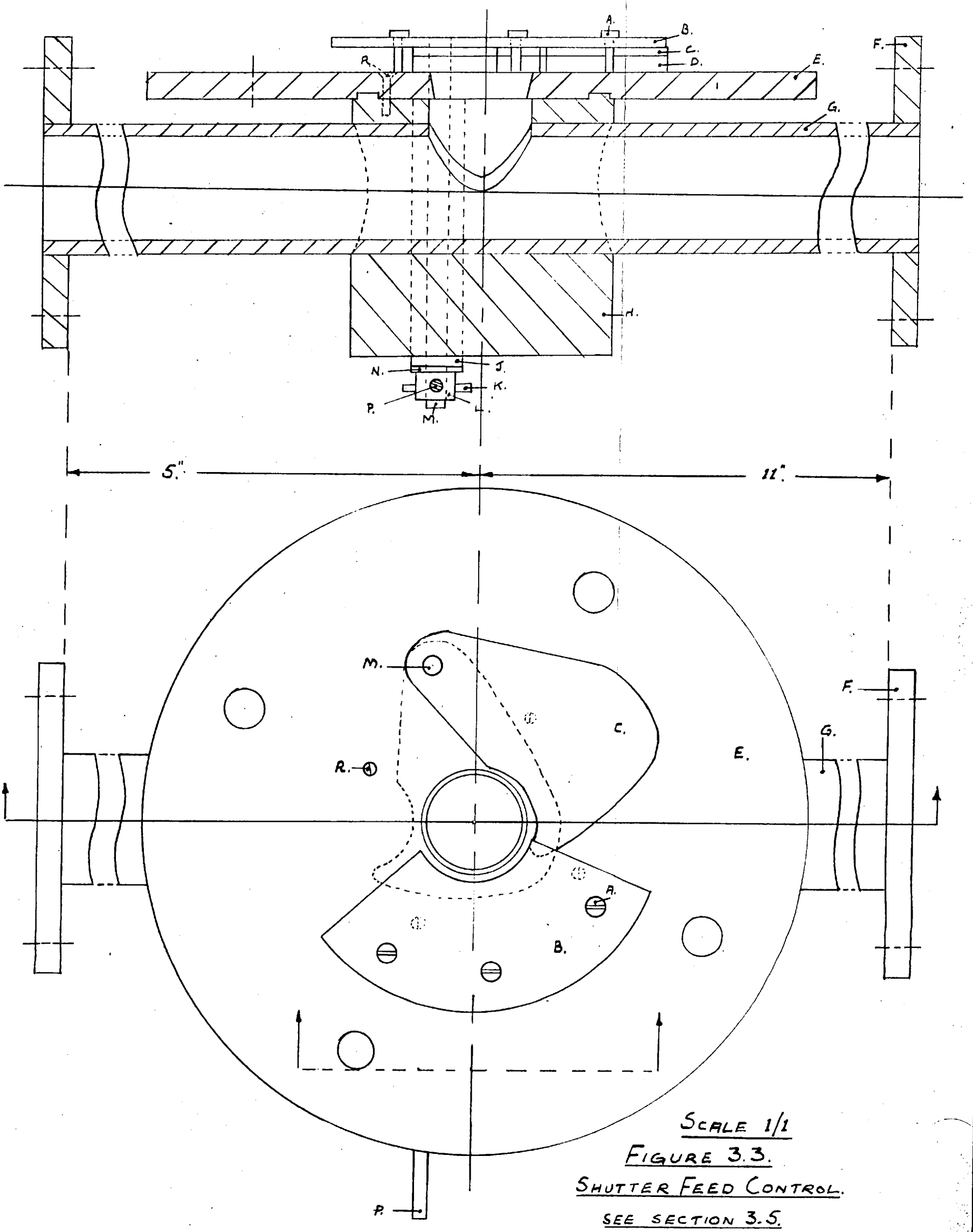


IRIS FEED CONTROL.

SCALE 1/1

FIGURE 3.2.

((SEE SECTION 3.5.))



SCALE 1/1

FIGURE 3.3.

SHUTTER FEED CONTROL.

SEE SECTION 3.5.

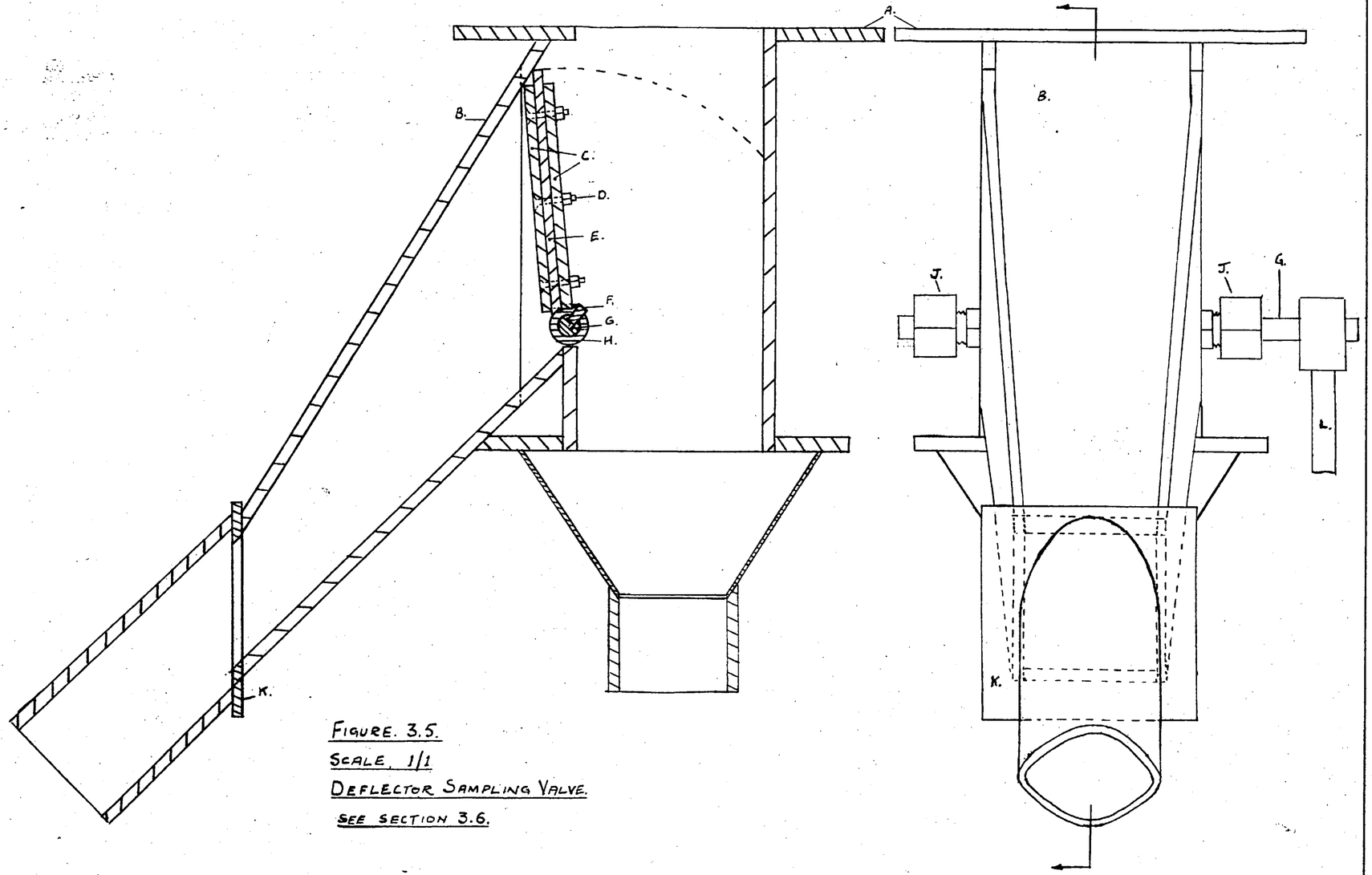


FIGURE. 3.5.
SCALE. 1/1
DEFLECTOR SAMPLING VALVE.
SEE SECTION 3.6.

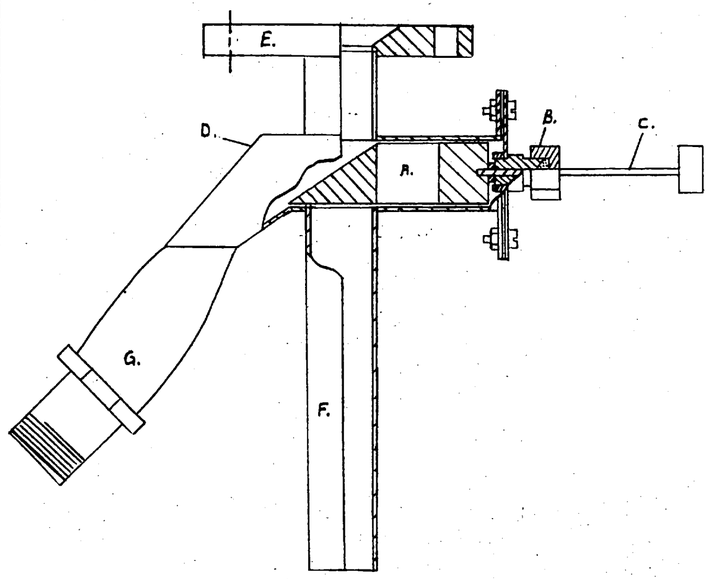
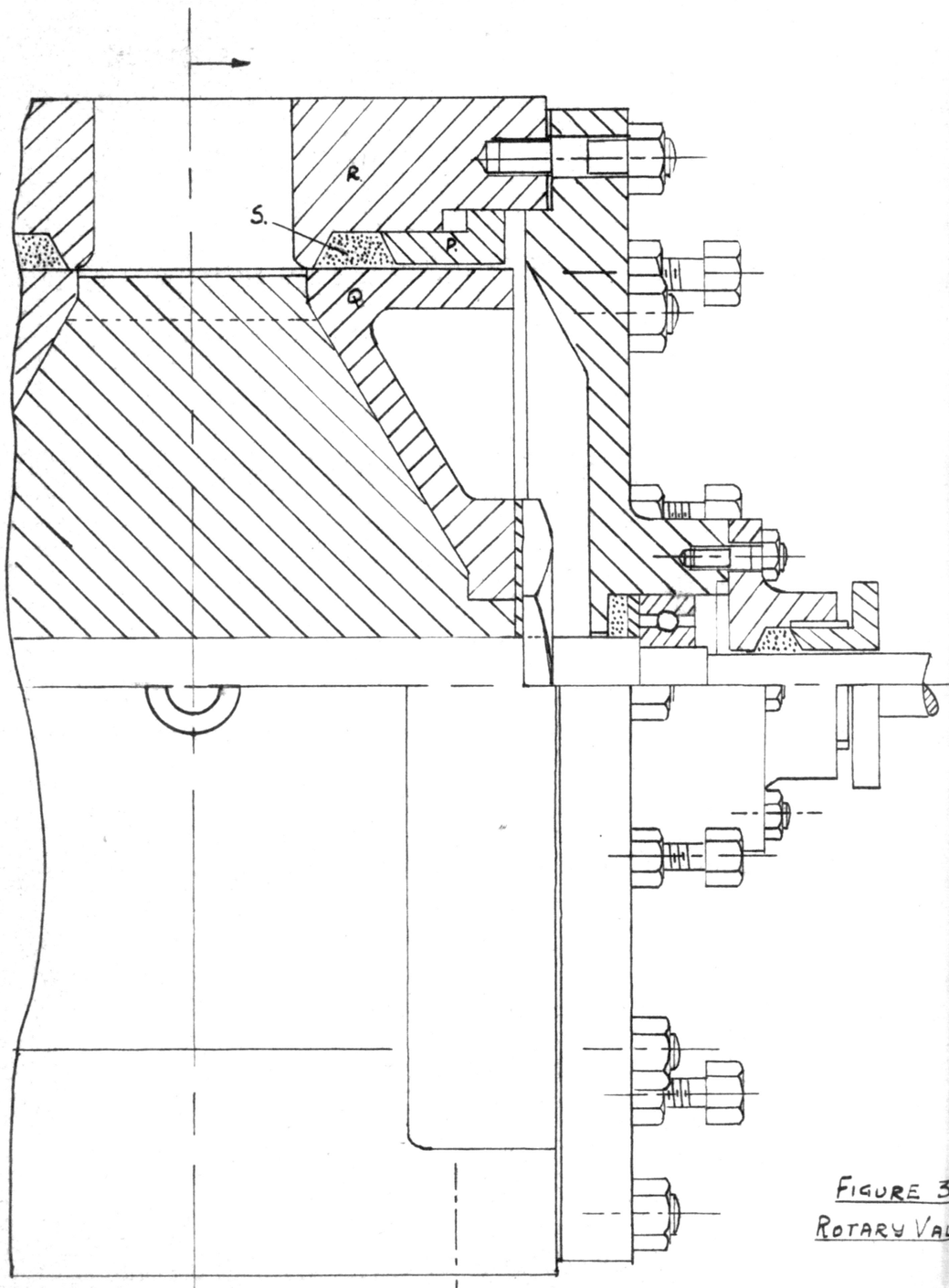


FIGURE 3.4.
SCALE 1/2.
SLIDE SAMPLING VALVE
SEE SECTION 3.6.



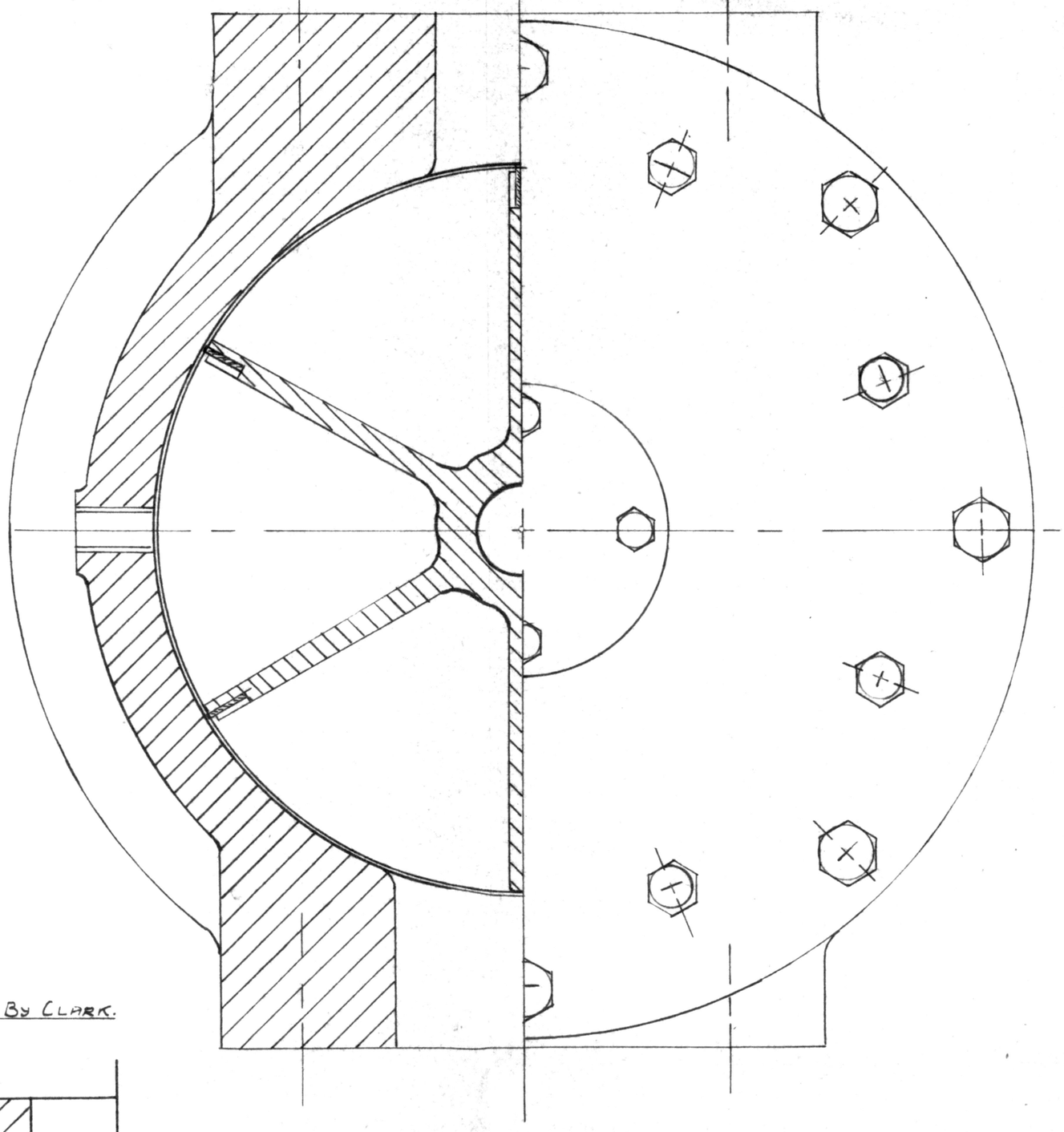
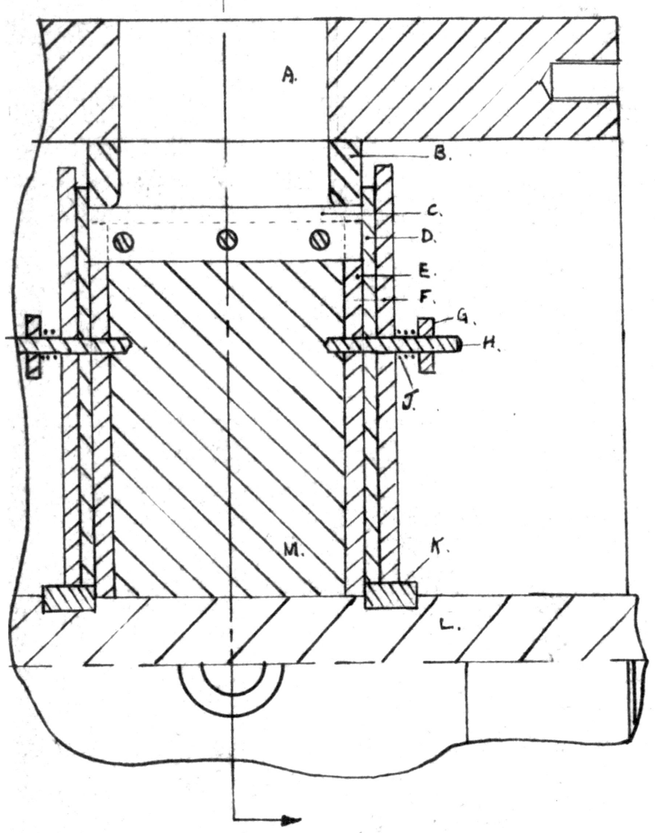


FIGURE 3.6.
ROTARY VALVE DESIGNED BY CLARK.



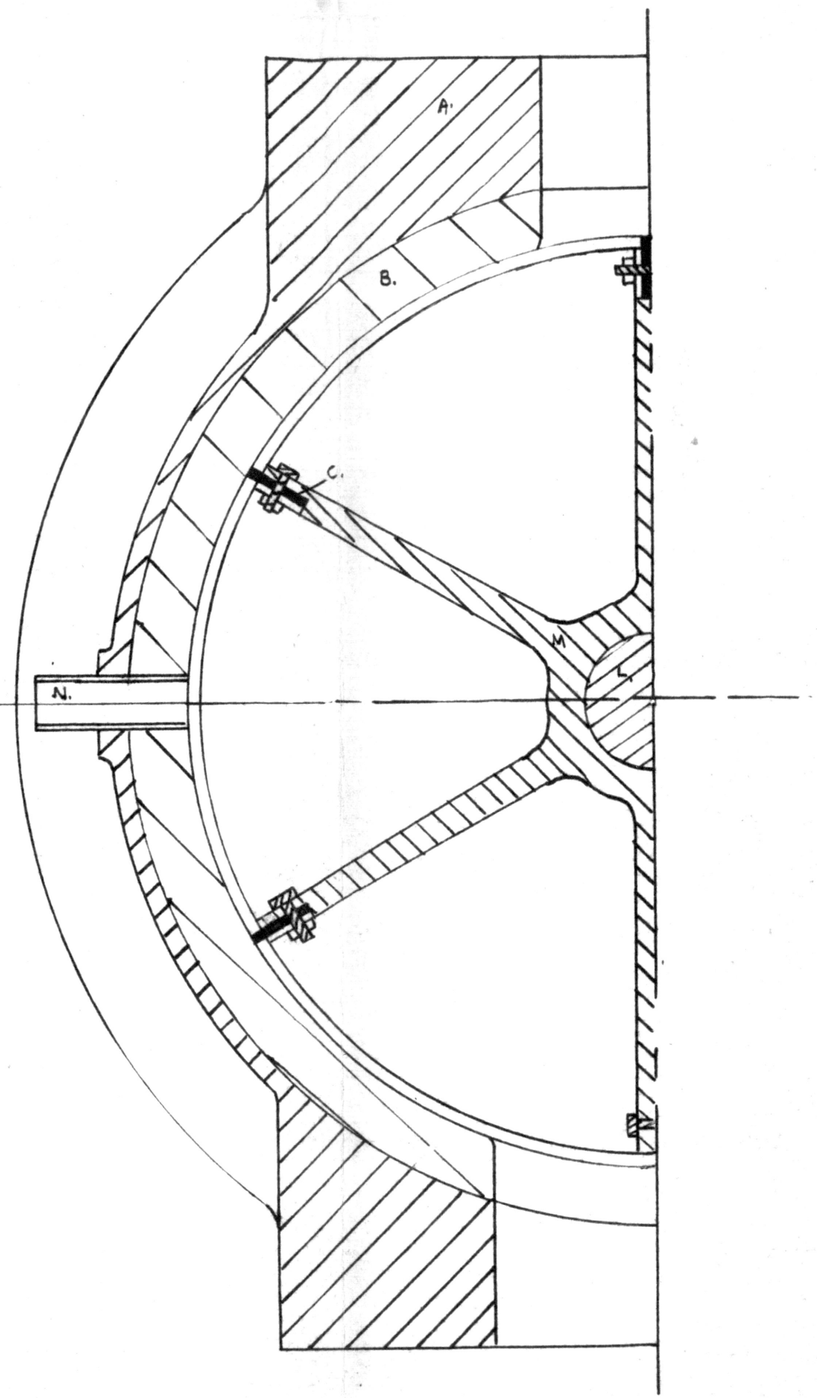


FIGURE 3.7.

REDESIGNED ROTARY VALVE

ALL FIGS. :- SCALE 3/4.
:- SEE SECTION 3.7

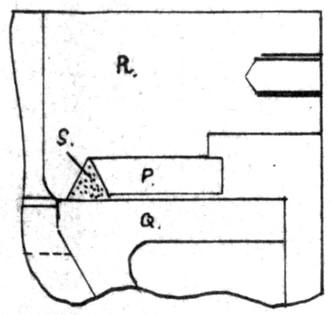


FIGURE 3.6A.

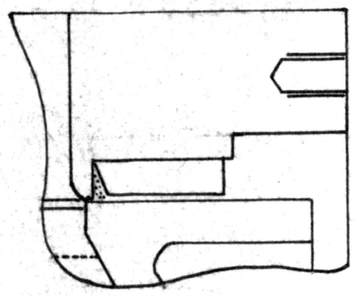


FIGURE 3.6B.

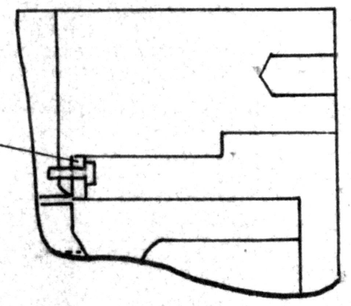
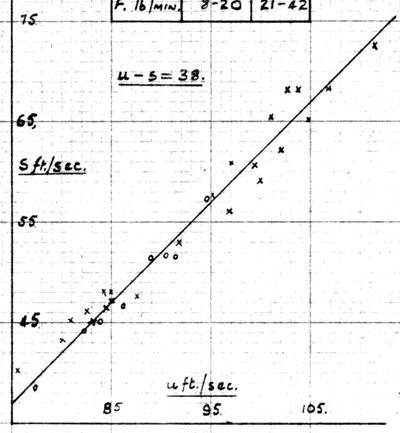


FIGURE 3.6C.

LEAD. GRAPH 6.1.

F. lb/min.	x	o
	8-20	21-42

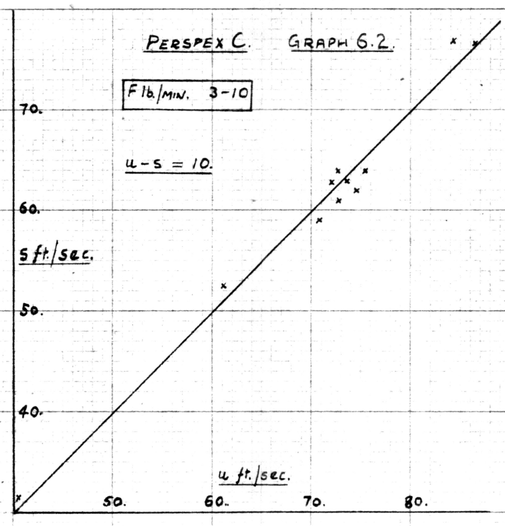
u-s = 38.



PERSPEX C. GRAPH 6.2.

F lb/min. 3-10

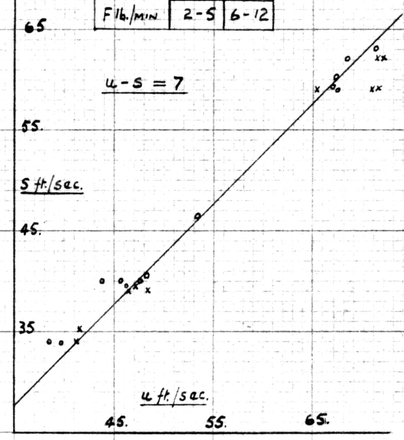
u-s = 10.



POLYSTYRENE. GRAPH 6.3.

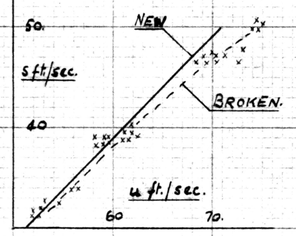
F lb/min	x	o
	2-5	6-12

u-s = 7



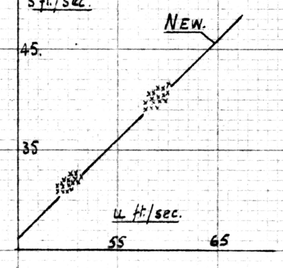
RADISH GRAPH 6.4.

u-s = 21



RAPE GRAPH 6.5

u-s = 19



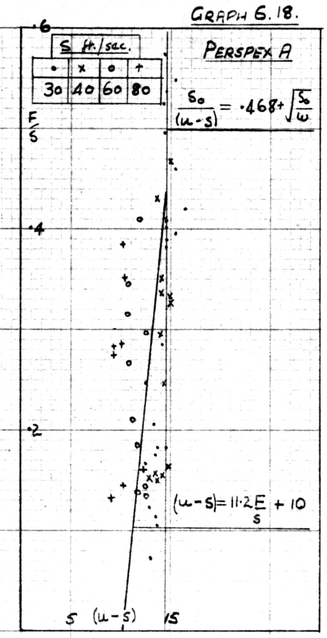
KEY

- u ft/sec. AIR VELOCITY.
- S ft/sec. SOLID VELOCITY.
- F lb./min. FEED RATE.
- S_o ft/sec. FALLING VELOCITY.
- w lb/cu.ft. DENSITY (SOLIDS).

PERSPEX A

S ft./sec.			
•	x	o	+
30	40	60	80

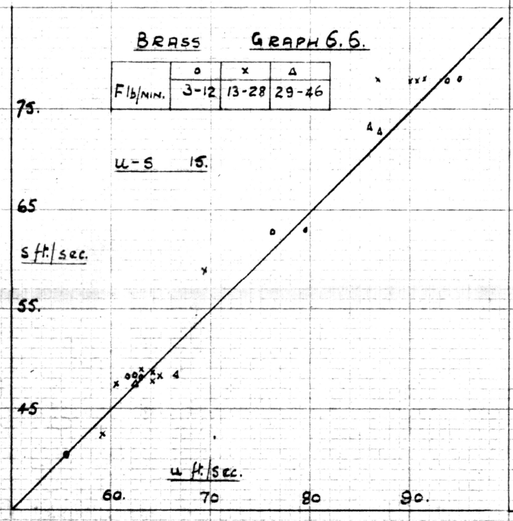
$\frac{S_o}{(u-s)} = .468 + \sqrt{\frac{S_o}{w}}$



BRASS GRAPH 6.6.

F lb/min.	o	x	Δ
	3-12	13-28	29-46

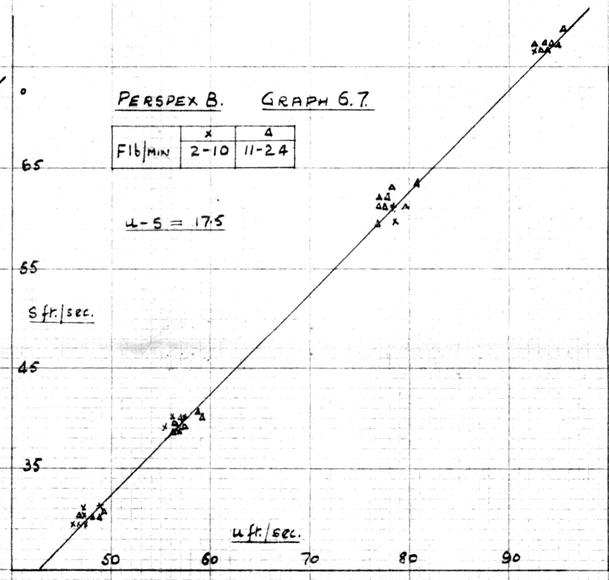
u-s 15.



PERSPEX B. GRAPH 6.7.

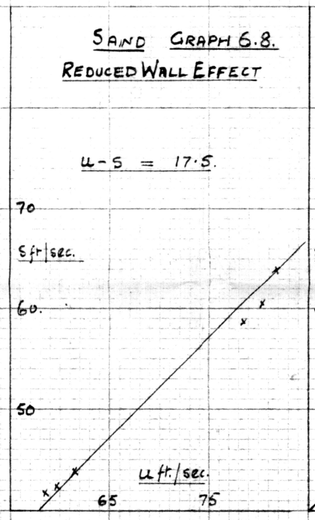
F lb/min	x	Δ
	2-10	11-24

u-s = 17.5



SAND GRAPH 6.8.
REDUCED WALL EFFECT

u-s = 17.5.



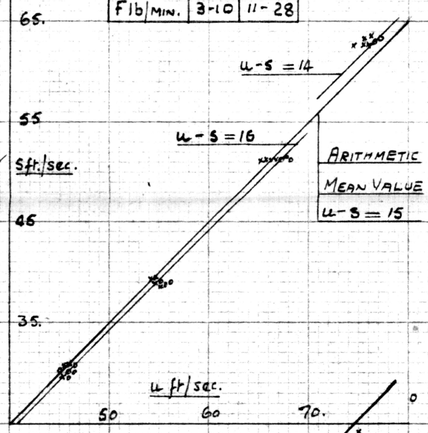
COAL E GRAPH 6.9.

F lb/min.	o	x
	3-10	11-28

u-s = 14

u-s = 16

ARITHMETIC MEAN VALUE u-s = 15



CORRELATION GRAPH 6.17.

$$(u-s) = \frac{S_o}{.468 + \sqrt{S_o/w}} + \frac{29.5}{\sqrt{S_o}} \cdot \frac{F}{S}$$

S_o FALLING VELOCITY.
u-s - RELATIVE VELOCITY.
S - SOLID VELOCITY ft./sec.
F - FEED RATE lb./min.
w - DENSITY $lb./ft^3$

SOLID VELOCITY S ft/sec.					
	•	x	+	o	'
ALUMINIUM	30	40	-	60	80
COAL A	30	35	37.5	-	-
COAL B	30	46	56	66	77
COAL C	30	40	50	60	75

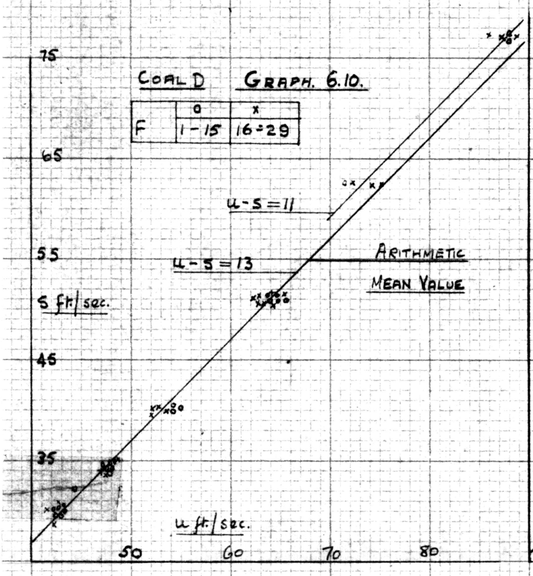
COAL D GRAPH. 6.10.

F	o	x
	1-15	16-29

u-s = 11

u-s = 13

ARITHMETIC MEAN VALUE

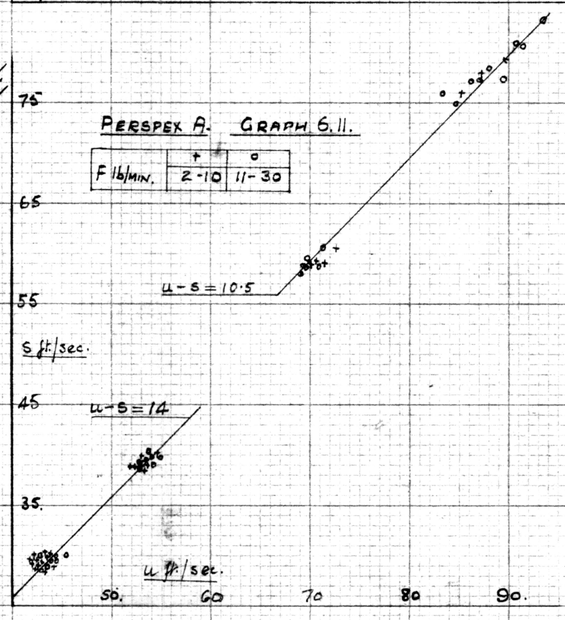


PERSPEX A. GRAPH 6.11.

F lb/min.	+	o
	2-10	11-30

u-s = 10.5

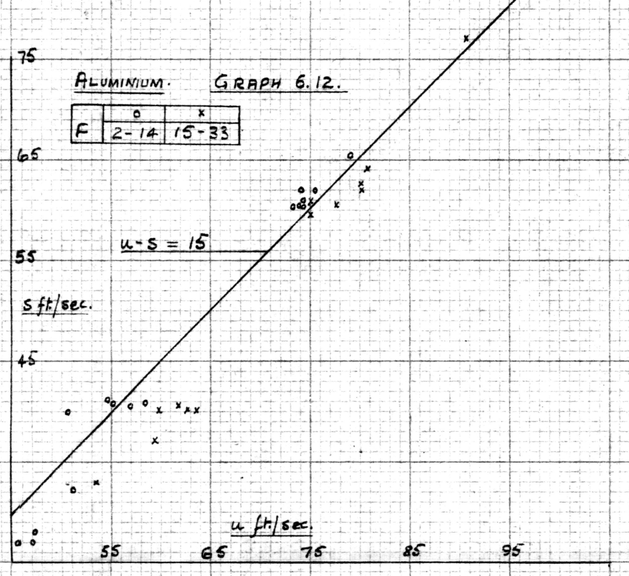
u-s = 14



ALUMINIUM. GRAPH 6.12.

F	o	x
	2-14	15-33

u-s = 15

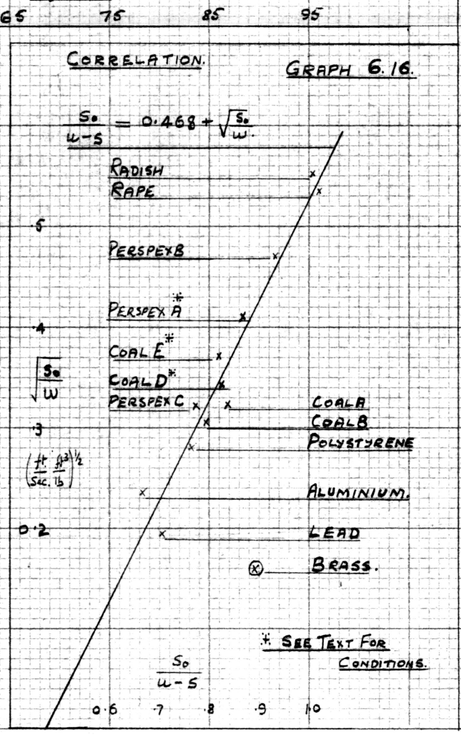


CORRELATION. GRAPH 6.16.

$\frac{S_o}{u-s} = 0.468 + \sqrt{\frac{S_o}{w}}$

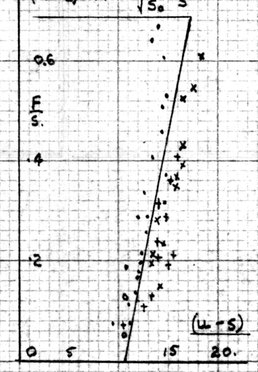
RADISH
RAPE
PERSPEX B
PERSPEX A*
COAL E*
COAL D*
PERSPEX C
COAL A
COAL B
POLYSTYRENE
ALUMINIUM.
LEAD
BRASS.

* SEE TEXT FOR CONDITIONS.



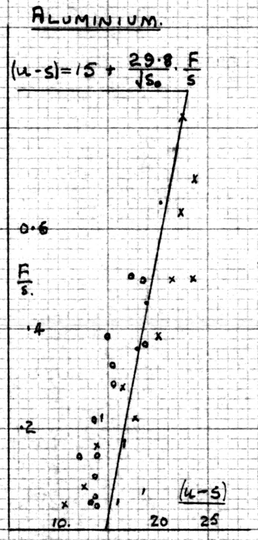
COAL A.

$(u-s) = 11 + \frac{27.7}{\sqrt{S_o}} \cdot \frac{F}{S}$



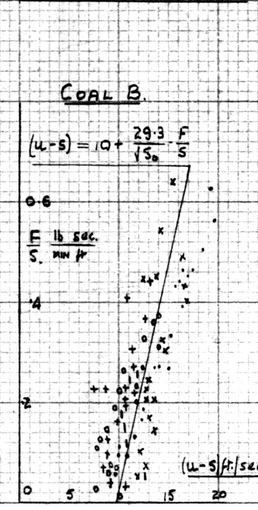
ALUMINIUM.

$(u-s) = 15 + \frac{29.8}{\sqrt{S_o}} \cdot \frac{F}{S}$



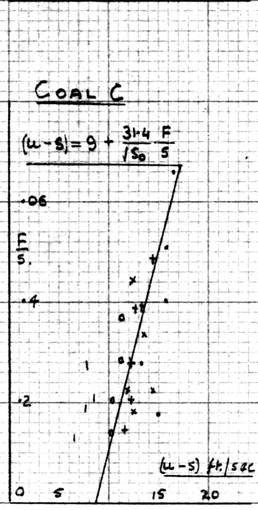
COAL B.

$(u-s) = 10 + \frac{29.3}{\sqrt{S_o}} \cdot \frac{F}{S}$



COAL C

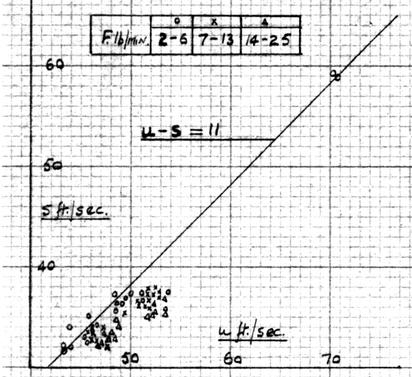
$(u-s) = 9 + \frac{31.4}{\sqrt{S_o}} \cdot \frac{F}{S}$



COAL A GRAPH 6.13.

F lb/min.	o	x	Δ
	2-6	7-13	14-25

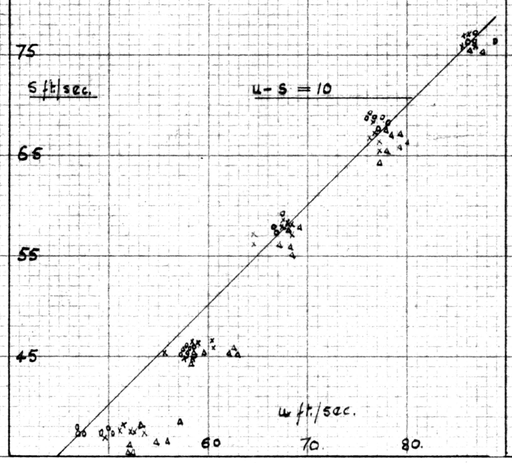
u-s = 11



COAL B GRAPH 6.14.

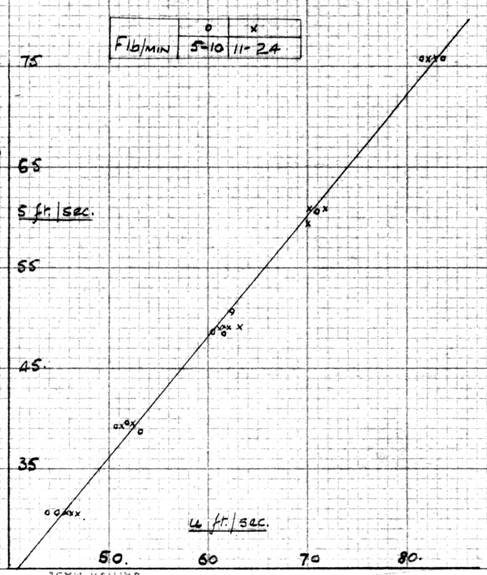
F lb/min.	o	x	Δ
	1-8	9-15	16-25

u-s = 10



COAL C. GRAPH 6.15.

F lb/min	o	x
	5-10	11-24



BRITISH MADE

LEAD GRAPH 7.3.

S ft/sec.	•	x
	45-50	51-72

$\frac{\Delta p_x \cdot S^2}{\Delta p \; F} = 24.4.$

$\frac{\Delta p_x \cdot S}{\Delta p}$ ft/sec

$\frac{F}{S}$ $\frac{lb}{min.}$ $\frac{sec.}{ft}$

BRASS GRAPH 7.4.

S	x	+	o
	40-50	70-80	55-65

$\frac{\Delta p_x \cdot S^2}{\Delta p \; F} = 62$

$\frac{\Delta p_x \cdot S}{\Delta p}$

F/S

PERSPEX A GRAPH 7.5

S	•	x	o	+
	30	40	60	80

$\frac{\Delta p_x \cdot S^2}{\Delta p \; F} = 57$

$\frac{\Delta p_x \cdot S^2}{\Delta p \; F} = 64 - \frac{3\,S}{F}$

$\frac{\Delta p_x \cdot S}{\Delta p}$

F/S

POLYSTYRENE GRAPH 7.6.

S	•	x	+	o
	35	40	46	60

$\frac{\Delta p_x \cdot S^2}{\Delta p \; F} = 132$

$\frac{\Delta p_x \cdot S}{\Delta p}$

F/S

RADISH. GRAPH 7.7

S - 40

$\frac{\Delta p_x \cdot S^2}{\Delta p \; F} = 40$

$\frac{\Delta p_x \cdot S}{\Delta p}$

F/S

RAPE GRAPH 7.8.

S - 40

$\frac{\Delta p_x \cdot S^2}{\Delta p \; F} = 37$

$\frac{\Delta p_x \cdot S}{\Delta p}$

F/S

NOTE F IN lb/MIN.

ALUMINIUM. GRAPH 7.9

S	•	x	o	+
	30	40	60	80

$\frac{\Delta p_x \cdot S^2}{\Delta p \; F} = 77$

$\frac{\Delta p_x \cdot S}{\Delta p}$

F/S

COAL C GRAPH 7.10

S	•	x	+	o	Δ
	30	40	50	60	80

$\frac{\Delta p_x \cdot S^2}{\Delta p \; F} = 106$

$\frac{\Delta p_x \cdot S}{\Delta p}$

F/S

COAL B. GRAPH 7.11.

S	•	x	+	o	Δ
	38	46	56	67	80

$\frac{\Delta p_x \cdot S^2}{\Delta p \; F} = 98$

$\frac{\Delta p_x \cdot S}{\Delta p}$

F/S

COAL A. GRAPH 7.12.

S	•	x	o
	32-34	35-37	60

$\frac{\Delta p_x \cdot S^2}{\Delta p \; F} = 90$

$\frac{\Delta p_x \cdot S}{\Delta p}$

F/S

GASTERSTADT'S DATA - WHEAT. GRAPH 7.18

u-S = 15 DIA. = 3·5/3·75"

u	x	⊛	⊕	⊞	o	Δ	□
	48	55	60/65	70	73/77	84/86	96/101

$\frac{\Delta p_x \cdot S}{\Delta p}$

F/S.

COAL D GRAPH 7.13

S	•	o	x	+	Δ	Δ
	30	35	40	50	60	80

$\frac{\Delta p_x \cdot S^2}{\Delta p \; F} = 82$

$\frac{\Delta p_x \cdot S}{\Delta p}$

F/S

COAL E GRAPH 7.14.

S	•	x	+	o	Δ
	30	40	60	60	75

$\frac{\Delta p_x \cdot S^2}{\Delta p \; F} = 66$

$\frac{\Delta p_x \cdot S}{\Delta p}$

F/S

PERSPEX B GRAPH 7.15

S	•	x	o	+
	30	60	60	80

$\frac{\Delta p_x \cdot S^2}{\Delta p \; F} = 31$

$\frac{\Delta p_x \cdot S^2}{\Delta p \; F} = 38.5 - \frac{2.5\,S}{F}$

$\frac{\Delta p_x \cdot S}{\Delta p}$

F/S

PERSPEX C GRAPH 7.16.

S - 60 ft/sec.

$\frac{\Delta p_x \cdot S^2}{\Delta p \; F} = 100 - \frac{4.5\,S}{F}$

$\frac{\Delta p_x \cdot S}{\Delta p}$

F/S

SEGLER'S DATA - WHEAT. GRAPH 7.17.

(u-S) ASSUMED CONSTANT = 15 ft/sec.

u ft/sec.	•	x	+	o	Δ
	63	66	69	72	75

DIA. 2" $\frac{\Delta p_x \cdot S^2}{\Delta p \; F} = 48.5$

DIA. 4" $\frac{\Delta p_x \cdot S^2}{\Delta p \; F} = 25$

DIA. 12" $\frac{\Delta p_x \cdot S^2}{\Delta p \; F} = 100$

DIA. 16" $\frac{\Delta p_x \cdot S^2}{\Delta p \; F} = 6.8$

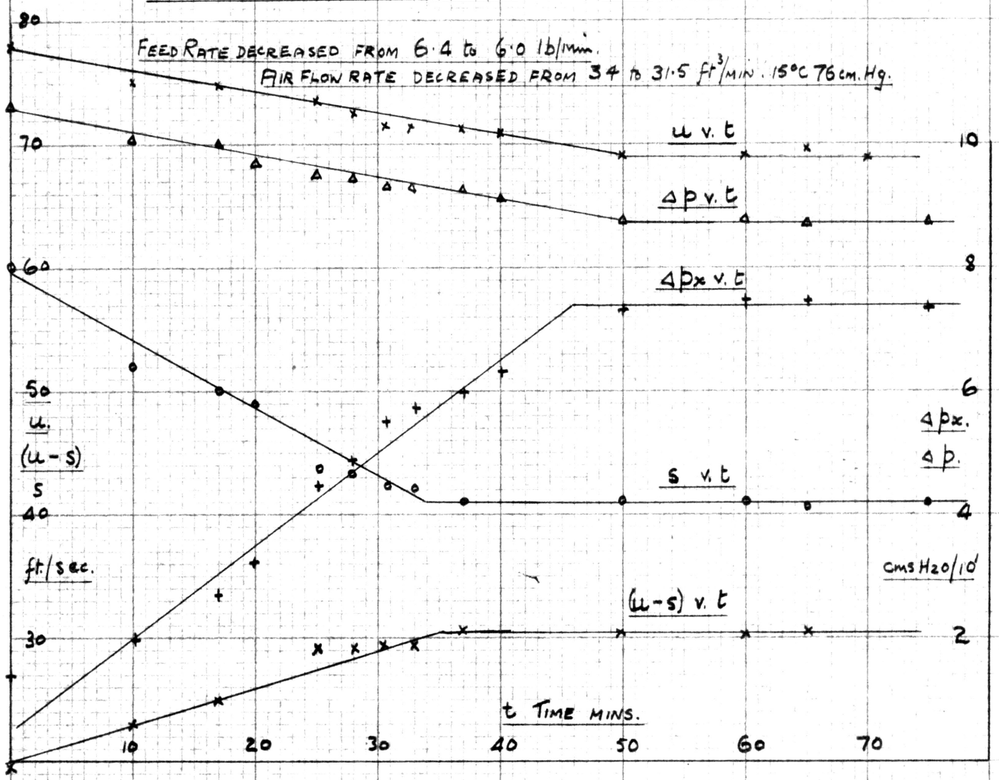
$\frac{\Delta p_x \cdot S}{\Delta p}$

F/S

BRITISH MADE

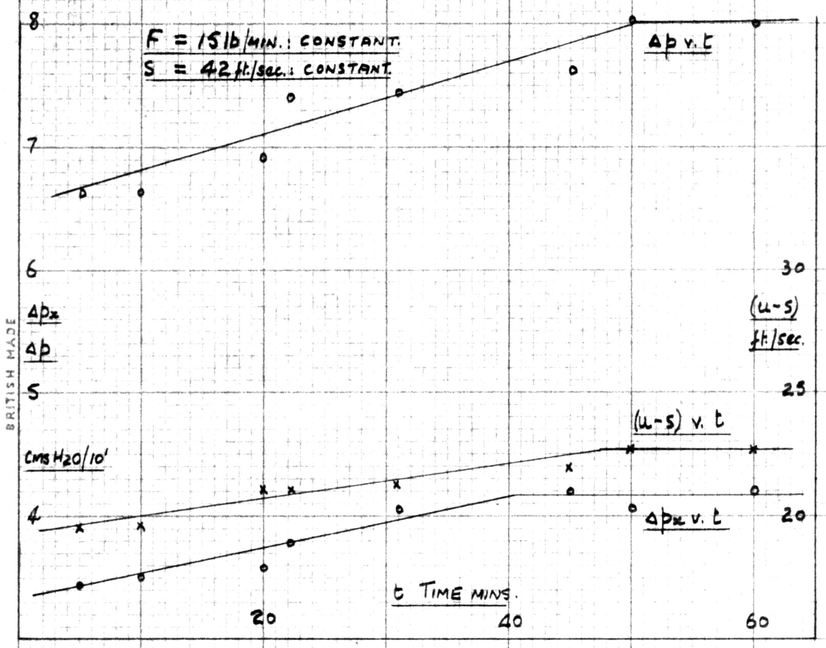
Build-up of the Wall Effect. Graph. 9.1.

Feed Rate decreased from 6·4 to 6·0 lb/min.
Air flow rate decreased from 34 to 31·5 ft³/min. 15°C 76 cm. Hg.

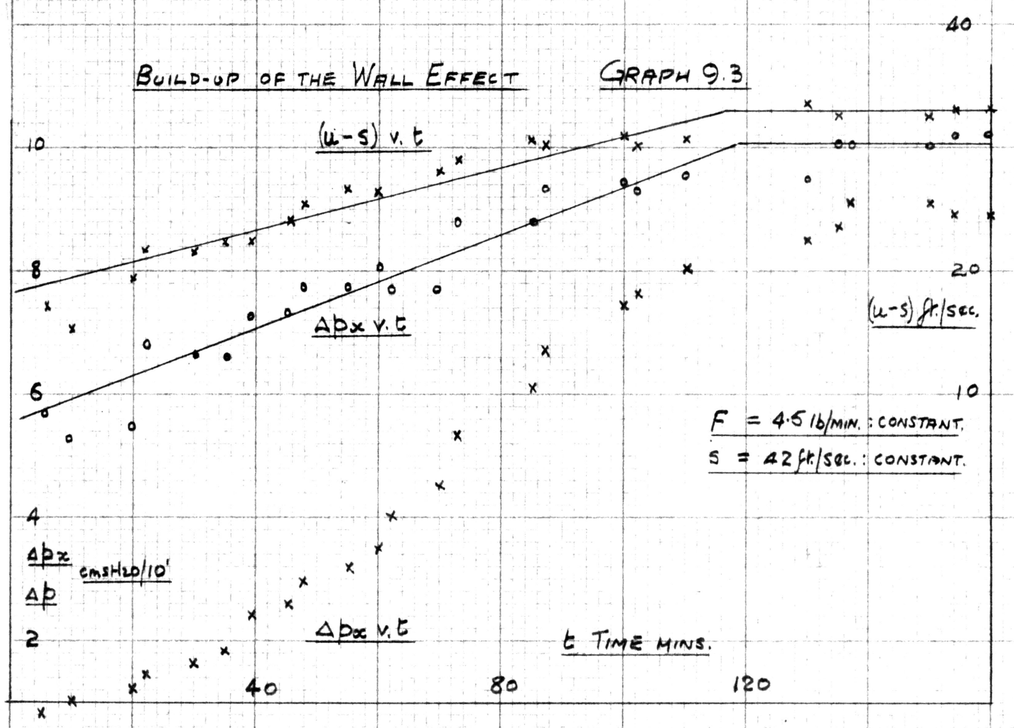


Build-up of the Wall Effect. Graph 9.2.

F = 15 lb/min.: constant.
S = 42 ft./sec.: constant.



Build-up of the Wall Effect. Graph 9.3

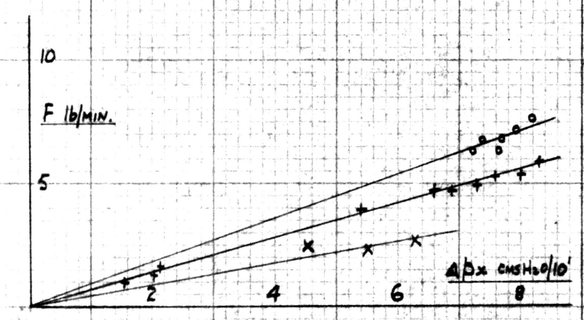


F = 4·5 lb/min.: constant.
S = 42 ft./sec.: constant.

Equilibrium Values. Graph 9.4.

S = 40 ft/sec.: constant.

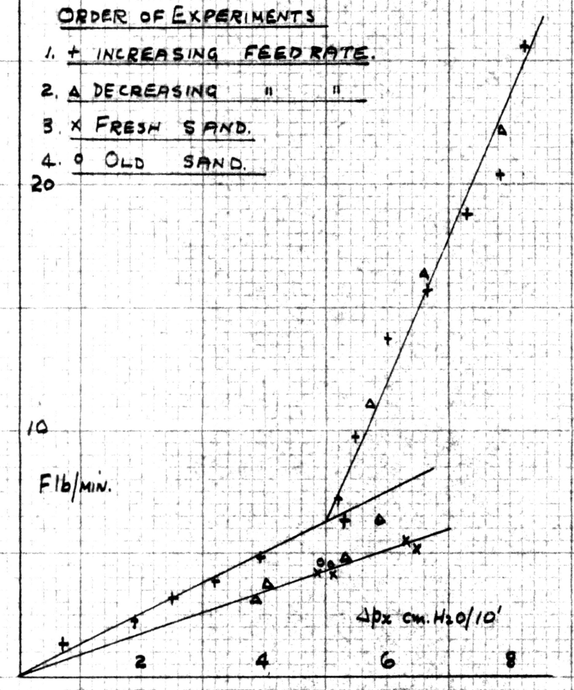
- o 1st day.. results during 50 min. } period after
- + 2nd " : " " 85 " } equilibrium
- x 3rd " : " " 115 " } was reached.



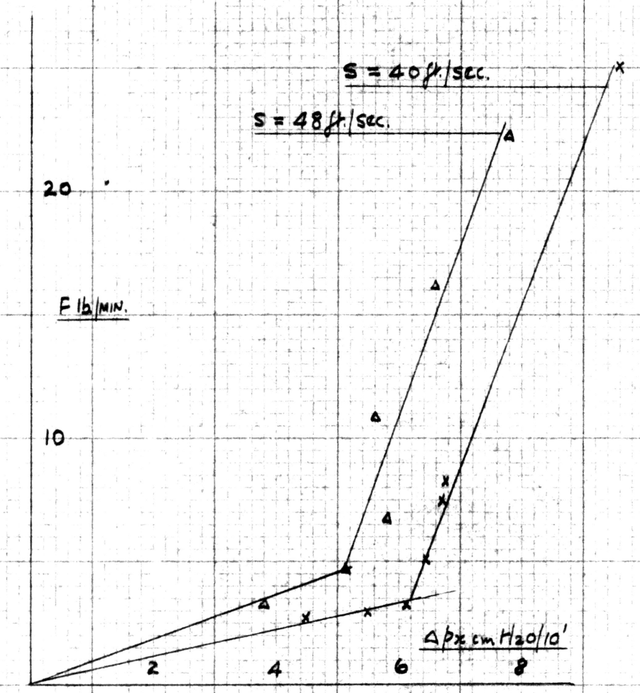
Equilibrium Values. Graph 9.5.

S = 48 ft/sec.: constant.

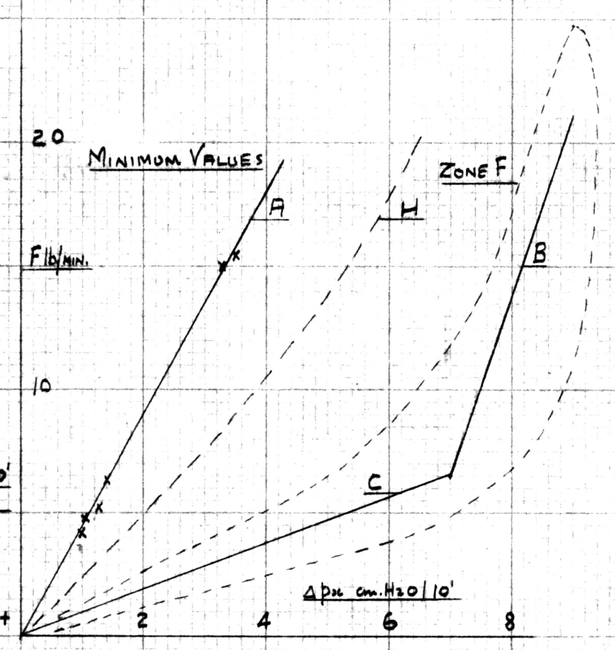
Order of Experiments
1. + increasing feed rate.
2. Δ decreasing " "
3. x Fresh sand.
4. o Old sand.



Equilibrium Values. Graph 9.6.

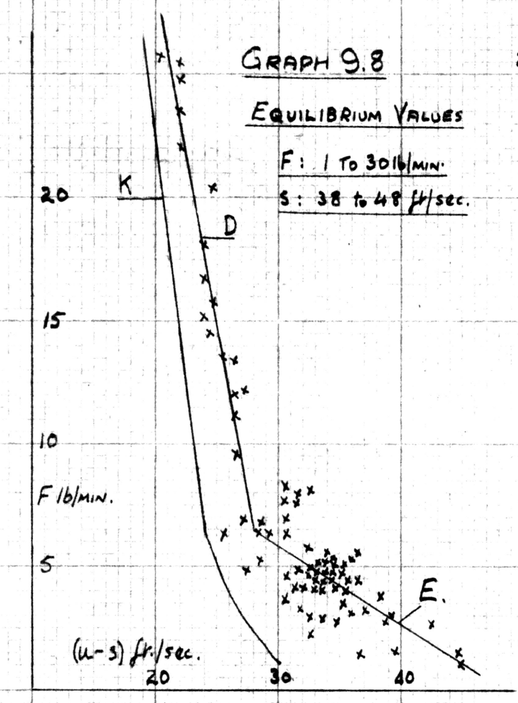


Pattern of the Wall Effect Graph 9.7.



Graph 9.8

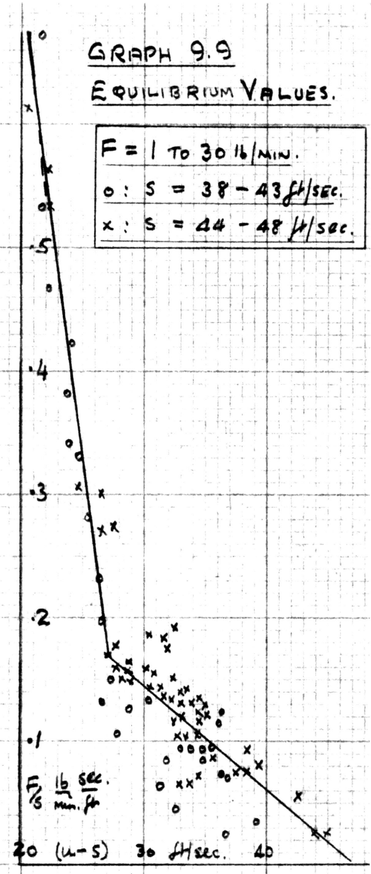
Equilibrium Values
F: 1 to 30 lb/min.
S: 38 to 48 ft/sec.



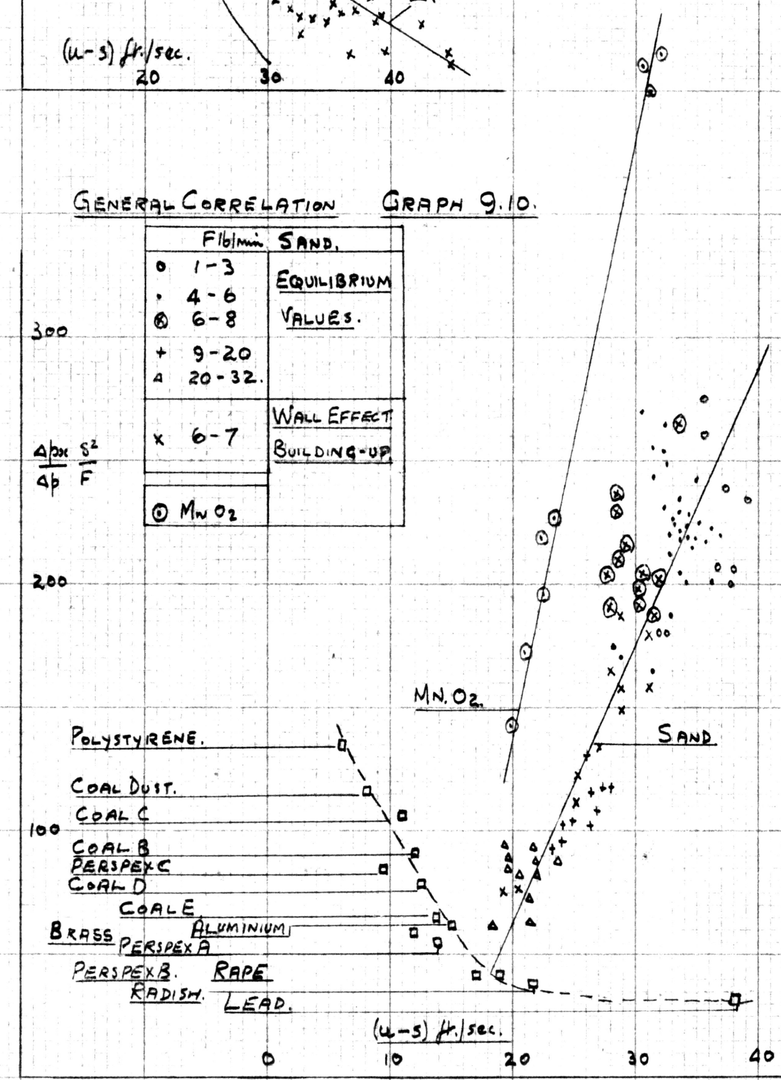
Graph 9.9

Equilibrium Values.

F = 1 to 30 lb/min.
o: S = 38 - 43 ft/sec.
x: S = 44 - 48 ft/sec.



General Correlation Graph 9.10.



BRITISH MADE